THE NATURE OF REACTIONS BETWEEN SODIUM SULPHIDE SLAG AND CARBON-SATURATED-IRON AND -COPPER ALLOYS

THE NATURE OF REACTIONS BETWEEN SODIUM SULPHIDE SLAG AND CARBON-SATURATED-IRON AND -COPPER ALLOYS

By

YAVUZ A. TOPKAYA, B.Met.

A Thesis

Submitted to the School of Graduate Studies

in Partial Fulfilment of the Requirements

for the Degree

Doctor of Philosophy

McMaster University

October, 1974

DOCTOR OF PHILOSOPHY (1974)
(Metallurgy)

McMASTER UNIVERSITY
Hamilton, Ontario

TITLE: THE NATURE OF REACTIONS BETWEEN SODIUM SULPHIDE SLAG AND CARBON-SATURATED-IRON AND -COPPER ALLOYS

AUTHOR: YAVUZ ALI TOPKAYA, B.Met. (Sheffield University)

SUPERVISOR: Professor W-K. Lu

NUMBER OF PAGES: (xiv), 216

SCOPE AND CONTENTS:

The nature of reactions between sodium sulphide slag and carbon-saturated-iron and -copper alloys were studied to obtain a more clear understanding of slag/metal reactions as well as to enhance the knowledge with respect to decopperization and desulphurization reactions. A model has been developed for the kinetics of reactions, taking into consideration the chemical reactions at the gas/slag and metal/slag boundaries as well as diffusion of sodium vapour in the gas phase. The rate constants have been determined by comparing the experimental results with the proposed model of the system using a CDC 6400 computer. Some understanding of the thermodynamics of sulphide solutions, never studied before, was accomplished through calculations. Suggestions were made for the most efficient use of sulphide slags for removing copper and sulphur from carbon-saturated iron melts. It is hoped that this work will open a new area of research on the fundamentals of slag/metal reactions involving sulphides. Such investigations may be helpful in understanding the slag/metal systems involving oxides.

ACKNOWLEDGEMENTS

The author wishes to express his sincere gratitude to his research supervisor, Dr. Wei-Kao Lu, whose direction and encouragement throughout different stages of the work led to a successful completion of the project. Special thanks are also due to Dr. M. Tokuda, whose help in the development of the kinetic theories was invaluable.

The author would like to extend his thanks to the members of the staff and graduate students of the McMaster University, who through many discussions contributed to the solution of various problems.

Finally, the author gratefully acknowledges the following groups for their financial support: the National Research Council of Canada, the Department of Metallurgy and Material Science and the Maden Tetkik ve Arama Enstitüsü of Turkey.

TABLE OF CONTENTS

LIST OF FIGURES

LIST OF TABLES

CHAPTER 1

INTRODUCTION

Pyrometallurgy is a branch of extractive metallurgy dealing mainly with the winning of crude metals from their ores and their subsequent refining, to obtain products of desired specifications, at elevated temperatures. Since some desired reactions become possible, thermodynamically, and/or practical kinetically only at high temperatures, the pyrometallurgical approach becomes necessary. Furthermore, the product phase (liquid metal) and the gangue phase (oxide or sulphide slags) have very limited mutual solubility and are quite different in densities, and thus readily separable.

Historically, the development of metallurgical industry, in many instances, has been far ahead of the scientific understanding of the chemical reactions involved. This is mainly due to the difficulties in carrying out measurements during the reaction at high temperatures, and the nature of multicomponent phases. Pyrometallurgical systems normally consist of at least three phases (gas, slag and metal), with chemical reactions taking place at the phase boundaries and heat and mass transport, through the bulk phases. Except for processes involving simple exchange reactions at interfaces, important industrial processes such as ironmaking, steelmaking, copper, nickel and lead smelting involve at least these three phases.

In view of such complexity, the fundamental understanding of pyrometallurgical processes, especially kinetic behaviour, is still far

from satisfactory. The kinetics of coupled reactions, at the slag/metal interface during desulphurization in ironmaking, have been studied only in the last two decades. The proper, although qualitative, interpretation appeared only in the very recent literature. To the best of our knowledge, there is no adequate investigation on important systems, such as steelmaking reactions, taking into consideration the gaseous oxidation of slag and the slag/metal boundary reactions as a single system.

The main objective of the present investigation is to study the coupling of interfacial reactions at both slag/metal and gas/slag boundaries. It is a pioneering study for more complicated but important systems. The choice of Na_2S slag, instead of ordinary silicate melts, is not only to avoid the complex anions in the slag and multiple reactions at slag/metal interface at this stage of investigation but also to shed some light on the nature of reactions in decopperization and desulphurization of iron alloys by sodium sulphide. Carbon, which is chemically inert in this work, is used as crucible material as well as a solute to lower the melting point of iron alloys.

In addition to the primary purpose stated above, it was thought that some thermodynamic information about sulphide mixtures could be obtained. In spite of the metallurgical importance of sulphide mattes, almost all research on the physical chemistry of melts has been devoted to halides and to oxide mixtures, especially silicates. With the present interest in decopperizing iron, more should be known about the thermodynamics of sulphide systems, such as activity coefficients of copper,

manganese and iron sulphides, at low concentrations, in sodium sulphide and other sulphides. Unfortunately, measurements of these activities are not easily made at high temperatures because of the high volatility of some of the compounds. It is anticipated that a clear understanding of both kinetics and thermodynamics of the present system may eventually lead to an economical process, of industrial importance, for decopperization and desulphurization of iron alloys.

CHAPTER 2

LITERATURE SURVEY

2.1 Kinetics of slag/metal reactions

This literature survey is limited, in its scope, to iron- and steel-making systems and it is aimed at establishing the electrochemical nature of the reactions involved. It deals mainly with the kinetics of sulphur transfer. Fundamental work on the coupling of reactions at both gas/slag and slag/metal boundaries seems to be lacking.

K.M. Goldman, G. Derge, and W.O. Philbrook[1] reported that the rate of transfer of sulphur from carbon-saturated iron to oxide slags is considerably increased by "deoxidizers", such as silicon, manganese, and aluminum. The data was interpreted in terms of a three-stage mechanism. However, the rate constants evaluated were not independent of concentrations for the elements mentioned above. S. Ramachandran, T.B. King and N.J. Grant[2] also reported the effect of silicon and aluminum in accelerating the sulphur transfer. Their results show that the rate of sulphur transfer is equivalent to the sum of the rates of transfer of silicon, aluminum, iron and the rate of CO evolution. If $\dot{n}$ represents rate of transfer or evolution in moles per second, the positive sign being used for metal to slag transfer, then

$$2\dot{n}_S = 2\dot{n}_{Fe} + 4\dot{n}_{Si} + 3\dot{n}_{Al} + 2\dot{n}_{CO}$$

This stoichiometric relation maintains the system electrically neutral.

Ramachandran et al. reached the conclusion that the reactions in their system are electrochemical in nature and have proposed a number of half-cell reactions. A treatment of the rate of CO evolution, in terms of the "two-film hypothesis" of mass transport, has been given.

A comprehensive analysis of the kinetics of slag/metal reactions, involving both interfacial reactions and mass transport, has been given by Wagner.[3] Wagner has considered slag/metal reactions of the type,

$$[Mn] + (Fe^{++})\ \text{slag} \longrightarrow (Mn^{++})\ \text{slag} + [Fe]$$

Two limiting cases were pointed out: (a) transport control, (b) chemical reaction control. An exchange reaction, as represented above, involves a sequence of steps including transport processes to and from the slag/metal interface and phase-boundary chemical reactions. It is most important to know the rate-determining step, for which Wagner developed the concept of the virtual maximum rate.

In dealing with kinetics of transport-controlled reactions, Wagner pointed out that mass transport generally consists of atomic diffusion and convection (natural and forced). So the mass transport equation must be written to account for atomic diffusion as well as convective mass transport in the form:

$$J_i = - D_i \frac{\partial C_i}{\partial x} + C_i V_x - E \frac{\partial C_i}{\partial x}$$

where the first, second and third terms in the equation above are for atomic diffusion, convective flow and eddy diffusion, respectively. V_x is the x-component of the convective flow velocity, D_i is the diffusion

coefficient of species i, C_i is the concentration of species i and E is the coefficient of eddy diffusion. The relative importance of the last two terms in comparison with atomic diffusion will depend on the fluid mechanical properties of the system. In most systems, mechanical stirring would reduce any concentration gradient near the interface provided the interface remains undisturbed. Consequently atomic diffusion is generally thought to be always operative within the so called "boundary layer". The "boundary layer" refers to the film of liquid near the interface in which concentration gradients are considered to exist, but beyond which a uniform bulk composition is maintained by turbulent or convective flow.

By describing the driving force in terms of concentration and boundary layer thickness, δ, and rewriting the flux in terms of moles, time, and interfacial area, then:

$$\frac{dn_i}{dt} = \frac{DA}{\delta} [C_i(\text{interface}) - C_i(\text{bulk})]$$

Using these concepts as a basis, theoretical models have been derived for cases where one particular diffusion step in the overall reaction is rate-limiting.

In dealing with kinetics of phase-boundary reactions, Wagner suggested that phase-boundary reactions occur randomly over the interface as simultaneous cathodic and anodic reactions, with regard to both space and time. The idea is similar to that used as the basis of the Wagner-Traud theory of corrosion of a homogeneous metal surface.[4] A Butler-Volmer type expression was suggested by Wagner to be applicable here for

describing the relationship between the current density, carried by a particular chemical species undergoing chemical reaction, and the electrical potential difference across the slag/metal interface. It is reproduced as follows:

$$J_i = k_i C_i \exp[(1 - \alpha_i) Z_i EF/RT] - k_i' C_i' \exp[-\alpha_i Z_i EF/RT]$$

where E is the electrical potential difference across the interface, k_i and k_i' are the rate constants for anodic and cathodic processes, respectively, for component i, C_i and C_i' are the interfacial concentrations of component i in the metal to be oxidized anodically and that of ions to be reduced cathodically, α_i is the symmetry factor whose value lies between zero and unity.

King et al.[5] and Eyring and co-workers[6] have attempted to explain the reported data of sulphur transfer in terms of Wagner's formalism. Eyring et al. proposed that the electrical potential difference across the slag/metal interface may be evaluated empirically, based on the irreversible reaction of CO evolution and is common for all interfacial reactions. They also assumed that the activity of oxygen in the slag is independent of time because of its high concentration. This assumption is certainly debatable. With the above mentioned assumptions, Eyring et al. fitted the experimental concentration vs. time curves for silicon and iron, obtained by King et al., with the empirically evaluated potential difference as a function of time and four adjustable parameters. It was found that the values of these parameters are sensitive to the initial silicon content of the melt.

W.O. Philbrook[7] and W-K. Lu[8,9] used the changes in electrochemical potentials, instead of chemical potentials, as the driving forces and using irreversible thermodynamics formulation reached, independently, very similar conclusions. It was shown that the exact form of the Butler-Volmer equation and the one according to Prigogine's formulation[10] are equivalent. However, the approximate forms are rather different. However, only the one based on irreversible thermodynamics is meaningful. They have reduced the simultaneous kinetic equations to functions of concentration and time (with the assumption that the overall reaction is controlled by chemical reaction). The lack of information, on the concentration of free oxygen as a function of slag composition, prevented the authors from giving a quantitative treatment of the data reported in the literature. Qualitative interpretations were given by Philbrook and Lu. Up to the present time, a general analysis, including both coupled chemical reactions and coupled diffusion, is not available.

In the present work, a sulphide slag was used to avoid the problem of free oxygen concentration. Then, the coupling between reactions at both slag/metal and gas/slag interfaces, and mass transport steps could be studied quantitatively.

2.2 Literature survey related to the use of sodium sulphide

The possibility of using sodium sulphide slags to remove sulphur and copper from ferrous alloys was first suggested by J.F. Jordan,[11,12] and two U.S. patents were granted to the above named investigator in 1950. In his patents, Jordan claimed to have lowered the sulphur content of a

molten pig iron containing 1.09wt%Mn and 0.045wt%S, to 0.007%S with molten sodium sulphide. In the case of another molten pig iron containing 4.25%C, 1.25%Si, 0.08%Mn and 0.097%S, sodium sulphide lowered the sulphur to 0.010% and manganese to 0.06%. He also claimed that the addition of aluminum to the molten metal would greatly improve the effectiveness of sodium sulphide as a desulphurization agent. In the tests carried out with melts containing copper, it was found possible to lower the copper from 0.30% to 0.04%, provided that sufficient sulphur additions were made to the molten pig iron before the commencement of slag/metal reactions. Jordan stated that the process of removal of copper by sulphide slag essentially depended on the preferential affinity of sulphur for copper rather than iron at liquid-iron temperatures. In his patents, Jordan made very general claims without specifying experimental conditions precisely.

Subsequent to the work mentioned above, several scientific and investigative reports about the desulphurization and decopperization of ferrous metals with sodium sulphide slags have been published in literature.[13-23]

In their investigation of removal of copper from Fe - Cu - C - S alloys, F.C. Langenberg and R.W. Lindsay[13,14,15,16] quoted final sulphur levels as low as 0.015%. Their work showed that sodium sulphide was capable of removing copper and sulphur from the melt at the same time. As a conclusion, they stated that alkali sulphides, such as sodium sulphide, as used in the Orford process, seemed to have the desirable characteristics of utilizing the affinity of copper and sulphur to remove copper, with

simultaneous lowering of sulphur content. The authors did not go into the thermodynamics and kinetics of the reaction but only tabulated the composition of the metal phase before and after treatment, with some quantitative explanation of what was happening during the reaction.

In more recent investigations, by H. Schenck and G. Perbix,[17] of decopperization of cast iron and lead by $Na_2S \cdot 9H_2O$, final sulphur content of iron was found to vary with temperature. Final sulphur levels of 0.025wt% at 1200° to 1300°C, 0.05wt% at 1400°C and 0.11wt% at 1500°C were quoted, whereas the partition ratio of copper $n_{Cu} = (\%\ Cu)_{Na_2S} / [\%\ \underline{Cu}]_{Fe} = 7.4$ was found to be constant in the temperature range 1400° to 1500°C and composition range $0 < [\%\ \underline{Cu}]_{Fe} < 2$. The investigation did not go beyond determination of the distribution coefficient of copper in slag and metal.

During the last decade, sodium sulphide has been tested on a larger scale for decopperization purposes by the Bureau of Mines and their findings have been published as investigation reports.[18,19,20,21] The findings confirmed the results obtained on smaller scale apparatus in various laboratories. According to their findings, the process now appears sufficiently defined to permit demonstration on commercial-scale melts. Practical applications would include treatment of ductile iron melts from bundled auto scrap to permit greater utilization of such scrap in the furnace charge.

More recently, H. Schenck, H. Roth and E. Steinmetz,[22] for the first time, tried to put forward a theory to explain the transfer of copper and other elements between molten iron, within the range of carbon

saturation, and sodium sulphide slags. In their paper, the authors discussed the experiments to remove copper from pig iron by means of sodium sulphide, by utilizing batch or counter flow processes. Extensive large pilot plant scale experiments have been conducted to determine the distribution constants and transfer coefficients. Schenck et al. reported a decrease in the sulphur level of the metal from 0.16 to 0.04wt% in the first 2 minutes of treatment, but after this period, there was a steady increase in the sulphur level with increasing time. Their reported distribution coefficient for copper n_{Cu} = 7.7 in the temperature range 1250° to 1500°C agrees quite well with the above mentioned work of Schenck and Perbix. Finally, an electrochemical interpretation of the copper transfer was given in this paper. Although Schenck et al. have also tried to set up a theoretical reaction model by making use of the ideas developed for desulphurization of iron under oxide slags, they have not attempted to correlate the derived theoretical equations with the experimental results. The main reasons given were the lack of information about activities in the slag phase and the disturbance of the system by the vaporization of Na_2S .

Finally, A. Safaiah and F. Sale[23] have investigated the influence of carbon level on the removal of copper from iron melts with sulphide slags. It was shown that sulphide slags were not as effective in removing copper from low-carbon melts as from high-carbon melts and this was explained by the relative activities of the copper in the various iron solutions. It was also found that sulphur pick-up occurred during the sulphide treatment of all melts when the initial sulphur content was low. The extent of

sulphur pick-up was found to be dependent on the carbon content of the metal bath. The effect of carbon upon the residual sulphur level of the metal baths was explained by a consideration of the effect of carbon on the activity of sulphur in liquid iron. Carbon significantly increases the activity of sulphur in iron and so it was apparent that a given sulphur potential above liquid-iron melt would result in a higher sulphur pick-up in low-carbon melts than in carbon-saturated ones.

Apart from the investigations mentioned above there have been a number of other studies involving other sulphide mixtures, A study by F.D. Richardson[24] investigated the thermodynamic properties of Na_2S - Cu_2S mixtures in the molten and solid states. Measurements were made of the equilibria between H_2 - H_2S, Cu and Cu_2S and H_2 - H_2S, Cu and Cu_2S - Na_2S in the temperature range 527° to 1152°C. The results were used to calculate the thermodynamic properties of solid Cu_2S and the activities of Cu_2S in both solid and liquid solutions containing up to 37 mole%Na_2S. For the equimolar mixture of Na_2S and Cu_2S, $a_{Cu_2S} = a_{Na_2S} = 0.19 \pm 0.05$ was reported at 820°C which suggests that the mixture is not ideal.

Various investigations of decopperization of lead and other non-ferrous metals by sulphide slags also exist.[17,25,26] It has even been suggested that the soda process for desulphurization of pig iron is very effective owing to the large solubility of FeS in the dross, which is rich in Na_2S.[27]

CHAPTER 3

GENERAL REVIEW OF SULPHIDES AND PROPERTIES OF COMPONENTS OF SLAG/METAL SYSTEM

3.1 General review of sulphides for decopperization and desulphurization purposes

Although copper is sometimes added to steel or cast iron to impart some specific physical or chemical property, its presence as a tramp element has become an important factor in scrap utilization. To be acceptable to the steel industry scrap should contain less than 0.15 wt% copper, and although the presence of small amounts of copper does not adversely affect many types of steel, concern has been expressed over the increasing amounts of copper in all types of steel. This increase is due to the recycling of ferrous scrap and the inability to remove copper from liquid iron or steel under the oxidizing conditions of the steelmaking processes.[28,39,30] The presence of copper in excess of the above given value is considered harmful for hot-working and deep-drawing processes.

One way of solving this problem is to use a sulphide slag to remove copper from liquid-iron melts. For the desulphurization and decopperization of ferrous metals with sulphide slags, the sulphide must be essentially immiscible in the molten metal that is to be treated; must be a solvent for the sulphides which are to be extracted from molten metal; must be the sulphide of a metal whose affinity for sulphur exceeds the affinity for sulphur exhibited by the molten metal that is to be treated; and must not be volatile at iron- and steel-making temperatures.

For the purpose of discussion, the sulphides can be classified into two groups:[31,32] volatile sulphides, those which lose weight chiefly by volatilizing as such, and non-volatile sulphides, those which dissociate rather than evaporate. This classification superimposed on a periodic table is shown in Table I.

The temperatures usually encountered during iron- and steel-making cover the range 1150° to 1800°C. When the stabilities of sulphides under these conditions are considered in relation to the periodic table classification by reference to Table I, two general classes of sulphides emerge. The sulphides of elements of group II B and of groups further to the right are volatile, while those sulphides of group I B and of groups further to the left are non-voltatile solids or liquids. The sulphides described as volatile may be dismissed as unsuitable at iron- and steel-making temperatures. The stabilities of the more favourable non-volatile sulphides under the anticipated conditions must be studied more closely.

From Table I, it can be seen that alkali sulphides exist as liquids in the temperature range of interest. In the absence of moisture they are non-reactive. However, at 1400°C their dissociation pressures are quite high, of the order of 10^{-2} atm. The alkali-earth sulphides melt above 2000°C and are unsuitable to be used alone. The transition metal sulphides TiS, VS, CrS and MnS melt within the range 1400°C to 2000°C. TiS and VS can be ignored because of their high melting points, whereas MnS is soluble in molten metal and is not suitable. The group VIII sulphides FeS, CoS and NiS and the group I B sulphides Cu_2S and Ag_2S melt below 1200°C so that the stability of the liquid sulphides are of interest but

I A	II A	III B	IV B	V B	VI B	VII B	VIII B			I B	II B	IIIA	IV A	V A
Li_2S 847°C	BeS													
Na_2S 1175	MgS >2000											Al_2S_3 1100		
K_2S 835	CaS 2400	ScS	TiS 1930	VS 1900	CrS 1550	MnS 1610	FeS 1195	CoS 1100	NiS 797	Cu_2S 1100	ZnS S1185	Ga_2S_3 1250	GeS 625	As_2S_3 300
Rb_2S d530	SrS >2000									Ag_2S 842	CdS s980	In_2S_3 1098	SnS 880	Sb_2S_3 546
Cs_2S d520	BaS 2200									Au_2S d197	HgS S446	Tl_2S 449	PbS 1114	Bi_2S_3 706

H_1 → | H_2 →

NON-VOLATILE SULPHIDES ← → VOLATILE SULPHIDES

H_1 = HYGROSCOPIC SULPHIDES

H_2 = HYDROLYZABLE SULPHIDES

d = Decomposes

s = Sublimes

Table I: Probable volatility and stability relationship of metallic sulphides

unfortunately some of these sulphides are either soluble in molten metal or have very low melting points.

A close examination of the free energy-temperature diagram for sulphides of metals,[33,34] indicates that Cu_2S, ZnS, MnS, Al_2S_3, Na_2S, K_2S, Li_2S, MgS, BaS, SrS, CaS and CeS are more stable than FeS, Fig. 1. As it can be seen from Table I, ZnS is volatile and can be ignored, as can MgS, BaS, SrS, CaS and CeS due to their very high melting points. Finally MnS is soluble in molten metal. This leaves us with Al_2S_3, Na_2S, K_2S and Li_2S. Among these Na_2S has the best prospect for use because of its higher melting point compared to the other three.

The above argument is given for refining of ferrous metals with a single sulphide slag alone. Mixtures of sulphides can be developed with desulphurization and decopperization potentials. By employing the non-volatile solute effect, the boiling point of the sulphide can be elevated by dissolving a solute which is non-volatile.

3.2 Properties of Components of Slag/Metal System

3.2.1 Properties of sodium sulphide

Anhydrous sodium sulphide is a white crystalline solid, having a density of 1.856 g/cc at 20°C.[35] It has a fluorite-type ionic lattice with a lattice constant 6.526 A°, in which the Na-S distance is 2.83 A°.[36] Its melting point has been given as 1180 ± 10°C[37] or 1200°C,[38] both these values being higher than those previously reported.[39] The boiling point is estimated to be above 1600°C.[40]

The heat of formation from the solid elements at 25°C has been

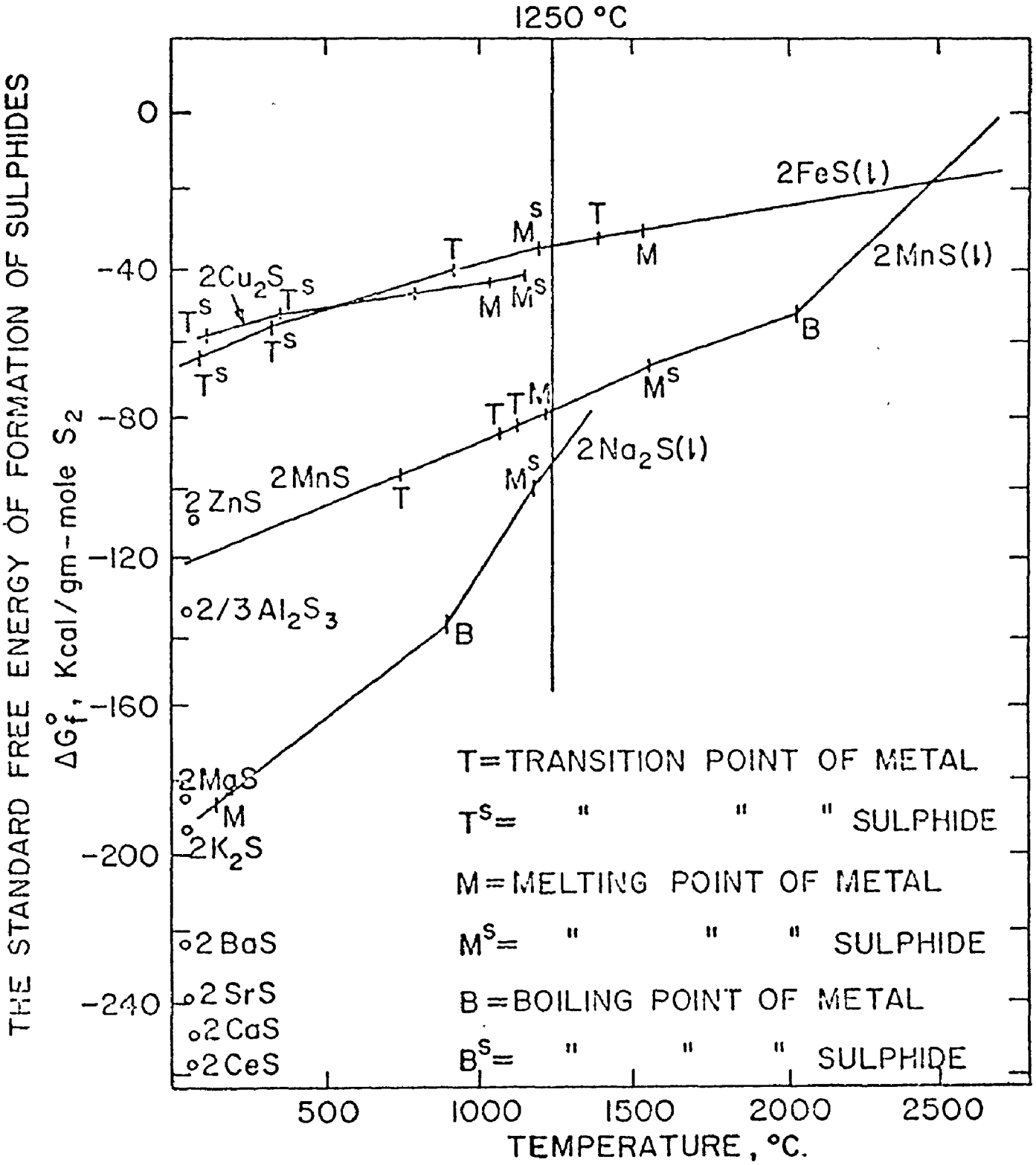

Fig. 1: The free energy-temperature diagram of sulphides

given as -89200 cal/mole.[41,42] The entropy of solid sodium sulphide at 25°C is reported as 23.6 g.cal/°C/mole.[33] The free energy change for the reaction

$$2Na(s,\ l,\ or\ v) + \frac{1}{2} S_2(v) \rightleftharpoons Na_2S(s\ or\ l) \qquad (3.1)$$

is tabulated in the range 298° - 3000°K by JANAF Thermochemical Tables[43] and it has been reproduced in Table II.

Sodium sulphide dissolves in water with the evolution of 15.6 K.cal/mole in the formation of a dilute solution.[44] As a result both the anhydrous salt and its hydrates are deliquescent.

Sodium sulphide is readily oxidized either dry or in solution. Although dry sodium sulphide is unattacked by dry air or oxygen at moderate temperatures, it is rapidly oxidized in the presence of a small amount of water. At temperatures of about 160 - 250°C, the product is mainly sodium sulphite, with smaller quantities of thiosulphate. At temperatures above 250°C, sodium sulphate is also formed. During storage, sodium sulphide oxidizes in contact with air, forming largely thiosulphate and deliquescing.[45]

Powdered mixtures of Na_2S and iron react at 1250°C and the reaction is accompanied with the evolution of sodium vapour. At 1350°C, with more vaporization of sodium, the sodium flames become 5 cm long. Reaction subsides with time but increases with increasing temperature. The final product is a mixture of iron sulphide and sodium sulphide melt and residual solid iron powder.[26]

Fused sodium sulphide attacks metals, including silver, gold and

Properties of sodium sulphide

Appearance: White crystalline solid, deliquescent

Molecular wt: 78.048

Melting point: 1180°C ± 10°C

ΔH_m(melting) = 1600 cal/gm-mole

$$2Na(s,l,g) + \frac{1}{2} S_2(g) \longrightarrow Na_2S(s,l)$$

Metal(Na), M.P. = 371°K $\quad \Delta H_m$ = 622 cal/gm-atom

B.P. = 1163°K $\quad \Delta H_v$ = 21280 cal/gm-atom

Sulphide M.P. = 1453°K $\quad \Delta H_m$ = 1600 cal/gm-mole

Structure: CaF_2 type cubic

Density: 1.856 g/cc

Boiling point: Above 1600°C

Solubility: 15.4 grams per 100 cc of cold water

57.2 grams per 100 cc of hot water

TABLE II: JANAF thermochemical table

DISODIUM SULFIDE (Na_2S) (Liquid)

Mol. Wt. = 78.048 $H^\circ_{f\ 298.15}$ = [-87.870] kcal.mole^{-1} $S^\circ_{298.15}$ = [24.136] cal.deg.$^{-1}$ mole^{-1}

T_m = 1223°K ΔH_m = 16 Kcal.mole^{-1}

T_m and ΔH_m are from National Bureau of Standards Circular 500 (1952).
Other data estimated

	cal.mole^{-1}deg.$^{-1}$			kcal.mole^{-1}			
T, °K.	C_p°	S°	$-(F^\circ-H^\circ_{298})/T$	$H^\circ-H^\circ_{298}$	ΔH_f°	ΔF_f°	Log K_p
0							
100							
200							
298	17.618	24.136	24.136	.000	-87.870	-85.458	62.639
300	17.666	24.245	24.136	.033	-87.871	-85.441	62.241
400	19.445	29.603	24.855	1.899	-89.792	-84.494	46.163
500	20.341	34.048	26.262	3.893	-90.218	-83.117	36.329
600	20.848	37.806	27.881	5.955	-90.455	-81.672	29.747
700	21.162	41.045	29.536	8.056	-90.566	-80.176	25.031
800	21.368	43.885	31.155	10.183	-103.654	-79.956	21.842
900	21.511	46.410	32.713	12.328	-103.327	-77.012	18.700
1000	21.614	48.682	34.198	14.484	-102.992	-74.106	16.195
1100	21.690	50.746	35.610	16.650	-102.661	-71.238	14.153
1200	21.748	52.636	36.951	18.822	-148.813	-67.480	12.289
1300	21.794	54.379	38.226	20.999	-148.075	-60.730	10.209
1400	21.830	55.995	39.438	23.180	-147.335	-54.040	8.436
1500	21.860	57.502	40.592	25.365	-146.592	-47.404	6.906

continued

Table II: JANAF thermochemical table (continued)

	cal.mole^{-1}deg.$^{-1}$			kcal.mole^{-1}			
T, °K.	C_p°	S°	$-(F^\circ-H^\circ_{298})/T$	$H^\circ-H^\circ_{298}$	ΔH_f°	ΔF_f°	Log K_p
1600	21.854	58.914	41.694	27.552	-145.847	-40.813	5.575
1700	21.904	60.241	42.746	29.741	-145.099	-34.271	4.406
1800	21.920	61.494	43.753	31.933	-144.351	-27.774	3.372
1900	21.934	62.679	44.718	34.125	-143.603	-21.315	2.452
2000	21.947	63.804	45.645	36.319	-142.856	-14.901	1.628
2100	21.956	64.876	46.535	38.515	-142.106	- 8.524	.887
2200	21.965	65.897	47.392	40.711	-141.358	- 2.178	.216
2300	21.973	66.874	48.218	42.908	-140.610	4.129	- .392
2400	21.980	67.809	49.015	45.105	-139.864	10.410	- .948
2500	21.987	68.706	49.785	47.304	-139.116	16.653	- 1.456
2600	21.993	69.569	50.529	49.503	-138.373	22.871	- 1.922
2700	21.998	70.399	51.250	51.702	-137.632	29.056	- 2.352
2800	22.002	71.199	51.948	53.902	-136.895	35.213	- 2.748
2900	22.006	71.971	52.625	56.103	-136.159	41.352	- 3.116
3000	22.009	72.717	53.283	58.303	-135.431	47.461	- 3.457

continued

Table II: JANAF thermochemical table (continued)

DISODIUM SULFIDE (Na_2S) (Solid)

Mol. Wt. = 78.048 $H^\circ_{f\ 298.15} = -89$ kcal.mole^{-1} $S^\circ_{298.15} = 23.4$ cal.deg.$^{-1}$mole^{-1}

$T_m = 1223°K$ $\Delta H_m = 16$ kcal.mole^{-1}

	Cal.mole^{-1}deg.$^{-1}$			kcal.mole^{-1}			
T, °K.	C_p°	S°	$-(F^\circ-H^\circ_{298})/T$	$H^\circ-H^\circ_{298}$	ΔH°_f	ΔF°_f	Log K_p
0							
100							
200							
298	18.990	23.400	23.400	.000	-89.000	-86.368	63.307
300	19.000	23.517	23.400	.035	-88.999	-86.351	62.903
400	19.300	29.025	24.149	1.950	-90.871	-85.342	46.627
500	19.600	33.363	25.573	3.895	-91.346	-83.903	36.672
600	19.900	36.964	27.180	5.870	-91.670	-82.381	30.006
700	20.200	40.054	28.803	7.875	-91.877	-80.793	25.224
800	20.500	42.771	30.383	9.910	-105.057	-80.468	21.982
900	20.800	45.202	31.897	11.975	-104.810	-77.408	18.796
1000	21.100	47.409	33.339	14.070	-104.536	-74.377	16.254
1100	21.400	49.435	34.712	16.195	-104.246	-71.380	14.181
1200	21.700	51.309	36.018	18.350	-150.415	-67.489	12.291
1300	22.000	53.058	37.262	20.535	-149.669	-60.607	10.189
1400	22.300	54.700	38.449	22.750	-148.895	-53.787	8.396
1500	22.600	56.248	39.585	24.995	-148.092	-47.022	6.851
1600	22.900	57.716	40.673	27.270	-147.259	-40.309	5.506
1700	23.200	59.114	41.717	29.575	-146.395	-33.651	4.326
1800	23.500	60.448	42.721	31.910	-145.504	-27.045	3.284
1900	23.800	61.727	43.687	34.275	-144.583	-20.486	2.356
2000	24.100	62.955	44.620	36.670	-143.635	-13.982	1.528

platinum, but it does not attack graphite. Silica dissolves in fused sodium sulphide or fused mixtures containing sodium sulphide. Thiosilicates of the type $SiO_2.nNa_2S$ are said to be formed. Al_2O_3 does not react with Na_2S. If there is any reaction, it is due to impurities present.(44)

Several compounds of Na and S exist. The monosulphide Na_2S is the most stable sulphide at high temperatures. Manufactured sodium sulphide is often discoloured yellow, pink, or red depending on the degree of purity or non-stoichiometry. The yellow colour results from polysulphide content and the red colour from iron content.(40)

Fused mixtures of sodium sulphide with sodium sulphate and sodium carbonate have been studied. Sodium sulphide forms liquid mixtures with various other metallic sulphides, e.g., ferrous, cuprous, and plumbous, but zinc sulphide does not dissolve in the fused salt. With cuprous sulphide, a compound $Cu_2S.Na_2S$ is formed in the liquid phase with a free energy of formation of 7 K.cal/mole.(24)

3.2.2 Properties of the Fe-C-S, Cu-C-S and Fe-Cu-C ternary systems

The equilibrium diagrams for binary Fe-C, Fe-S, Cu-C and Cu-S systems are reported in Metals Handbook(46) and also by Hansen.(47) The effect of sulphur on the solubility of graphite in iron has been investigated by E. Turkdogan and A. Hancock.(48) Their results are summarized in Fig. 2 where the atom fraction of carbon at saturation is plotted against the atom fraction of sulphur. The figure shows that the solubility of carbon in iron is reduced by dissolved sulphur. The above named

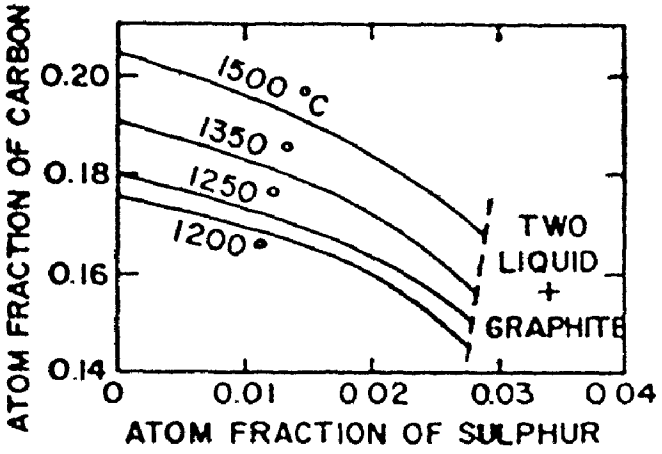

Fig. 2: Effect of sulphur on solubility of graphite in molten iron[48]

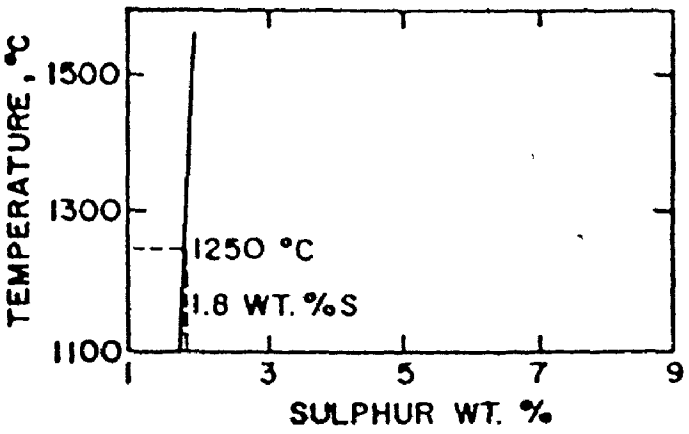

Fig. 3: Composition-temperature relationship in carbon-rich layer of two immiscible liquids in iron-sulphur-carbon melts[48]

authors also investigated the miscibility gap in carbon-saturated iron-carbon-sulphur melts. Figure 3 shows the relationship between the temperature and composition of the carbon-rich layer.

Data on the solubility of carbon in molten copper is represented in Fig. 4. The solubility, expressed in wt%C, was determined to be about 0.0001 at 1100°C, 0.00015 at 1300°C, 0.0005 at 1500°C and 0.003 at 1700°C. On the other hand, the change of solubility of sulphur in liquid copper with temperature can be seen in Fig. 5. The effect of a small amount of carbon on the solubility of sulphur is expected to be negligible.

There is also some reported information on the ternary Fe-Cu-C system. Investigations have shown that melts in this system separate into two layers. The results of these studies are summarized in Fig. 6, in which the phase boundary between single and double liquid phases is plotted along with the compositions of coexisting layers found by S. Smith and E. Palmer[49] at 1550°C.

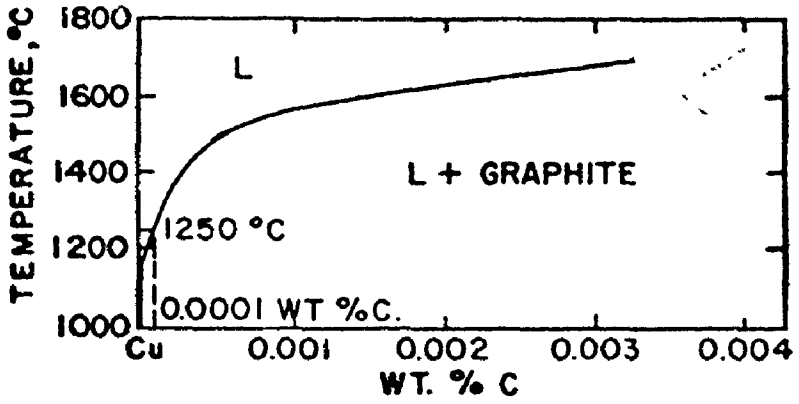

Fig. 4: Binary phase diagram of Cu - C system[46]

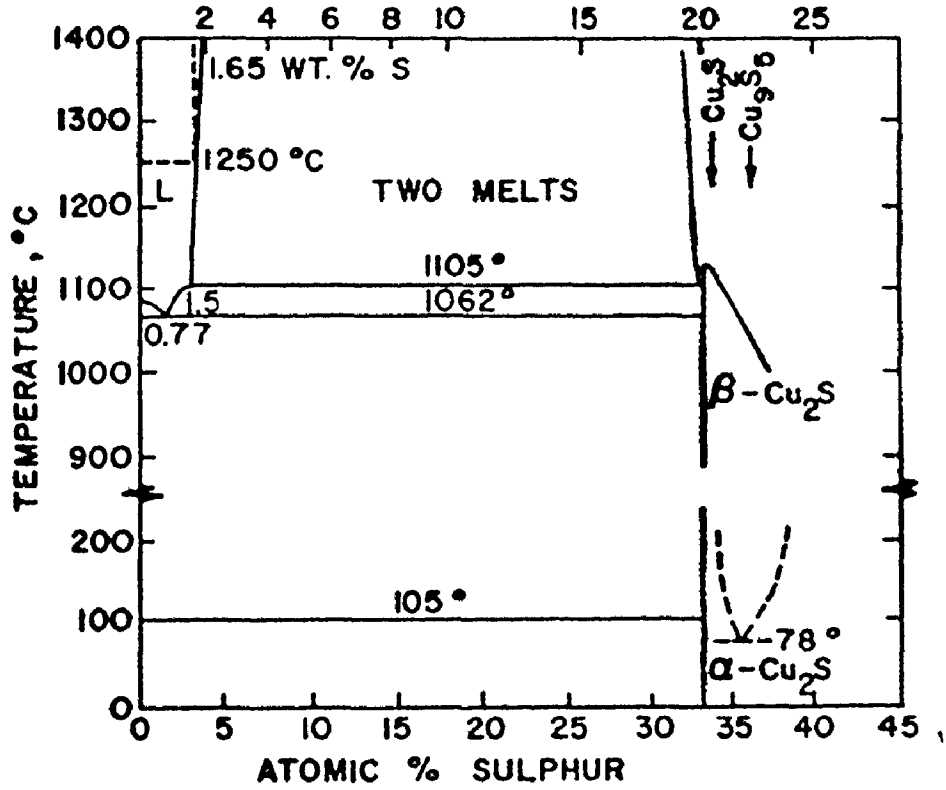

Fig. 5: Phase diagram of Cu - S system[47]

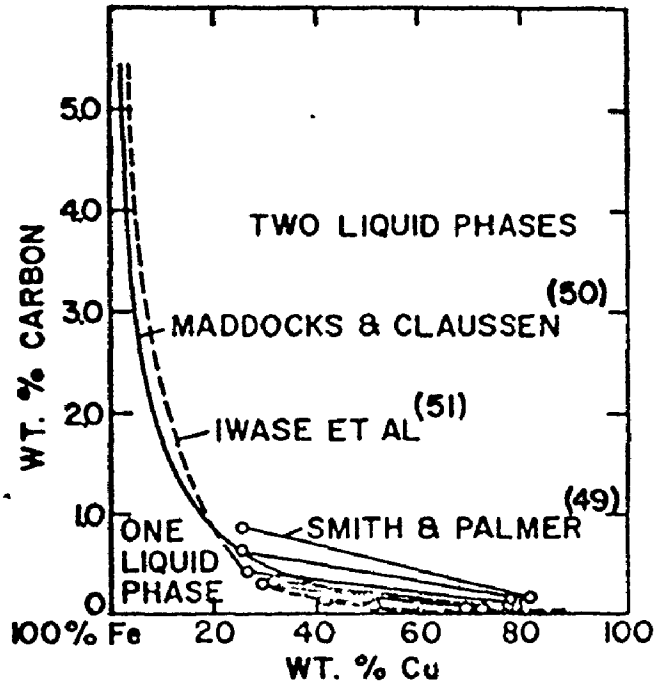

Fig. 6: Phase boundaries in the Fe - Cu - C system at 1550°C

CHAPTER 4

EXPERIMENTAL APPARATUS AND PROCEDURE

4.1 Introduction

For the purpose of study of the present system, it was necessary to control the temperature, reaction time, degree of vacuum and gas flow rate. Resistance furnace heating with a double crucible arrangement was the most suitable for a majority of investigations, since the reaction could be studied accurately over a wide range of temperatures and flow rates. A further advantage was that the slag and metal could be brought together at the desired moment. Thus, uncertainties introduced by cold additions of slag or metal were eliminated and a true zero time was achieved.

In addition to the double crucible experiments, studies were done using capillaries to find out the effect of stirring within the metal phase. Experiments with closed-systemshelped to understand the reversibility of the reaction. Details of the experimental apparatus and procedure used are given in detail in this chapter.

4.2 Furnace Assembly

The experimental work for this project was performed in a vertically wound molybdenum resistance furnace, Fig. 7. The alumina furnace tube, 3" O.D. x 2-3/4" I.D. x 27-1/2" in length, was wound, over a length of 13 inches with 0.050 inches diameter high purity molybdenum wire. The molybdenum resistance wire was wound on the tube by means of a lathe, starting 6 inches

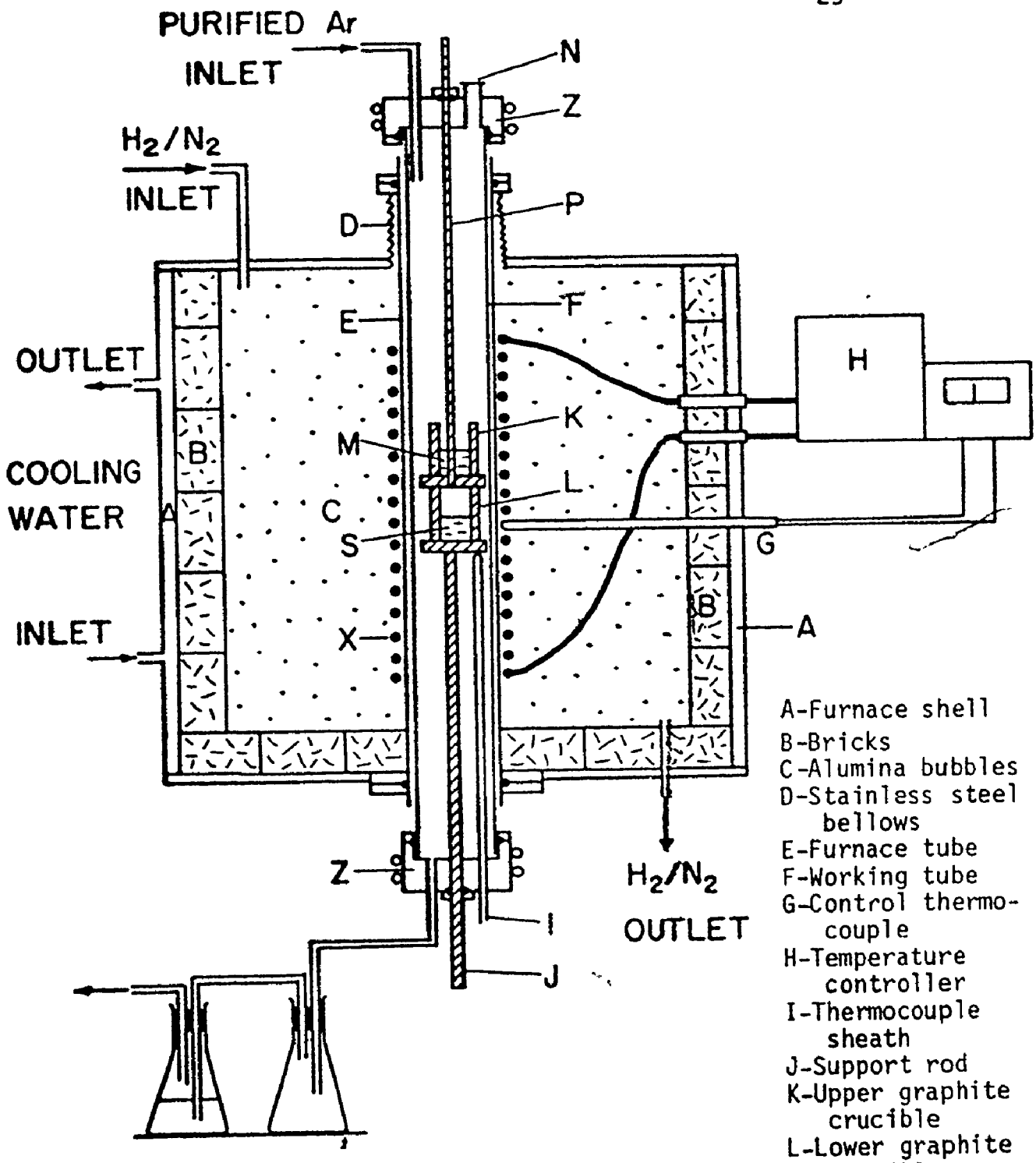

A-Furnace shell
B-Bricks
C-Alumina bubbles
D-Stainless steel bellows
E-Furnace tube
F-Working tube
G-Control thermocouple
H-Temperature controller
I-Thermocouple sheath
J-Support rod
K-Upper graphite crucible
L-Lower graphite crucible
M-Metal phase
N-Sighting hole
P-Graphite stopper rod
S-Slag phase
X-Molybdenum winding
Z-Brass caps

Fig. 7: The furnace and crucible assembly (not to scale)

from the botton end, and using 10 turns per inch for 2 inches, 9 turns per inch for 2-1/2 inches, 8 turns per inch for 4 inches, 9 turns per inch for 2-1/2 inches, and 10 turns per inch for 2 inches. In this manner, a flat temperature profile was enhanced by adding more heat to the ends of the winding. The molybdenum wire was completely covered by a thick layer of alumdum cement. The electrical extension leads consisted of molybdenum wire wound in triplicate to reduce the resistance and were connected to the power supply by connectors passing through the double walled furnace body.

The tube was centrally located in a bricklined cylindrical steel shell. The space between the inside layer of insulating brick and the furnace tube was filled with alumina bubbles ranging in size from approximately 1/64" to 1/8".

The furnace had a double walled outer jacket which permitted water cooling so that the outer wall was kept essentially at room temperature. The removable top plate was fitted with a water cooled "O" ring, for gas tightness, with the furnace body. The top plate was also fitted with 8" long, stainless steel bellows, in order to allow expansion and contraction of the refractory furnace tube. A gas entrance was located on the top plate to allow the introduction of the protective furnace gas, which was a 5% H_2 - 95% N_2 reducing gas mixture. The bottom plate of the furnace was welded to the furnace body and had a water cooled "O" ring assembly to maintain gas tightness on the furnace tube. The furnace gas outlet was located on the bottom plate.

The working tube was also of recrystallised alumina with dimensions

31" long, 2-1/2" O.D., 2-1/4" I.D., and was fitted at the top and the bottom with two gas-tight water-cooled brass caps. The bottom cap was fitted with a gas outlet and a swagelock opening to allow gas-tight entry of an alumina thermocouple protection sheath into the working tube. The bottom cap also had a centrally located swagelock for introducing the graphite crucible into the furnace. The top cap was equipped with a sight hole for continuous observation of the melt, a centrally located swagelock for introducing the upper crucible as well as for taking samples of the melt and a gas inlet for introduction of the inert argon gas. The swagelock fittings contained teflon ferrules, which maintained a gas tight seal on graphite support rods and allowed raising or lowering of the crucibles.

4.3 Temperature Control

Power to the furnace was supplied through a proportional power controller (Barber-Coleman Series 621) driven by a null balance millivoltmeter controller (Barber-Coleman Series 520) which received the output from the control thermocouple, which was placed inside a thin recrystallized alumina sheath located at the side of the furnace shell and extending up to the hot zone of the furnace tube.

The temperature profile of the furnace was determined with a vertical travelling thermocouple while there was a steady flow of argon through the reaction tube. The temperature profile obtained at 1250°C is shown in Fig. 8. The temperature variation at the hot zone of the furnace was ± 1°C over 1 inch and ± 3°C over 2 inches. The estimated error in temperature measurements was ± 5°C.

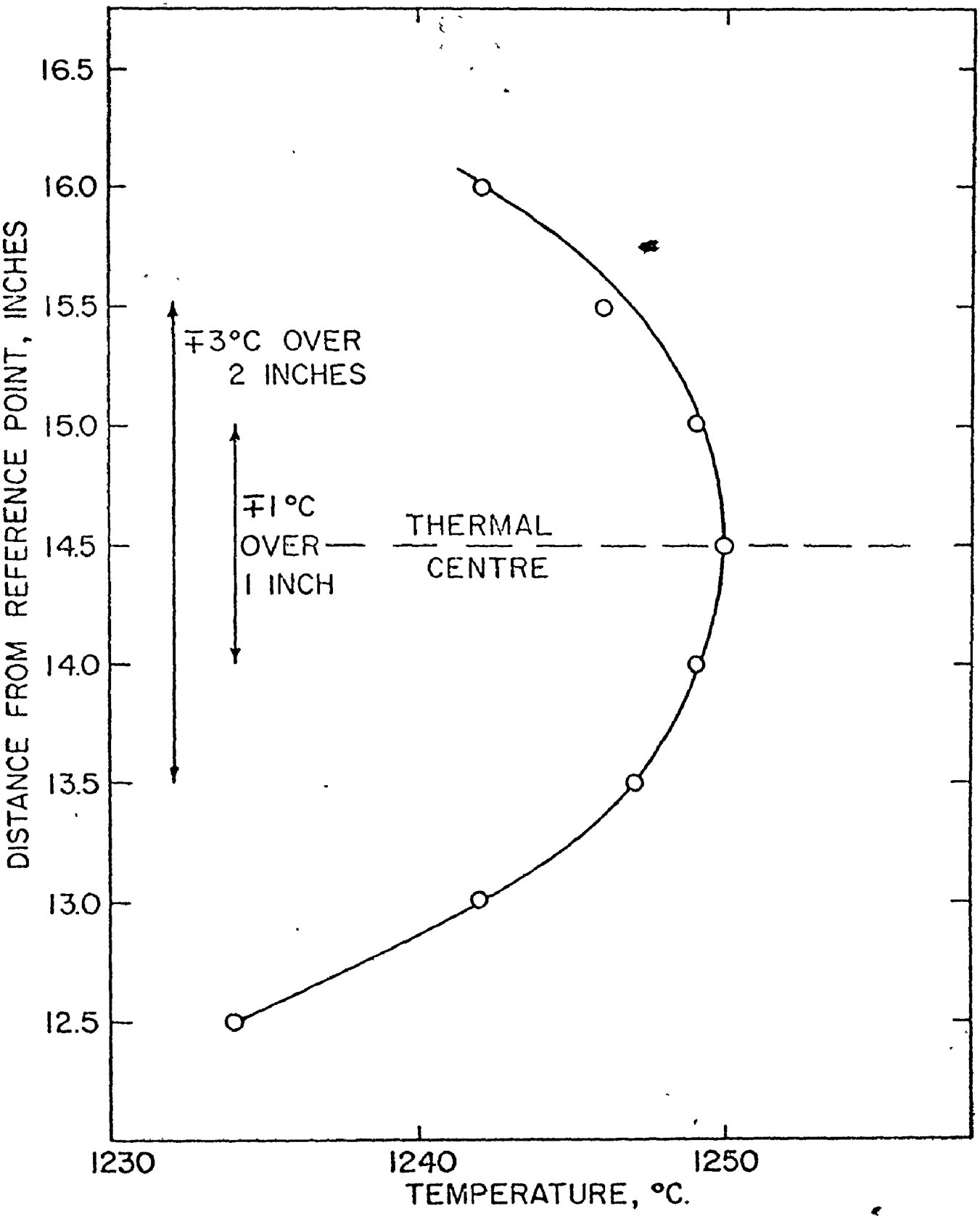

Fig. 8: Temperature profile of the resistance furnace at 1250°C

4.4 Furnace Atmosphere

The furnace atmosphere was controlled by 99.998% argon which was dried over silica gel and magnesium perchlorate and deoxidized over titanium strips at 875°C prior to admission to the furnace working tube. The flow rate of purified argon gas was kept constant during the experiments at 75 cc s.t.p./min. It was changed only when the effect of flow rate of argon on the rate of reaction was being studied.

4.5 Experimental Set-up

4.5.1 Thermal stability of Na_2S

For studying the high temperature stability of sodium sulphide, dehydrated sodium sulphide was heated in a graphite crucible machined to the same dimensions as those used in the slag/metal reactions, Fig. 9. The crucible was 1-1/2" high and 3/4" O.D. with a 5/64" wall thickness.

4.5.2 Double crucible experiments

The crucible assembly consisted of two graphite crucibles placed over one another, Fig. 10. Metal was melted in the upper graphite crucible and slag in the lower one. The upper crucible was provided with a graphite rod stopper which could be manipulated using the sighting hole. The lower graphite crucible was supported by a graphite rod which passed through the swagelock at the base of the reaction tube, by means of which the slag carrying graphite crucible could be moved up and down.

The crucibles were machined from Union Carbide CS grade graphite rods to fixed dimensions. In the preliminary experiments, the dimensions

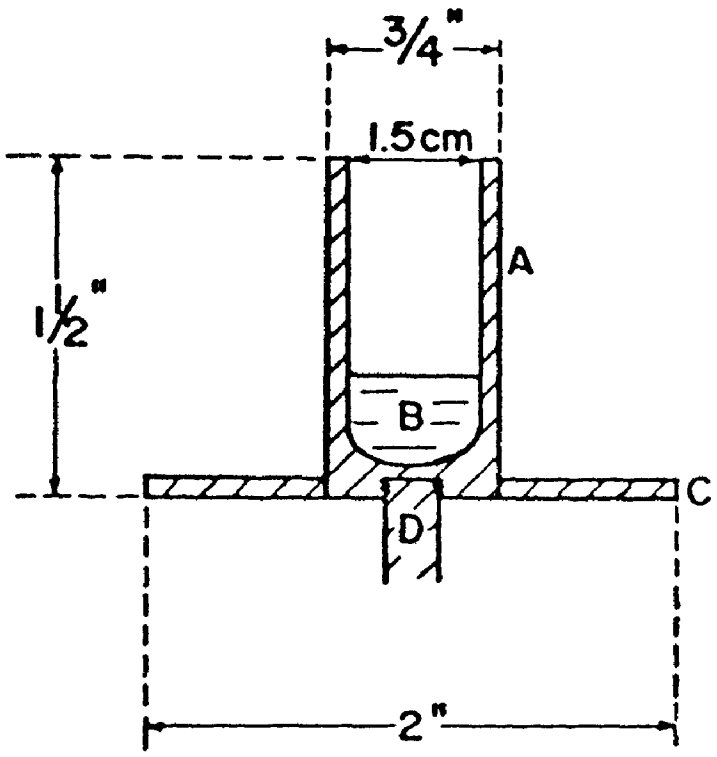

A – GRAPHITE CRUCIBLE
B – DEHYDRATED Na_2S SLAG
C – GRAPHITE DISC
D – 1/4" GRAPHITE SUPPORT ROD

Fig. 9: Crucible assembly for studying the thermal stability of dehydrated Na_2S

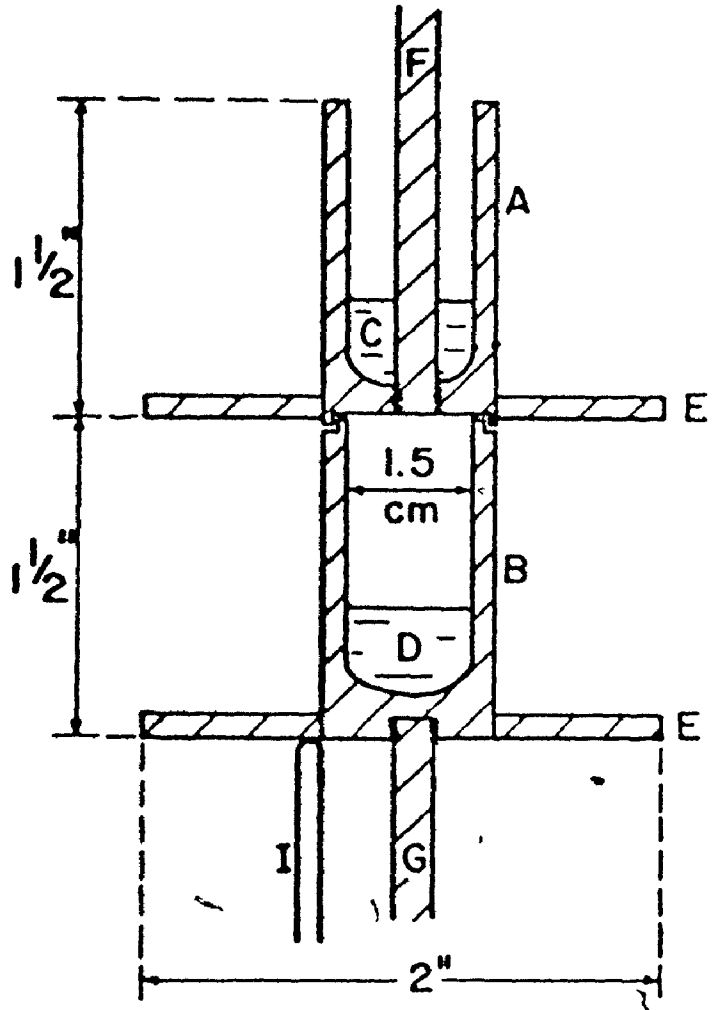

A – UPPER GRAPHITE CRUCIBLE
B – LOWER GRAPHITE CRUCIBLE
C – METAL PHASE
D – DEHYDRATED Na_2S SLAG
E – GRAPHITE DISCS
F – 1/4" GRAPHITE STOPPER ROD
G – 1/4" GRAPHITE SUPPORT ROD
I – Pt/Pt-13 % Rh THERMOCOUPLE

Fig. 10: Crucible assembly for the double-crucible slag/metal experiments

were 1-1/4" I.D., 1-3/4" O.D., 3" in length. However, in subsequent small crucible experiments, the dimensions were reduced to 19/32" I.D. (1.5 cm), 3/4" O.D., 1-1/2" in length. The graphite discs which were screwed onto the crucibles allowed crucibles to stand straight and acted as radiation shields. The temperature measuring thermocouple was introduced to the furnace through the opening in the bottom cap and was positioned such that its tip was located in the base of the lower graphite crucible.

4.5.3 Capillary experiments

(i) Metal Diffusion: The arrangement of liquid-liquid diffusion couple used for the determination of diffusivity of sulphur in carbon-saturated iron at 1250°C is shown in Fig. 11. The large graphite crucible with a graphite lid contained the Fe-C-0.77wt%S alloy of lower density. The Fe-C-0.17wt%S alloy of higher density was contained in the 2-3 mm diameter graphite capillaries. The graphite capillaries were screwed onto a graphite disc which could be immersed into the molten metal pool by lowering the graphite immersion rod.

The graphite lid served two purposes. It removed the excessive capillary sample resulting from thermal expansion and fusion before the holder was dipped into the reservoir melt; i.e., metal pool, and also insured the separation of the reservoir melt from the capillary sample when the holder was taken out of the reservoir.

(ii) Slag/metal reactions: The overall arrangement used was similar to the double crucible set-up but the lower crucible was now replaced by a capillary filled with the metal phase. The slag phase was

A-Graphite crucible
B-Graphite base
C-Capillaries
D-Metal pool
E-Graphite lid
F-1/4" graphite immersion rod
G-Graphite support rod
H-Capillary metal
Fe - C - 0.17wt%S
I-Graphite capillary material

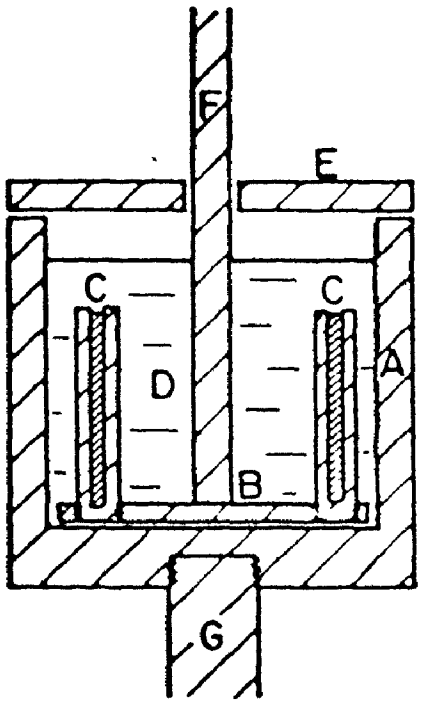

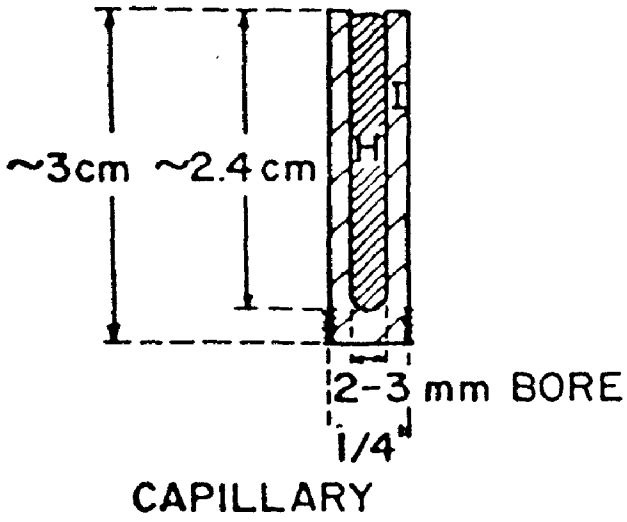

Fig. 11: Crucible assembly for the capillary experiments: Metal capillary-metal pool system

melted in the upper-graphite crucible, Fig. 12.

Various capillary shapes, materials and dimensions were tried to obtain meaningful results. Graphite, alumina and mullite capillaries with 1 to 3 mm bore, similar to those used in metal diffusion experiments, failed due to the penetration of the slag phase between the capillary wall and the metal phase. The most satisfactory results were obtained with double metallic capillaries in graphite. The inner capillary was 1 to 1.5 mm in diameter and the shorter, outer capillary had a maximum diameter of 4.25 mm. The inner and outer metallic capillaries were connected on top as shown in Fig. 12, so any slag penetration between the graphite and the metal affected only the outer capillary. For chemical analysis only the inner capillary metal was taken. Although, in all cases the slag wetted the graphite capillary material resulting in penetration of slag between the graphite capillary wall and the outer capillary metal, the effect of this slag penetration on the inner capillary was small. Another problem associated with this double crucible type of set-up was that the slag had to be poured onto the top of the capillary metal from the upper graphite crucible. But the slag did not run down completely due to sticking to the graphite crucible. So the initial slag weight could not be controlled exactly under the present set-up. In the absence of stirring within the metal phase, these slag/metal capillary experiments allowed determination of sulphur gradients in the metal phase.

(iii) Vacuum induction melting unit for filling of capillaries: A vacuum induction melting unit was constructed for melting and filling of graphite capillaries with Fe-C-S alloys under vacuum. Figure 13 shows

A-Upper graphite crucible
B-Graphite container
C-Graphite capillary material
D-Capillary metal Fe - C - 0.215wt%S
E-Na_2S slag
F-1/4" graphite stopper rod
G-Graphite discs
H-1/4" graphite support rod

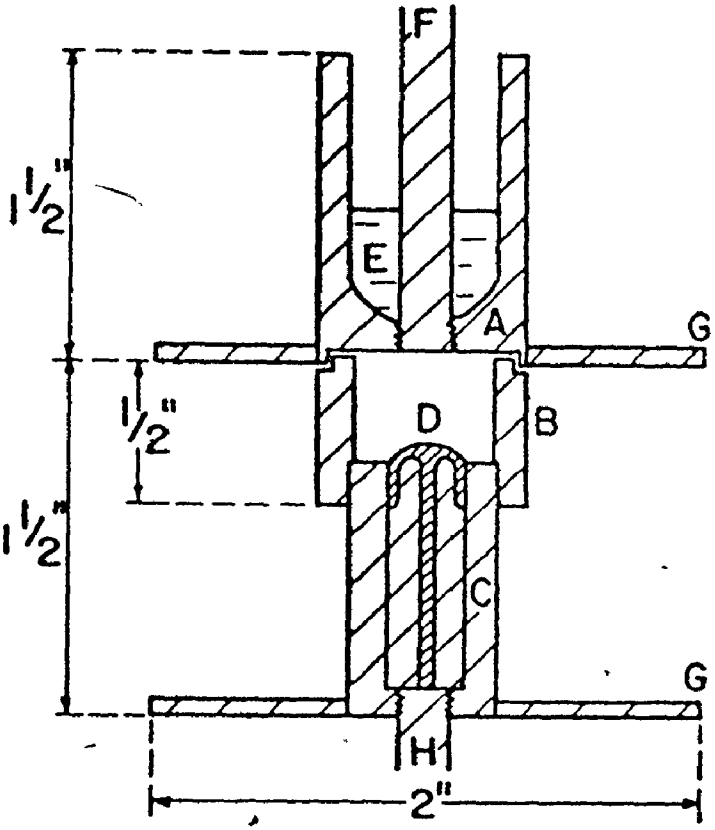

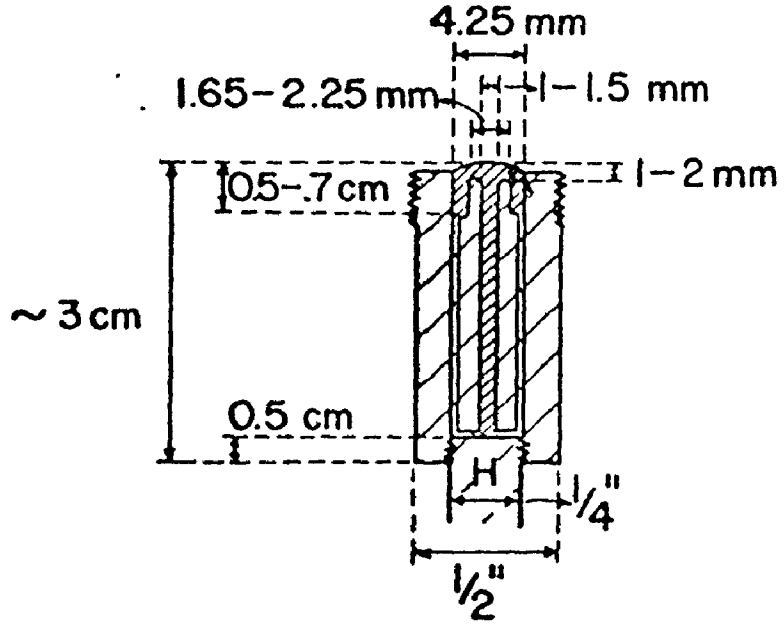

Fig. 12: Crucible assembly for the capillary experiments: slag/metal system

A-Large graphite crucible
B-Copper heating coil
C-Capillaries
D-Metal pool
E-Vycor tubing
F-1/4" graphite immersion rod
G-Al_2O_3 support tube
H-Vacuum pump
I-Brass cap
J-Thermocouple
K-Argon inlet
L-Valve
P-Pressure gauge

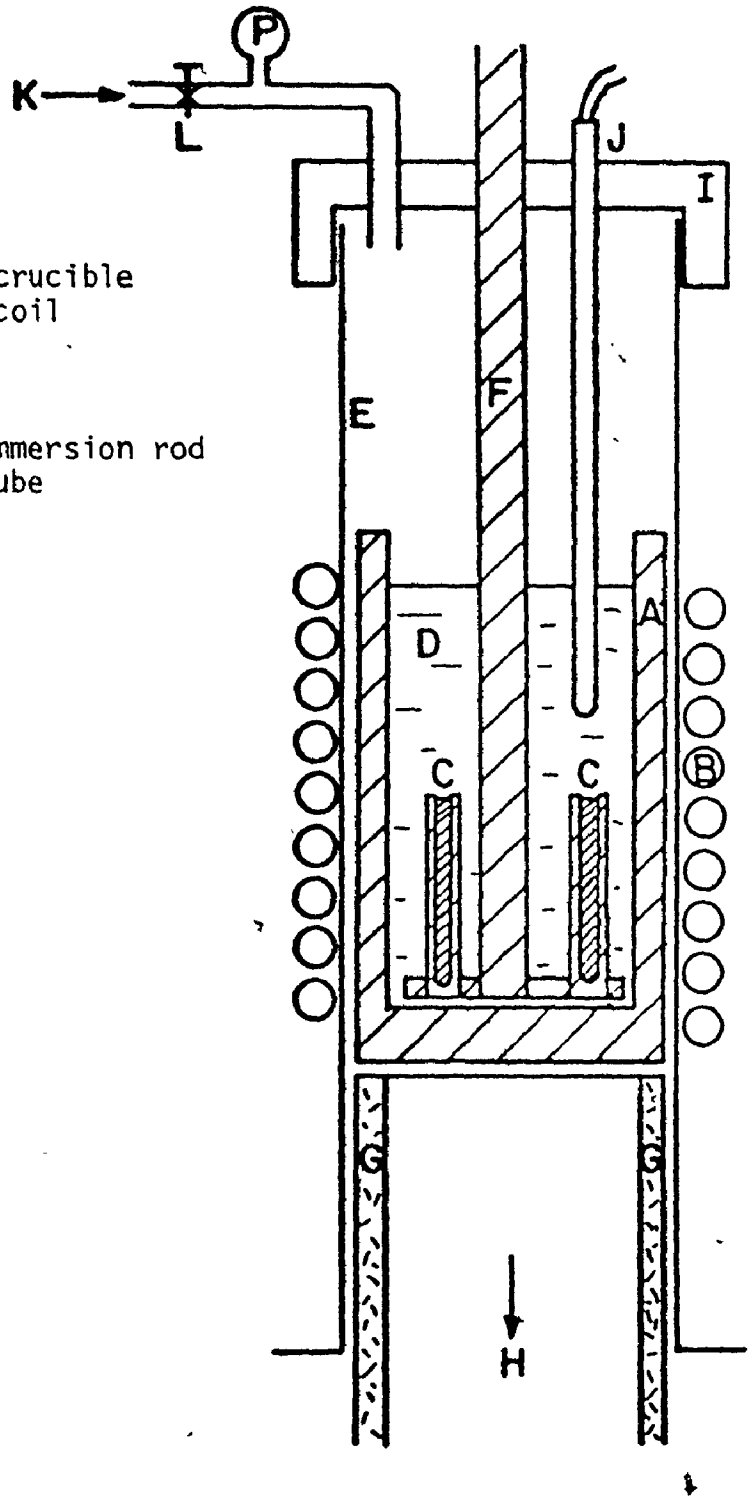

Fig. 13: Vacuum induction melting unit for filling capillaries.

the unit used for this purpose. The heating coil consisted of a 1/4" copper tubing wound over a length of 4 inches with 9 turns around a 18" x 2-1/4" O.D. x 2" I.D. vycor tube, open at both ends, the bottom end of which was connected to the vacuum unit consisting of a rotary pump and a diffusion pump. The brass cap for the top was fitted with a gas entrance hole, a swagelock for the thermocouple and a centrally located swagelock fitting to allow for raising and lowering of capillaries into the melt. The temperature was controlled by manual adjustment of the high frequency (300 Kc) power supply. This unit was utilized for filling single as well as double metallic capillaries used in diffusion and slag/metal reactions, respectively.

4.5.4 Closed-system experiments

To establish the reversibility of the reaction under study, a different kind of crucible combination was necessary due to requirements of gas tightness. Figure 14 shows a typical set-up for the experiments. It consisted of an outermost steel crucible with a lid which could be welded on to the bottom part and two inner crucibles. The innermost crucible was graphite which was machined to the same dimensions as those used in the slag/metal reactions. The recrystallized alumina crucible in between the two crucibles was for breaking the contact between graphite and steel. The innermost crucible contained the slag and metal phases. With this type of closed-system, it was possible to have equilibrium or near equilibrium state which in principle could not be obtained in the open-system, i.e., double-crucible experiments under flowing argon atmosphere.

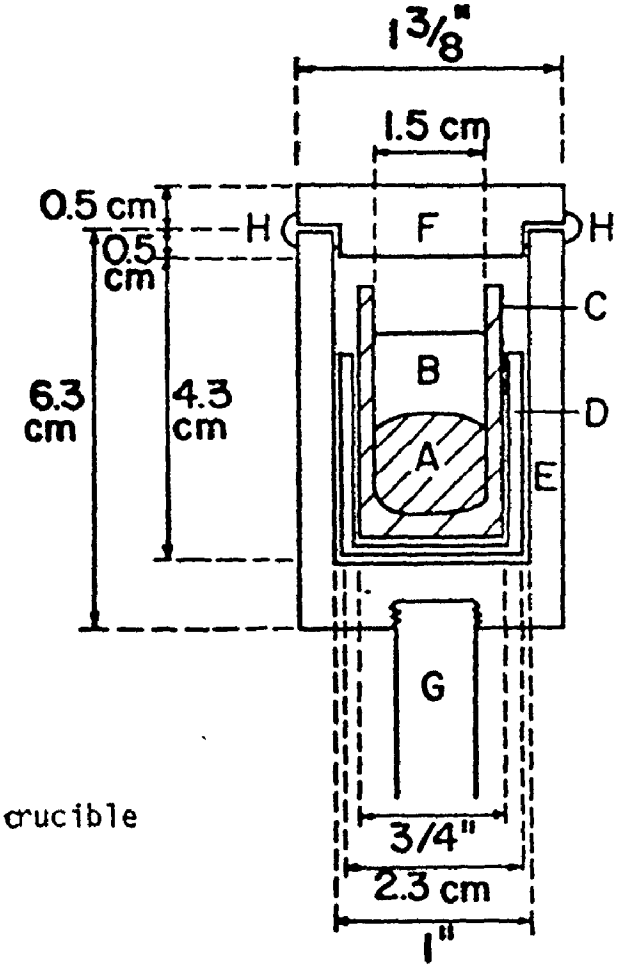

A-Metal phase
B-Slag phase
C-Graphite crucible
D-Recrystallized Al_2O_3 crucible
E-Steel crucible
F-Steel lid
G-Steel support rod
H-Welds

Fig. 14: Crucible assembly for the closed-system experiments

4.6 Preparation of Materials

4.6.1 Preparation of anhydrous sodium sulphide

Analytical reagent grade $Na_2S.9H_2O$ (typical analysis of this crystalline material is given in Table III) was used for preparing anhydrous sodium sulphide. Although there are several methods for obtaining anhydrous sodium sulphide, the most recent method developed by N.I. Kopylov[52] is the only way of obtaining pure anhydrous Na_2S by direct, single stage, low temperature drying. In this method, the crystalline $Na_2S.9H_2O$ was heated rapidly to 50-60°C at a residual pressure of 30-35 mm Hg, then the furnace temperature was raised by 15°C per hour to 150-160°C under vacuum and the sulphide held at that temperature for at least twelve hours. The apparatus used for the dehydration of $Na_2S.9H_2O$ is shown in Fig. 15. Figure 16 shows the equilibrium diagram of the Na_2S- H_2O system.

Although the anhydrous sulphide produced was chemically pure, it picked up water from the atmosphere during storage and handling. To avoid this, the sulphide was heated to 1250°C in a large graphite crucible under argon atmosphere and suction samples of the slag were taken with 3mm silica tubes. The firing of the sulphide also made sure that any oxide, thiosulfate, or sulphate that might have been present, was reduced by graphite resulting in a pure anhydrous sodium sulphide. The quenching of the slag was done in argon which prevented oxidation of the slag. As a precaution slag tips were discarded before use.

Anhydrous sodium sulphide so obtained was left in their silica tubes until use. The slag-containing silica tubes were then placed in

TABLE III: Chemical composition of $Na_2S.9H_2O$ crystals used in the preparation of dehydrated Na_2S

Certified A.C.S. (Fisher Scientific Company)

Reagent Grade

$Na_2S.9H_2O$	99.9%
Insoluble	0.002%
Ammonium NH_4	0.001%
Sulfite, thiosulfate(as SO_2)	0.05%
Iron	P.T.

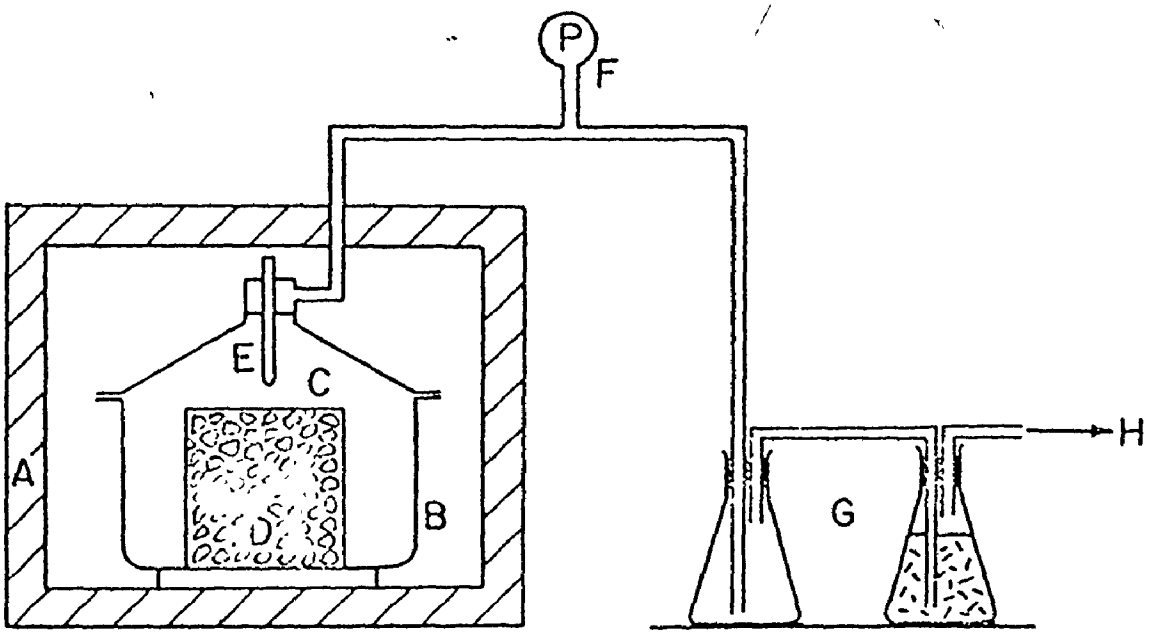

A – FURNACE
B – DESICCATOR
C – BEAKER
D – CRYSTALLINE $Na_2S \cdot 9H_2O$
E – THERMOMETER
F – PRESSURE GAUGE
G – WATER ABSORPTION SYSTEM
H – TO VACUUM PUMP

Fig. 15: Diagram of the apparatus used for the dehydration of $Na_2S \cdot 9H_2O$

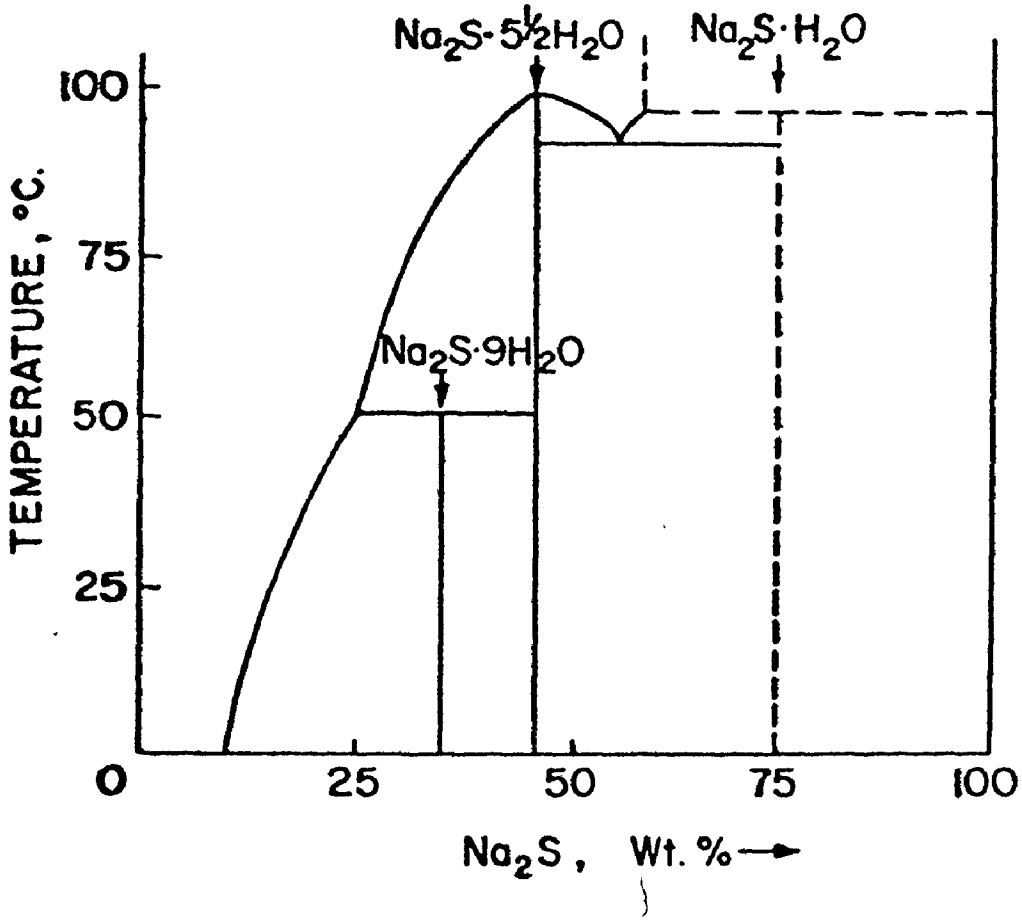

Fig. 16: Equilibrium diagram of the Na_2S - H_2O system[52]

air-tight bottles to avoid oxidation and deterioration of the sulphide slag. The handling of the final product was kept to a minimum because of its hygroscopic nature.

Chemical analysis of the sulphide, so produced, showed only slight departure from the stoichiometric composition. Average composition of the dehydrated sodium sulphide was 41.2wt%S, 58.55wt%Na and 0.25wt% impurities such as oxygen, graphite, etc.(stoichiometric composition: 41.08 %S and 58.92%Na).

4.6.2 Preparation of carbon-saturated alloys

Carbon-saturated alloys were prepared by melting electrolytic iron and copper-shot in graphite crucibles. The compositions of the raw materials used are given in Tables IV and V. Later, the melt was allowed to saturate with carbon at the desired temperature. Any alloying additions such as FeS, Fe-Mn, Cu or Si were made to the saturated melts in the furnace. Then, the alloy was sucked into 3 mm I.D. silica tubes using an aspirator bulb. The alloy rods so produced were surface ground to remove any oxide layer present and were used as master alloys in subsequent experiments.

4.7 Sampling of slag and metal

In the slag/metal reaction, samples from the metal phase were either taken by suction with a silica tube or the final metal phase was machined with a lathe. No samples were taken from the slag phase during the experiments. The slag remaining on top of the melt after an experimental

TABLE IV: Chemical composition of electrolytic iron used in the preparation of carbon-saturated iron alloys

Spectrographic Analysis (National - U.S. Radiator Corporation)

Aluminum	0.003%
*Arsenic	Nil
Carbon	0.004%
Chromium	0.003%
Cobalt	0.005%
*Copper	0.001%
Hydrogen	0.010%
Manganese	0.001%
Nickel	0.020%
*Oxygen	0.05%
*Sulphur	0.004%
Titanium	0.001%
Iron	99.875%

*Determined by chemical analysis

TABLE V: Chemical composition of copper metal shot

Used in the preparation of carbon-saturated copper alloys

Certified A.C.S. (Fisher Scientific Company)

Cu	At. wt. 63.54
Assay	99.9%
Insoluble in HNO_3	0.010%
Antimony and tin	0.005%
Arsenic	0.0005%
Iron	0.001%
Lead	0.001%
Manganese	0.0005%
Phosphorus	0.001%
Silver	0.0005%

run was used for chemical analysis.

4.8 Chemical Analysis

4.8.1 Sulphur analysis

The sulphur analysis was carried out in a Leco 518 titrator by a combustion-iodometric method. Details of the procedure can be found under A.S.T.M. method E 30-47.[53] Solutions of approximately 0.111 and 8.88 grams/litre of potassium iodate were used for metal and slag analysis, respectively. National Bureau of Standards samples were used to standardise the dilute titrating solutions. Reagent grade Na_2SO_4 and Na_2SO_3 were used for standardisation of concentrated solutions for slag analysis. The combustion method for the determination of sulphur is reliable and a degree of accuracy ± 0.003% for metal samples and ± 0.25% for slag samples or better can be obtained.[54]

4.8.2 Analysis of slag and metal for other elements

The metal phase was analysed with an atomic absorption spectrophotometer for copper and manganese. The slag phase was analysed by wet-chemistry methods as well as by atomic absorption spectrophotometry for sodium, iron, manganese, copper and silicon. In Table VI, detection limits and precision obtained with the atomic absorption spectrophotometer are given.[55] The metal and slag phases were also analysed for carbon and oxygen in a number of cases. For the oxygen analysis of the samples a Leco inert gas fusion apparatus was used, which was calibrated with standards provided by manufacturers. A standard combustion technique was

Table VI: Detection Limits and precision of Atomic absorption spectrophotometer

Detection Limit		Wavelength
For Na	0.005 µg/cc	5890 A°
Fe	0.05 µg/cc	2483 A°
Mn	0.01 µg/cc	2795 A°
Cu	0.01 µg/cc	3247 A°

Precision

Precision better than 0.3% of the present can be achieved.

used to determine carbon in samples. The sample was melted in a Leco induction unit, the carbon was oxidized to CO_2 and the CO_2 was absorbed in a potassium hydroxide solution.

(i) Wet chemical analysis of Na_2S: A solution containing Na_2S was analysed by two titrations[56]

(a) with acid, to the methyl-red end point,

$$Na_2S + 2\ HCl \longrightarrow 2\ NaCl + H_2S$$

one equivalent of Na neutralized one equivalent of acid, whether sulphur was present or not.

(b) with silver nitrate, on another sample, adding an excess along with ferric alum, and back-titrating with ammonium thiocyanate until a pink colouration was obtained

$$Na_2S + 2\ AgNO_3 \longrightarrow 2\ NaNO_3 + Ag_2S$$

one equivalent of sulphur reacted with one equivalent of silver nitrate.

(ii) Wet chemical analysis for iron in the slag phase: The iron analysis of the slag was performed by a potassium dichromate titration method.[57] The sample was dissolved in concentrated HCl and reduced at the same time to Fe^{++} by a stannous chloride solution. Excess stannous chloride was later neutralized by mercuric chloride additions at room temperature. The dilute solution was later titrated with potassium dichromate to a violet colour using a titrating mixture.

(iii) Wet chemical analysis for copper in the slag phase: The copper-containing slag sample was dissolved in acid and copper was deposited onto a platinum cathode.[58] Later, the weight increase was determined

gravimetrically. The copper contents of the slag and metal were determined within an accuracy of ± 0.02wt%.

(iv) Wet chemical analysis for silicon in iron: The metallic samples were analysed for silicon by the standard gravimetric method.[58] After dissolution of the sample in acid, silicon was oxidized to silica, collected and weighed.

4.8.3 Precautions and difficulties related to chemical analysis

Every slag melt containing Na_2S oxidized rapidly if left in air and an odour of hydrogen sulfide arose from the action of moisture. The final slag would crumble to a powder in a short time if left in the open air. All samples were therefore preserved in sealed containers or analysed immediately after an experimental run.

In all cases graphite was also present as suspended particles within the slag phase from the walls of the graphite crucible as well as rejected graphite from metal phase. In addition to the difficulty due to suspended graphite probably, there also was some inhomogeneity due to segregation during cooling and a certain amount of unavoidable oxidation of sodium sulphide to sulfate or thiosulfate. To avoid the segregation problem, whenever possible all of the slag was taken for chemical analysis so that average values for the components of the slag could be obtained.

As mentioned before, the chemical analysis of the system was done by wet-chemistry methods as well as by atomic absorption spectrophotometry. Due to the large dilution factors involved in analysis of sodium in the slag phase by atomic absorption, the values obtained from wet-chemical

analysis were found to be more reliable. The instability of read-out in the case of iron analysis on the atomic absorption unit was a problem. As before, the values reported here are mostly from wet-chemical analysis. In the case of sulphur analysis in the slag, the readings obtained from the Leco instrument were more reliable and reproducible than those obtained by titration.

4.9 Experimental Procedure

4.9.1 Thermal stability of Na_2S

For determination of thermal stability of sodium sulphide, the graphite crucible containing 3 grams of dehydrated sodium sulphide was introduced into the resistance furnace by pushing the graphite support rod through the swagelock, located on the bottom furnace cap. At the same time, the furnace was continuously flushed with purified argon to prevent oxidation of the slag. A thermocouple was also introduced from the bottom into the furnace tube. When the crucible was in the hot zone of the furnace and reached the desired temperature, the timing of the reaction was started.

After a pre-determined period of time of reaction, the crucible was quenched in argon in the lower part of the furnace tube. Later the weight loss from the system was determined as well as the composition of the final slag. It was also observed that the crucible was not attacked by the slag during an experimental run.

4.9.2 Double crucible experiments

A similar procedure to the one described above was used in these experiments. In this case, the lower graphite crucible contained the slag phase of known weight, the upper graphite crucible was charged with a desired amount of the master alloy. Then, both crucibles were brought to the desired temperature under a stream of argon gas. When the temperature of the reaction was reached, the metal was allowed to drop into the slag by unscrewing the graphite stopper from the upper graphite crucible. In some experiments, samples of the alloy were taken at definite intervals after removal of the graphite stopper. As before, at the end of each experimental run, the lower graphite crucible containing the slag and metal phases was quenched in argon in the lower portion of the furnace tube, which was followed by chemical analysis.

In experiments which used mechanical stirring, the upper graphite crucible was rotated by an external motor. An extension of the graphite stopper rod stirred both slag and metal.

4.9.3 Filling of capillaries

Initially, graphite capillary material was machined to desired dimensions with great care and accuracy. Then, these graphite capillaries were filled with alloys of known composition using the vacuum induction melting unit. For this purpose, the metal phase was melted under vacuum in a graphite crucible. When the desired temperature was reached, the graphite capillaries were immersed into the metal pool and vacuum was released to force the liquid metal into the small capillary tubes. Later,

the capillaries were pulled out of the melt and quenched in argon in the upper part of the vycor tube. As an experimental precaution against a large carbon flux, the capillaries were filled and diffused at identical temperatures so that carbon-concentration gradients would be minimized substantially.

4.9.4 Diffusion of sulphur from the capillary to the metal pool

To determine the diffusivity of sulphur at 1250°C, graphite capillaries filled with Fe-C-0.17wt%S alloy were immersed into a pool of metal of composition Fe-C-0.77wt%S for a pre-determined time period. Initially, the tips of the capillaries were just outside the surface of the metal pool. When the thermal equilibrium was established between the capillary metal and the metal pool, the capillaries were gently immersed into the pool of molten metal. The metal pool itself was located within the furnace so that there was a positive temperature gradient of about 5°C from the top to the bottom, i.e., the top of the capillaries and the metal pool were at a higher temperature than the bottom. This reduced convective mixing in the experiments. At the end of each experimental run, the capillaries were removed from the molten pool of metal, by raising the graphite support rod, and were quenched in the upper part of the furnace tube. Purified argon was kept flowing through the reaction tube to protect the sample and reservoir liquids from oxidation during experiments. Finally, the sulphur content of the capillary metal was determined chemically.

4.9.5 Reaction of capillary metal with slag

The double capillary filled with Fe-C-0.215wt%S alloy using the vacuum induction melting unit was fitted with a graphite container on top so that the slag from the upper graphite crucible could be poured into it from above, Fig.12. The slag, which was now in the upper graphite crucible, and the capillary were brought to the desired temperature under a stream of argon gas, as in the double crucible experiments. Inside the resistance furnace, the capillary was positioned so that the top of the capillary was at a higher temperature than the bottom which resulted in reduced convective mixing. When the system reached the desired temperature, the slag was allowed to run onto the top of the metal phase. As before the system was quenched in argon in the lower part of the furnace at the end of each experimental run. Later, the inner metallic capillary was analysed for sulphur.

4.9.6 Closed-system experiments

In the closed-system experiments, the experimental procedure was slightly different from that of the double crucible experiments. In this case, known amounts of metal and slag were placed in the same graphite crucible from the start of the experiments. Later, this graphite crucible was placed inside a recrystallized Al_2O_3 crucible Then, the bi-crucible assembly was put into a steel crucible. Before each experimental run, the system was evacuated and filled with argon gas to prevent oxidation of gaseous species that formed during experimental runs. Finally, the steel lid was welded onto the steel crucible by tungsten arc welding.

The closed-system so produced was then introduced from the bottom into the resistance furnace heated to a known temperature. The assembly was kept at the reaction temperature for a known time and later quenched in the lower part of the furnace. The lid was cut open and the graphite crucible containing the slag/metal system was removed for chemical analysis.

CHAPTER 5

EXPERIMENTAL RESULTS

5.1 Introduction

In this chapter, the experimental data obtained are presented in tabular and graphical form for various types of study undertaken during the course of this work.

5.2 Thermal Stability of Na_2S

A set of experiments were conducted on dehydrated sodium sulphide to find out the stability of the slag in the temperature range 1200° to 1400°C under flowing purified argon gas (75 cc s.t.p./min). The thermal stability of Na_2S under vacuum was also investigated at 1250°C. The weight loss from the system was used as a measure of thermal stability at high temperatures. The results are summarized in Table VII and Figure 17 shows the weight loss vs. time at 1250°C. The variation of composition of the slag with time is also given in Table VII.

5.3 Double Crucible Experiments

5.3.1 Preliminary experiments with large crucibles

In preliminary experiments, the weight of master alloy used was 100 grams and slag weight was 15 grams so that the sampling of the metal phase could be made as the reaction progressed. Since the suction samples were around 1 to 2 grams each, the relative weight of the metal phase

Table VII: Thermal stability of sodium sulphide

Total weight lost from 1.5 and 3.0 cm diameter crucibles in 1 hour

Experimental condition	Initial slag wt	Diameter of crucible, cm	Temperature °C	Total weight lost, grams
Argon flow	3.00	1.5	1200°C	0.07
"	3.00	1.5	1250	0.09
"	3.00	1.5	1300	0.14
"	3.00	1.5	1350	0.17
"	3.00	1.5	1400	0.20
"	6.00	3.0	1250	0.34
150 mm Hg vacuum	3.00	1.5	1250	0.15

Total weight lost for various times of heating at 1250°C

Diameter of graphite crucible = 1.5 cm

Initial slag weight = 3.00 grams

Time, Hours	0	1	3	8
Weight lost, grams	0.03	0.09	0.185	0.52
wt%Na	58.55	58.3	57.65	56.7
wt%S	41.20	41.3	41.9	42.9
Ratio S/Na	0.705	0.708	0.727	0.756

Initial wt%C in slag = 0.15 max. Initial wt%O in slag = 0.30 max.

Stoichiometric Ratio wt%S/wt%Na = $\frac{41.08}{58.92}$ = 0.697

Fig. 17: Weight lost from dehydrated Na_2S (grams) against time (hours) at 1250°C
Initial slag wt = 3.00 grams

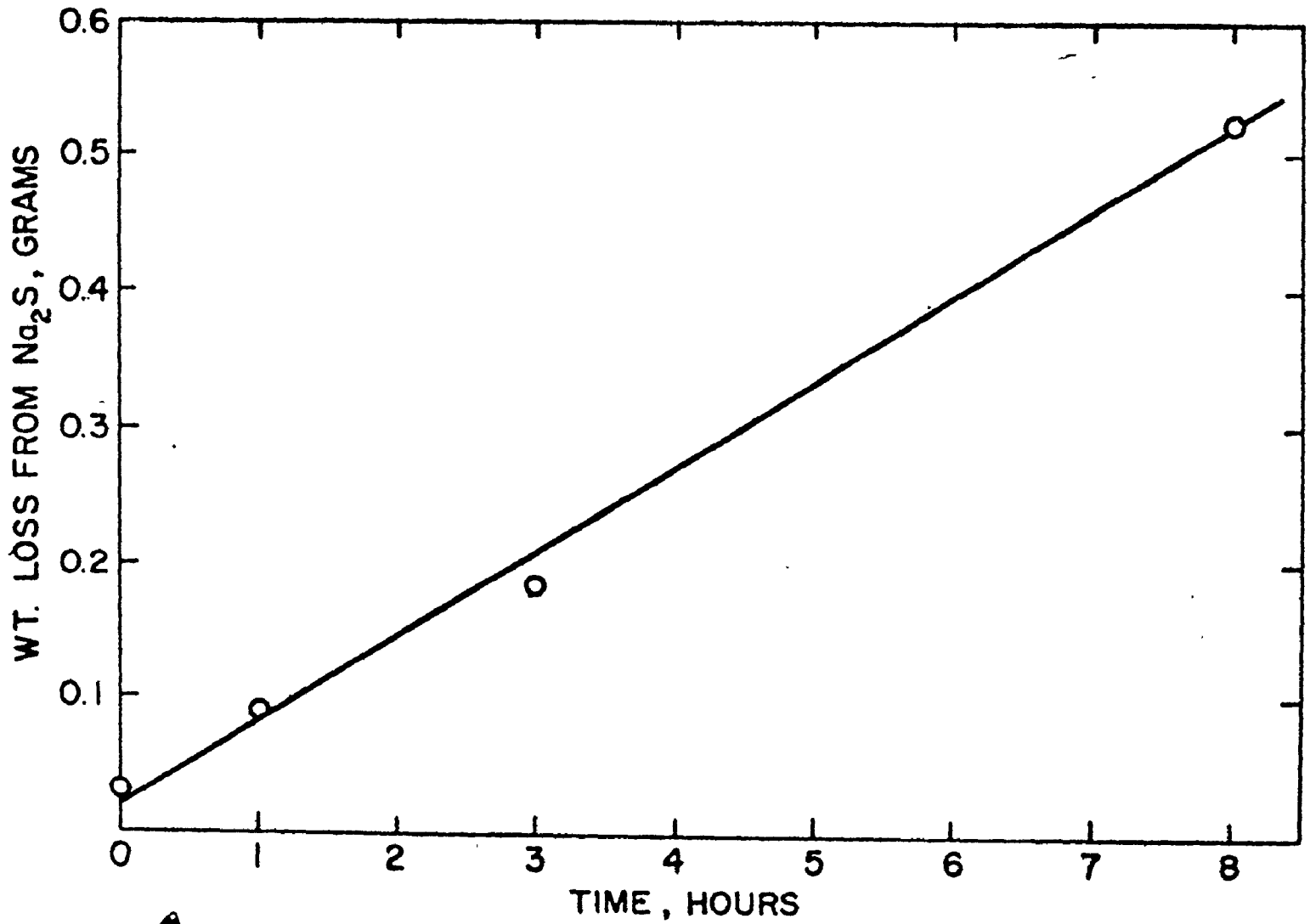

could only decrease between 5 to 10% due to sampling. So by analysing the metal samples it was possible to follow desulphurization of high sulphur melts. Initial composition of the master alloys was varied between 0.06wt%S and 0.76wt%S. Table VIII summarizes the sulphur change with time up to 3 hours at 1250°C. Figure 18 illustrates typical time-concentration curves obtained for sulphur in the metal phase in this investigation. In most cases, each point in this figure represents an average of at least three experimental determinations with a variation of ± 0.003wt%S for the low sulphur values.

A few preliminary experiments were also done with Fe- C - Mn - S and Fe - C - Si - S alloys. Table IX summarizes results obtained for different experimental durations at 1250°C.

5.3.2 Experiments with smaller crucibles

Due to the relatively large amounts of metal and slag required, as well as their large thermal mass, the large crucible experiments were discontinued and most experiments were done under identical conditions but using double graphite crucibles of smaller size. In most cases, each crucible had an inside diameter of 1.5 cm. In order to determine the rate-limiting steps for the reaction under consideration, the effects of changes in several variables on the rate of each reaction were studied.

(i) Effect of "nature of the metal phase": Carbon-saturated iron of four different compositions and carbon-saturated copper were reacted with the slag for different times up to 48 hours. In most experiments the maximum time of reaction was 8 hours. In each case, there was no

Table VIII: Desulphurization of Fe - C - S alloys, large double crucible experiments

All experiments employed:

1. carbon-saturated iron (4.5wt%C)
2. Graphite crucibles of 1-1/4" I.D., 1-3/4" O.D., 3" in length
3. 15 grams of dehydrated sodium sulphide slag
4. 100 grams of Fe - C - S alloys
5. No forced stirring
6. Reaction temperature of 1250°C

Sample Number	Time, minutes	wt%S	wt%S	wt%S
1	0	0.06	0.34	0.76
2	2	0.021	0.042	0.072
3	5	0.014	0.016	0.030
4	10	0.011	0.011	0.020
5	15	0.009	0.009	0.013
6	30	0.007	0.009	0.012
7	60	0.008	0.011	0.012
8	120	0.009	0.016	0.017
9	180	0.015	0.019	0.022

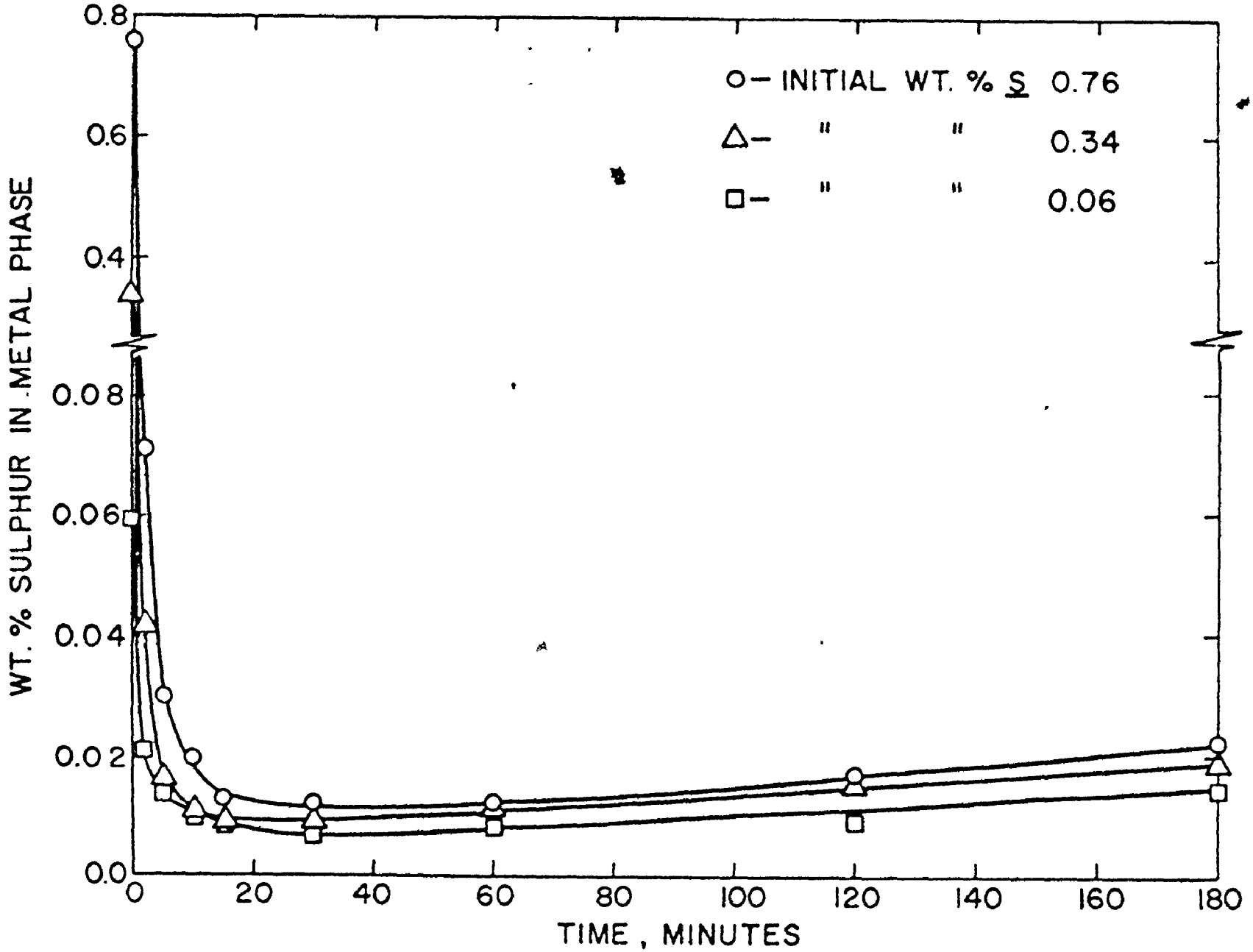

Fig. 18: wt%S against time (minutes)

Table IX: Desulphurization of Fe - C - Mn - S and Fe - C - Si - S alloys, large double crucible experiments

All experiments employed:

1. Carbon saturated iron
2. Graphite crucibles of 1-1/4" I.D., 1-3/4 O.D., 3" in length
3. 15 grams of dehydrated sodium sulphide slag
4. 100 grams of Fe - C - Mn - S or Fe - C - Si - S alloy
5. No forced stirring
6. Reaction temperature, 1250°C

Alloy Fe - C - 0.7 wt%Mn - 0.06 wt%S

Sample No	Time, mins	wt%S	wt%Mn
1	0	0.06	0.7
2	10	0.0105	0.435
3	20	-	0.365
4	30	0.0075	0.33

Alloy Fe - C - 0.125wt%Mn - 0.36wt%S

Sample No	Time, mins	wt%S	wt%Mn
1	0	0.36	0.125
2	10	0.013	0.048
3	20	0.0105	0.0365
4	30	0.015	0.028

Alloy Fe - C - 0.85wt%Si - 0.76wt%S

Sample No	Time, mins	wt%S	wt%Si
1	0	0.76	0.85
2	5-1/2	0.031	0.845
3	20	0.028	-
4	42	0.024	0.86
5	104	0.026	0.80
6	180	0.024	0.82

Alloy Fe - C - 0.97wt%Si - 0.76wt%S

Sample No	Time, mins	wt%S	wt%Si
1	0	0.76	0.97
2	15	0.033	-
3	30	0.020	0.98

sampling during the experimental run. The final metal and slag phases were chemically analysed at the end of each experiment and the results were checked against those obtained gravimetrically after each run. Occasionally, the same experiment was repeated twice to check the reproducibility of the results. It was found that the variations were small as long as the experimental conditions were kept constant.

The initial metal compositions were as follows,

Fe - C - 0.005wt%S

Fe - C - 0.7wt%S

Fe - C - 0.005wt%S - 0.9wt%Cu

Fe - C - 0.005wt%S - 3.54wt%Mn

Cu - C - 0.002wt%S

All metal phases were saturated with carbon at the temperature of the reaction. Tables X to XVII summarize results and Figs. 19 to 26 show the variation of metal and slag compositions as a function of time for graphite crucibles of differing dimensions at a reaction temperature of 1250°C.

(ii) Effect of "temperature of reaction": For a better understanding of the kinetics of reaction, it was necessary to study the effect of temperature on the reaction of Fe - C - 0.005wt%S alloy with dehydrated Na_2S. The time of reaction and crucible size were kept constant but the reaction temperature was varied between 1200°C and 1400°C. Table XVIII summarizes the results obtained from such experiments.

(iii) Effect of "stirring rate": The effect of stirring on the rate of reaction was studied by stirring the slag and metal with a graphite stirrer which was rotated by an external motor at a known rate.

Table X: Change of slag and metal compositions with time of reaction

Initial metal composition Fe - C - 0.005wt%S
Diameter of graphite crucible = 1.5 cm
Reaction temperature = 1250°C
Initial metal wt. = 20.00 grams
Initial slag wt = 3.00 grams

Time, Hours	1/2	1	2	3	4	5	6	7	8
Slag Composition									
Na wt%	52.9	48.3	42.3	38.2	35.0	32.5	30.6	29.2	28.5
S%	39.0	39.2	39.1	39.0	39.0	38.7	38.6	38.40	38.0
Fe%	8.0	12.5	18.4	22.7	26.0	28.6	30.7	32.25	33.5
Final slag wt.g.	3.03	3.04	3.05	3.04	3.04	3.07	3.08	3.05	3.075
Fe lost to slag, g.	0.24	0.38	0.56	0.69	0.79	0.87	0.93	0.98	1.02
Na lost from slag, g.	0.17	0.30	0.45	0.58	0.68	0.73	0.80	0.86	0.88
wt%S in metal	0.0135	0.018	0.027	0.036	0.045	0.063	0.090	0.117	0.135

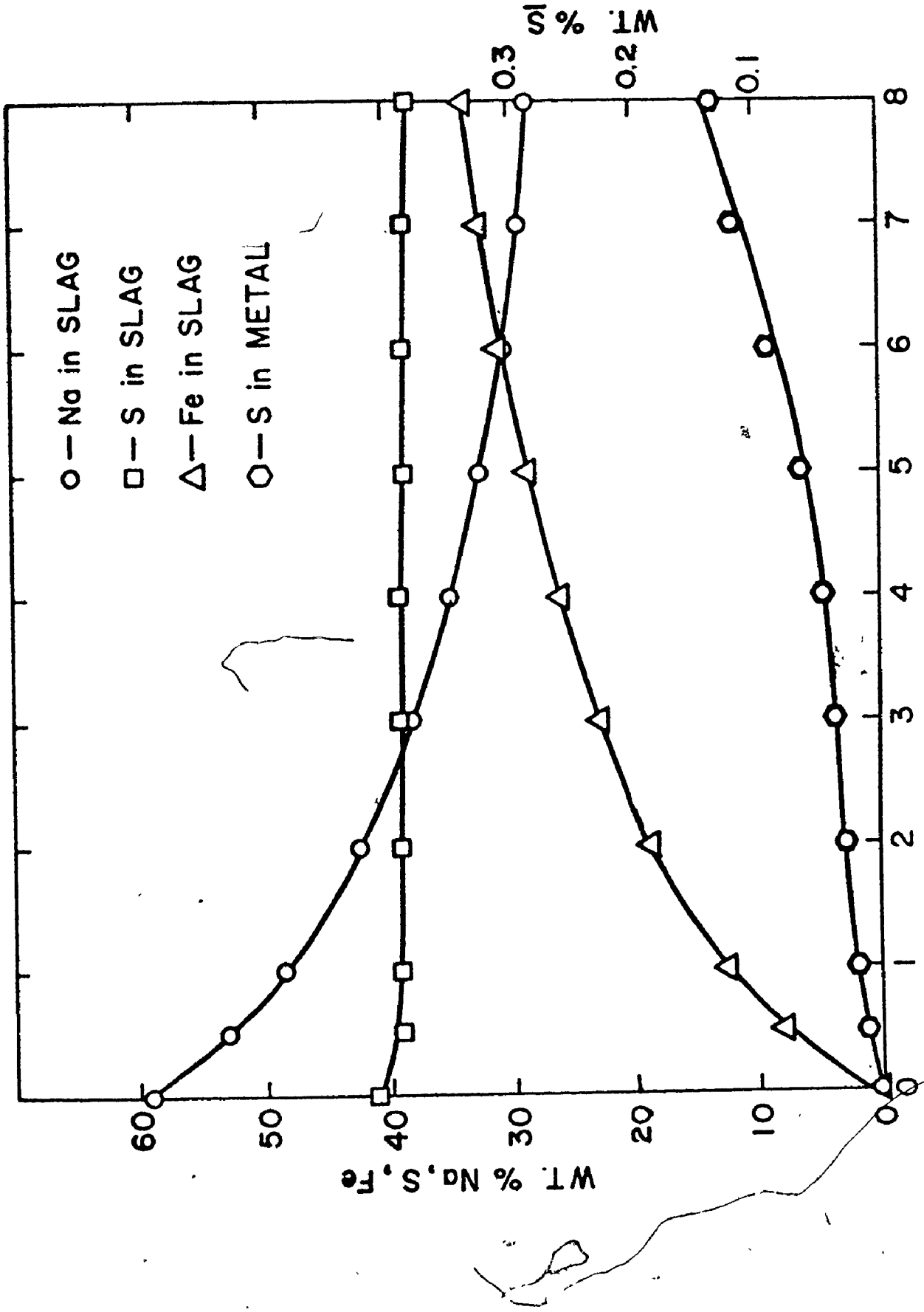

Fig. 19: Variation of compositions of slag and metal with time (For Fe - C - 0.005wt%S with Na_2S, 1.5 cm ϕ crucible)

Table XI: Change of slag and metal compositions with time

Initial metal composition: Fe - C - 0.005wt%S
Diameter of graphite crucible: 3.0 cm
Reaction Temperature: 1250°C
Initial metal wt: 40.00 grams
Initial slag wt : 6.00 grams

Time Hours	1	2	3	4	5	6	7	8
Slag Composition								
Na%	43.5	39.5	37.2	35.65	34.3	32.9	31.5	30.0
S%	40.0	39.8	39.65	39.60	39.4	39.5	39.5	39.45
Fe%	16.4	20.7	23.15	24.75	26.2	27.6	29.0	30.35
Final slag wt, grams	6.18	6.23	6.26	6.28	6.30	6.31	6.33	6.34
Fe lost to slag, g.	1.015	1.29	1.45	1.555	1.65	1.74	1.835	1.925
Ne lost from slag, g.	0.85	1.08	1.21	1.30	1.38	1.46	1.55	1.63
wt%S	0.027	0.0315	0.036	0.0405	0.045	0.054	0.072	0.090

Fig 20: Variation of compositions of slag and metal with time (For Fe - C - 0.005wt%S with Na_2S, 3.0 cm ϕ crucible)

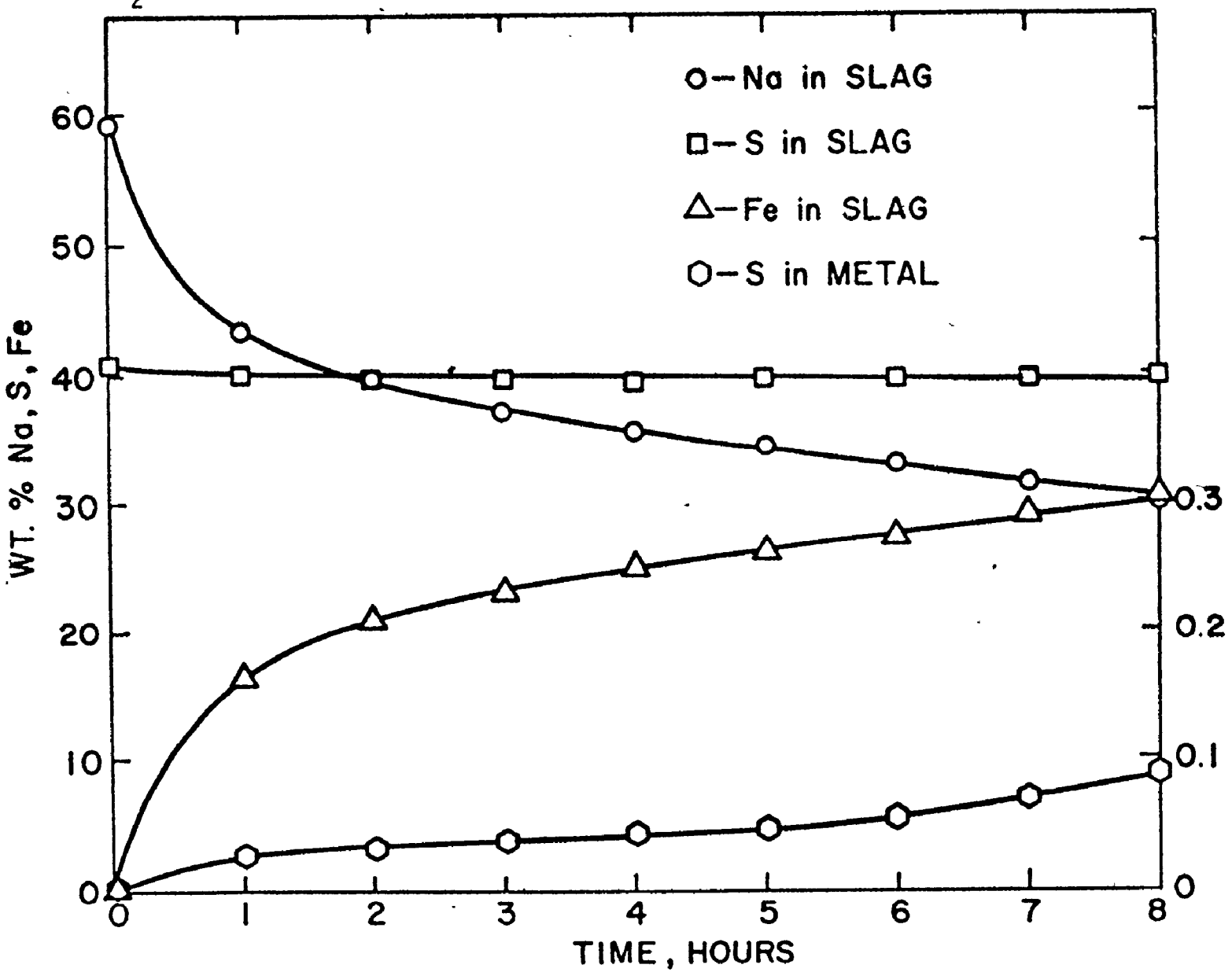

Table XII: Change of slag and metal compositions with time

Initial metal composition: Fe - C - 0.005wt%S
Reaction temperature: 1250°C
Initial metal wt: 20.00 grams
Initial slag wt : 6.00 grams

Dimensions:

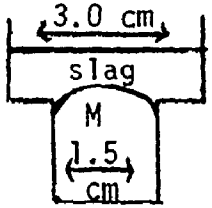

Time, Hours	1	2	3	4	5	6	7	8
Slag Composition								
Na wt%	45.9	41.6	39.5	37.9	36.5	35.2	34.0	32.9
S%	40.1	39.9	39.55	39.4	39.2	39.4	39.4	39.2
Fe%	14.0	18.5	20.85	22.5	24.1	25.4	26.6	27.9
Final slag wt, grams	6.155	6.21	6.235	6.255	6.27	6.29	6.30	6.32
Fe lost to slag, g.	0.86	1.15	1.30	1.41	1.51	1.60	1.68	1.76
Na lost from slag, g.	0.715	0.95	1.08	1.17	1.25	1.33	1.395	1.46
wt%S	0.0225	0.0315	0.038	0.0415	0.045	0.0485	0.054	0.063

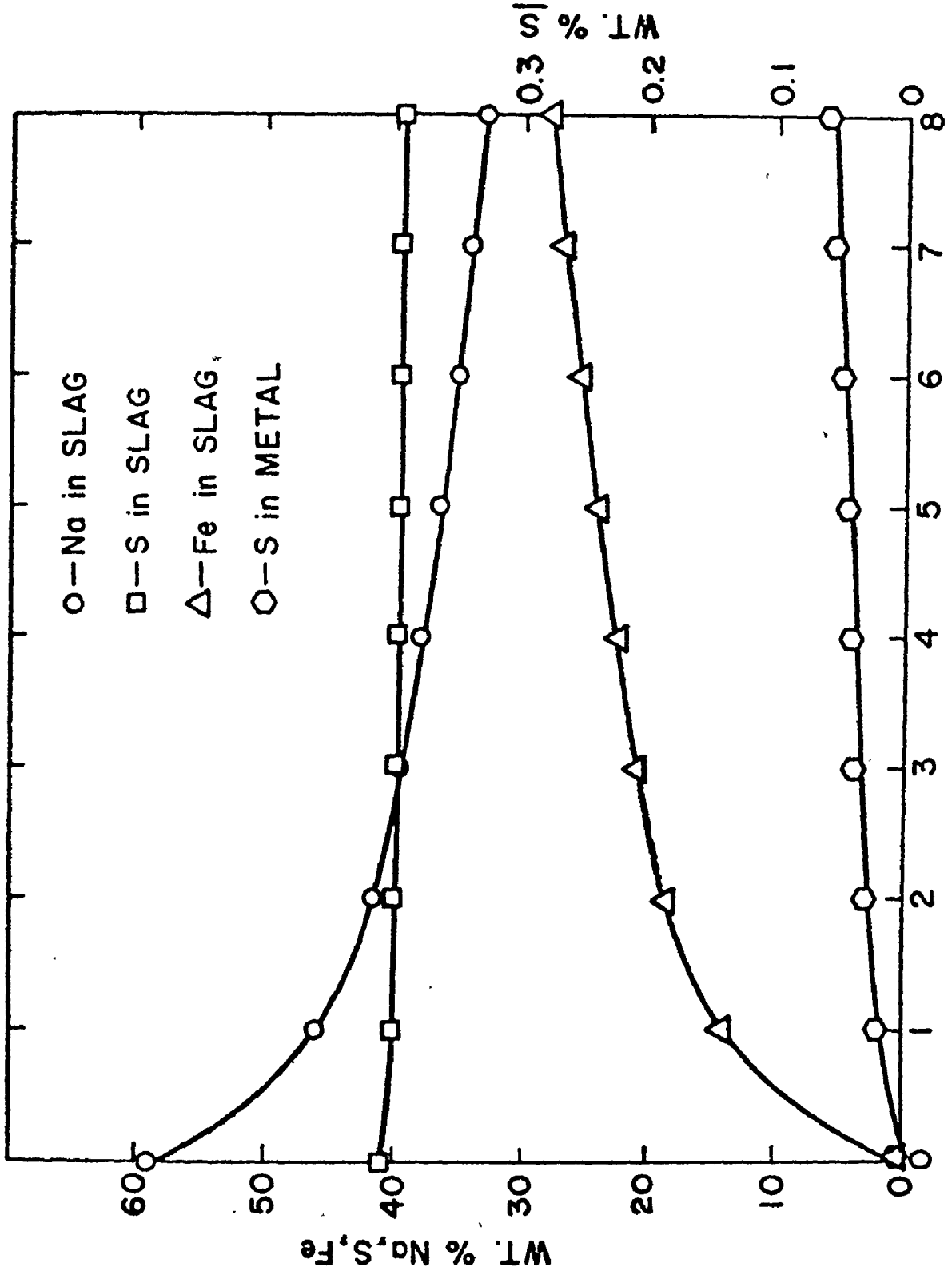

Fig. 21: Variation of compositions of slag and metal with time (For Fe - C - 0.005wt%S with Na_2S, 3.0/1.5 cm ϕ crucible)

Table XIII: Change of slag and metal compositions with time

Initial metal composition: Fe - C - 0.7wt%S
Initial metal weight: 20.00 grams
Initial slag weight: 3.00 grams
Reaction temperature: 1250°C
Diameter of graphite crucible: 1.5 cm

Time, Hours	1/2	1	3	8	24	48
Slag composition						
Na%	50.0	43.0	35.5	28.5	20.0	13.2
S%	39.75	40.0	39.25	38.0	38.1	37.3
Fe%	10.0	16.8	25.5	33.5	42.0	49.5
Final slag wt, grams	3.36	3.43	3.42	3.385	3.25	3.055
Fe lost to slag, g.	0.34	0.57	0.87	1.09	1.36	1.51
Na lost from slag, g.	0.09	0.30	0.56	0.805	1.12	1.365
wt%S	0.016	0.0215	0.050	0.207	0.57	0.94

Fig. 22: Variation of compositions of slag and metal with time (For Fe - C - 0.7wt%S with Na_2S, 1.5 cm ϕ crucible)

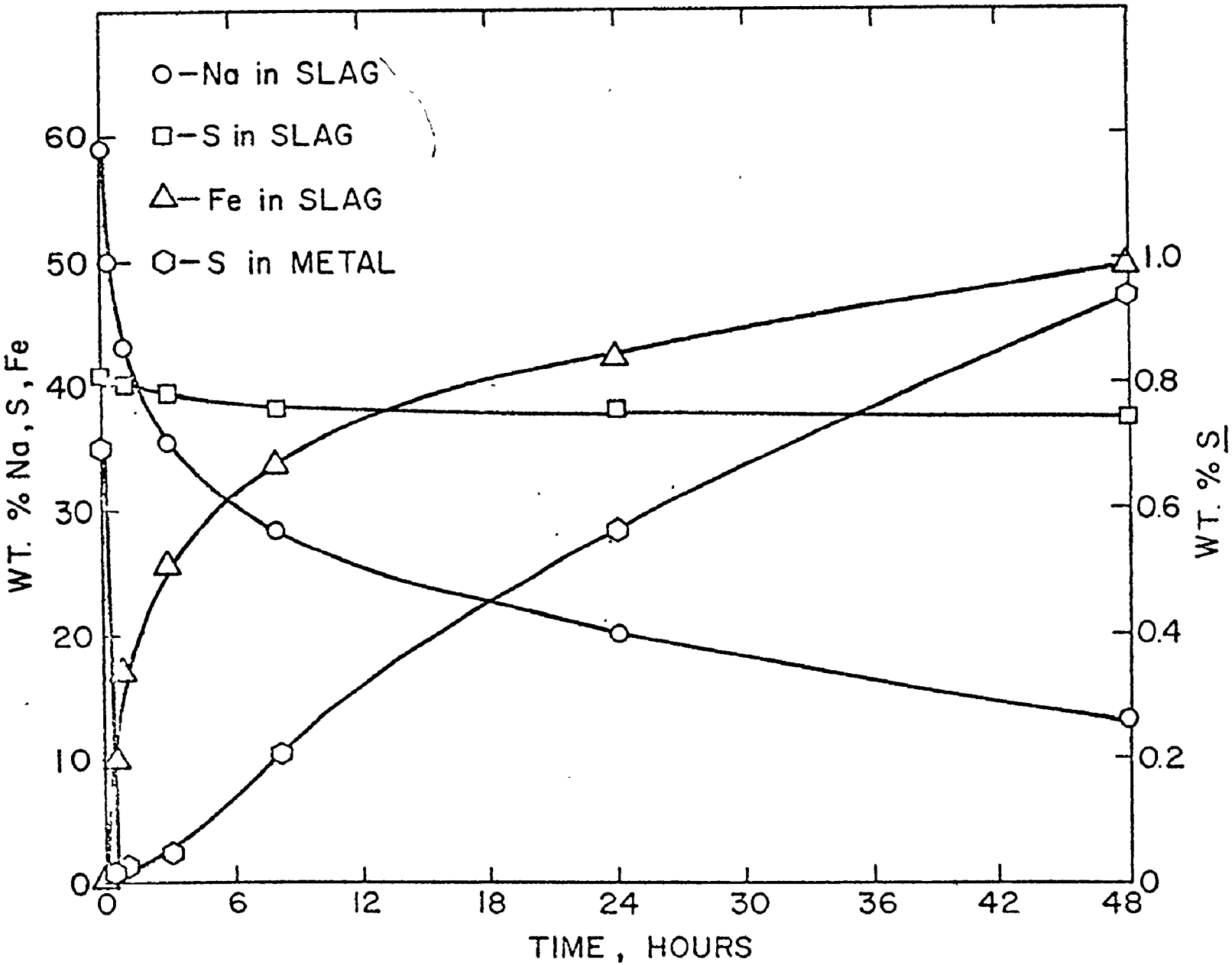

Table XIV: Change of slag and metal compositions with time

Initial metal composition: Fe - C - 0.9wt%Cu - 0.005wt%S
Initial metal weight: 20.00 grams
Initial slag weight: 3.00 grams
Reaction temperature: 1250°C
Diameter of graphite crucible: 1.5 cm

Time, Hours	1/2	1	2	3	4	5	6	7	8
Slag composition									
Na wt%	47.5	43.75	39.6	36.25	33.45	31.6	30.6	29.1	28.25
S wt%	38.5	39.0	38.0	37.5	37.9	37.5	36.7	36.4	35.75
Fe wt%	10.5	13.0	17.85	21.45	24.0	26.25	28.0	29.75	31.20
Cu wt%	3.4	4.05	4.5	4.6	4.6	4.6	4.6	4.6	4.6
Final slag wt grams	3.104	3.085	3.08	3.076	3.08	3.07	3.07	3.06	3.043
Fe lost to slag, g.	0.32	0.40	0.55	0.66	0.74	0.805	0.86	0.91	0.95
Na lost from slag, g.	0.295	0.42	0.55	0.655	0.74	0.80	0.83	0.88	0.91
wt%S	0.014	0.020	0.032	0.045	0.059	0.078	0.099	0.120	0.147
wt%Cu	0.37	0.275	0.21	0.19	0.19	0.19	0.195	0.195	0.20

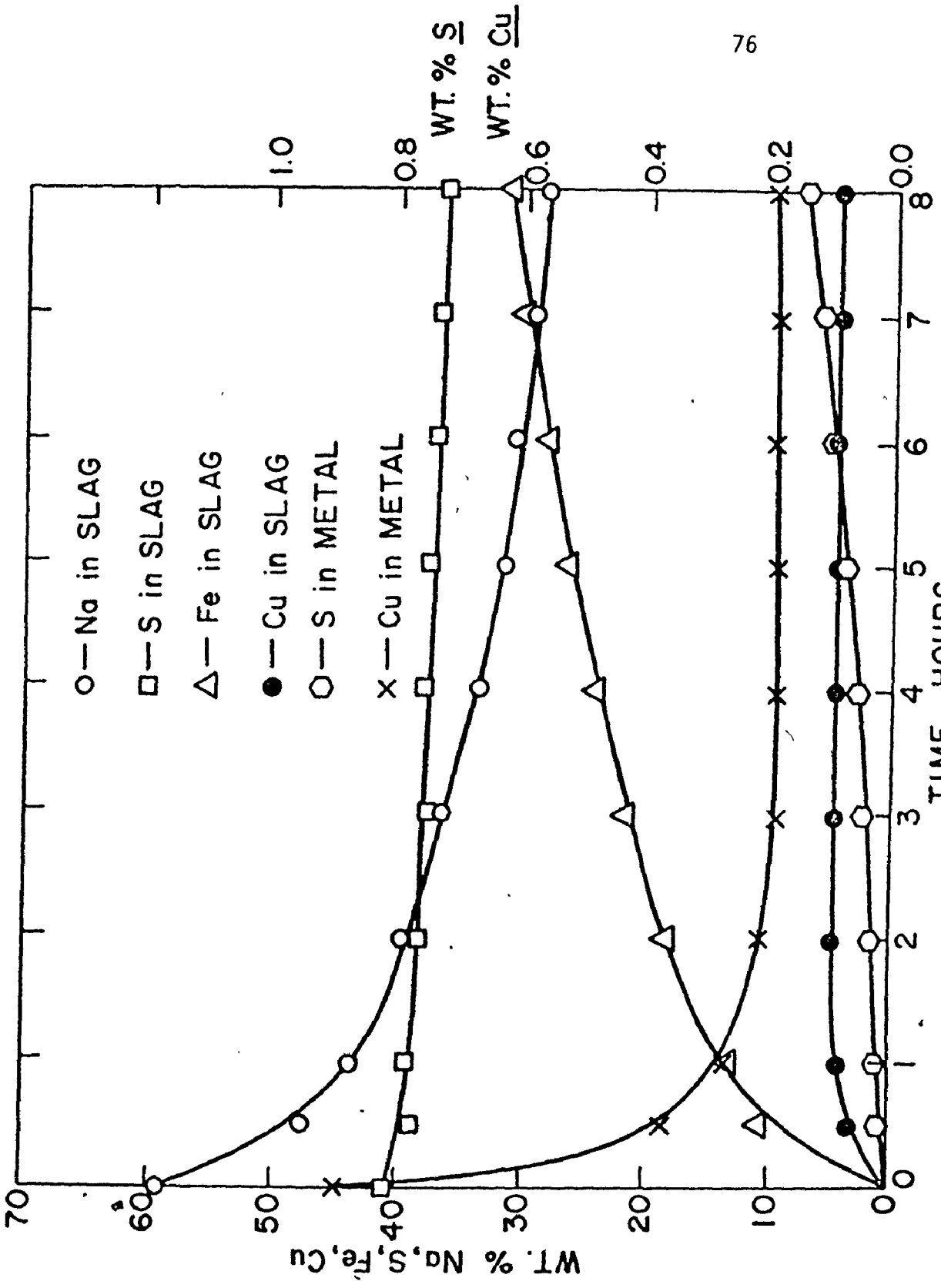

Fig. 23: Variation of compositions of slag and metal with time (For Fe - C - 0.9wt%Cu - 0.005wt%S with Na_2S, 1.5 cm ϕ crucible)

Table XV: Change of slag and metal compositions with time

Initial metal composition: Fe - C - 3.54wt%Mn - 0.005wt%S
Initial metal weight: 20.00 grams
Initial slag weight: 3.00 grams
Reaction temperature: 1250°C
Diameter of graphite crucible: 1.5 cm

Time, Hours	1/2	1	3	8
Slag Composition				
Na%	47.0	41.9	30.6	24.6
S%	40.1	40.0	38.0	39.0
Fe%	1.3	2.0	9.3	14.1
Mn%	11.6	16.1	22.0	22.2
Final slag wt, grams	3.021	3.04	3.054	3.058
Fe lost to slag, g.	0.04	0.06	0.28	0.43
Na lost from slag, g.	0.35	0.51	0.84	1.00
wt%S	0.007	0.0115	0.0525	0.124
wt%Mn	1.82	1.12	0.193	0.128

Fig. 24: Variation of compositions of slag and metal with time (For Fe - C - 3.54wt%Mn - 0.005wt%S with Na_2S, 1.5 cm ϕ crucible)

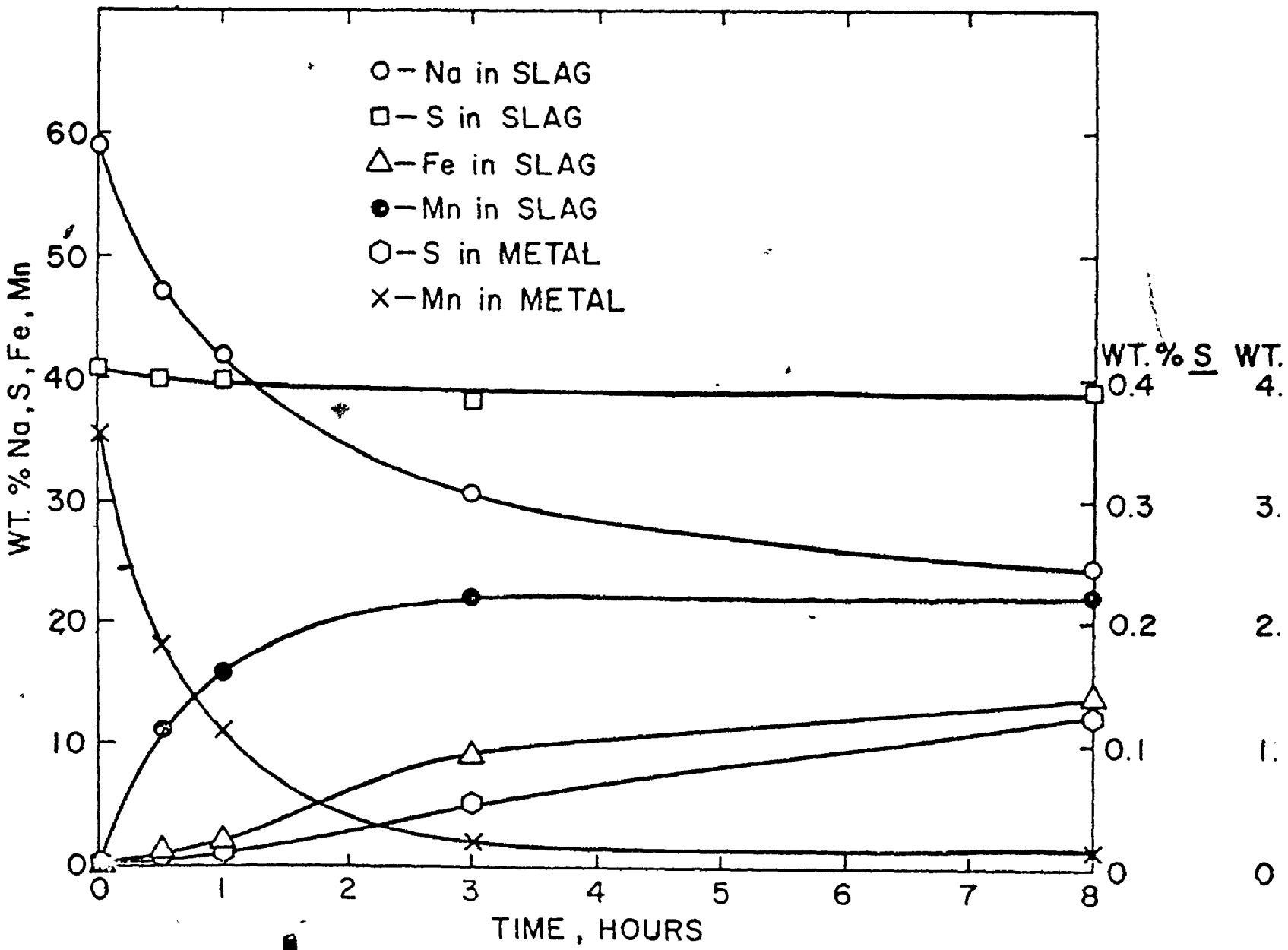

Table XVI: Change of slag and metal compositions with time

For initial metal composition: Cu - 0.0001wt%C - 0.002wt%S
Diameter of graphite crucible: 1.5 cm
Reaction temperature: 1250°C
Initial metal wt: 20.00 grams
Initial slag wt: 3.00 grams

Time, Hours	1/2	1	2	3	4	5	6	7	8
Slag Composition									
Na wt%	41.1	36.4	30.5	26.0	22.9	19.6	17.7	15.8	13.8
S%	34.0	32.3	30.1	29.5	28.9	27.5	27.0	26.0	25.6
Cu%	24.8	31.2	39.4	44.4	48.3	52.6	55.3	58.1	60.4
Final slag wt, g.	3.53	3.69	3.94	4.08	4.20	4.33	4.42	4.53	4.62
Cu lost to slag, g.	0.88	1.16	1.56	1.83	2.05	2.31	2.47	2.65	2.80
Na lost from slag, g.	0.32	0.43	0.58	0.69	0.78	0.885	0.955	1.03	1.10
wt%S	0.020	0.035	0.063	0.096	0.145	0.200	0.240	0.295	0.340

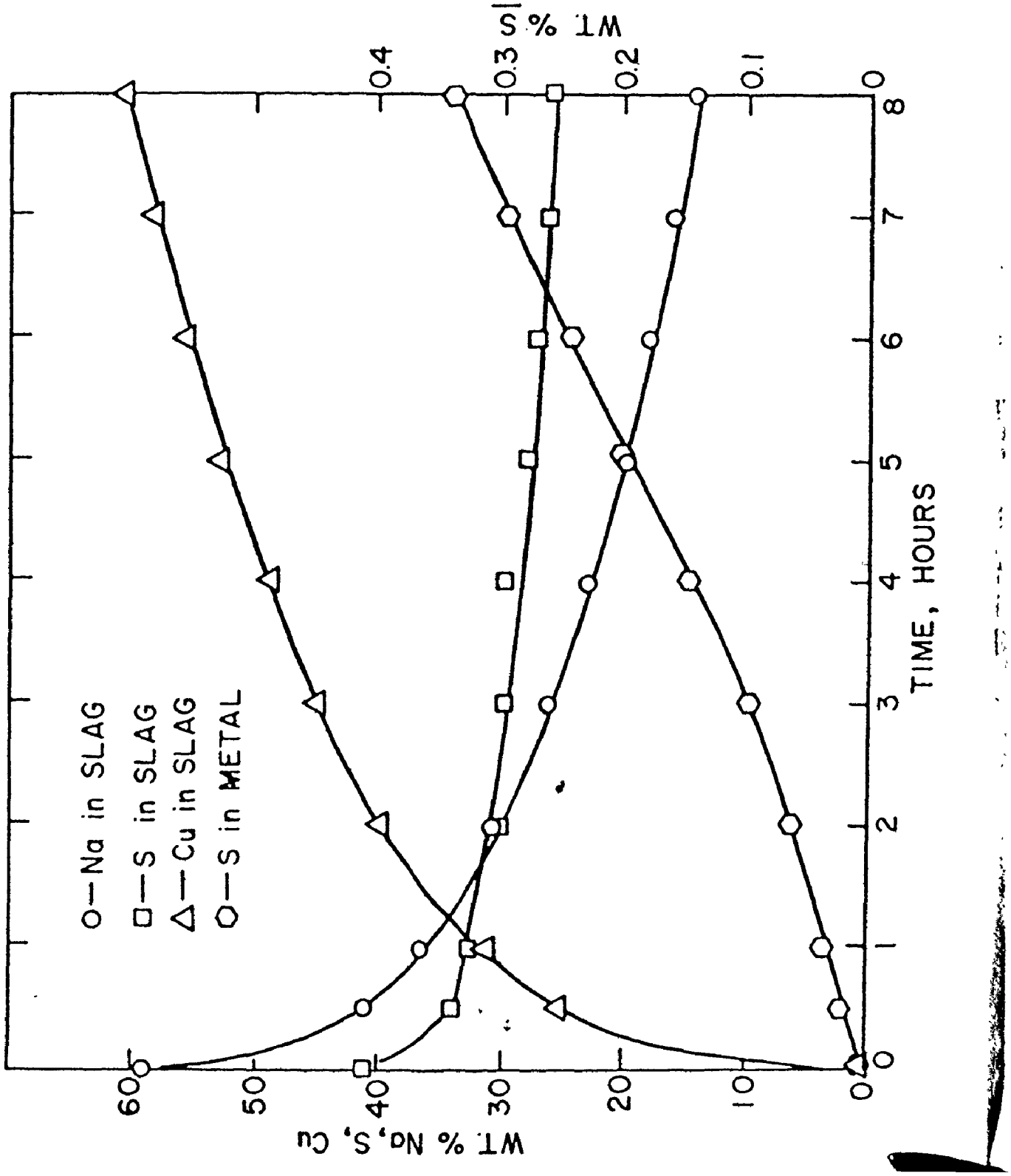

Fig. 25: Variation of compositions of slag and metal with time (For Cu - 0.0001wt%C - 0.002wt%S with Na_2S, 1.5 cm ϕ crucible)

For initial metal composition: Cu - 0.00[illegible] wt%
Diameter of graphite crucible: 3.0 cm
Reaction temperature: 1250°C
Initial metal wt: 40.00 grams
Initial slag wt: 6.00 grams

Time, Hours	1	2	3	4	5	6	7	8
Slag Composition								
Na wt%	32.0	27.45	25.1	23.2	21.35	20.0	18.8	17.8
S%	32.0	30.7	30.0	29.5	29.15	28.8	28.5	28.2
Cu%	36.0	41.85	44.9	47.3	49.5	51.2	52.7	54.0
Final slag wt, g.	7.80	8.195	8.415	8.60	8.78	8.92	9.05	9.16
Cu lost to slag, g.	2.81	3.43	3.78	4.07	4.35	4.57	4.77	4.95
Na lost from slag, g.	1.045	1.29	1.43	1.545	1.665	1.755	1.835	1.91
wt%S	0.0495	0.091	0.115	0.140	0.173	0.198	0.214	0.231

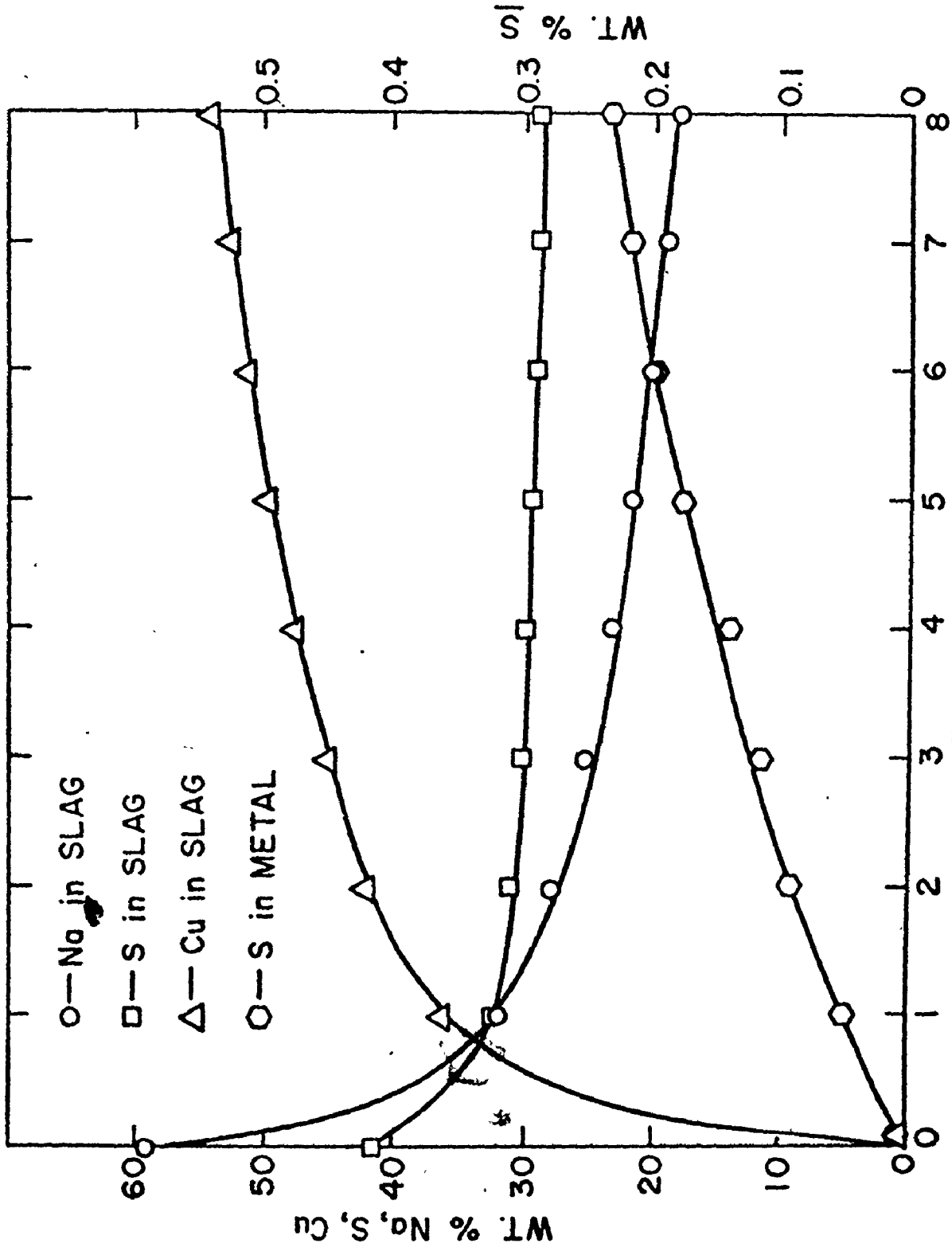

Fig. 26: Variation of compositions of slag and metal with time (For Cu - 0.0001wt%C - 0.002wt%S with Na_2S, 3.0 cm ϕ crucible)

Table XVIII: Effect of "reaction temperature"

Initial metal composition: Fe - C - 0.005wt%S
Initial metal weight: 20.00 grams
Initial slag weight: 3.00 grams
Graphite crucible size: 1.5 cm diameter
Time of reaction: 1 hour

Temperature °C	Fe lost to slag, grams	Na lost from slag, grams
1200	0.305	0.25
1250	0.38	0.30
1300	0.43	0.345
1350	0.53	0.44
1400	0.62	0.52

The rotation speed was determined by a stroboscope and kept constant during each experimental run. Table XIX summarizes results obtained with 3 cm diameter graphite crucibles at 1250°C. For the moderate stirring conditions employed in this study the interfacial areas would not be altered, as shown in room temperature transparent fluid studies of similar systems.

(iv) Effect of "gas/slag and/or slag/metal interfacial areas": To determine the effect of the two interfacial areas, crucibles of various shapes were machined. Figure 27 shows dimensions of the crucibles used in the experiments. In one case only the gas/slag interfacial area was increased. Conversely, in another case, only the metal/slag interfacial area was increased substantially. Finally, both interfacial areas were increased compared to those of the 1.5 cm diameter crucible. The results obtained are given in tabular form in Table XX for different reaction times.

(v) Effect of "length of graphite-gas-slag contact line": A graphite rod, as shown in Fig. 28, was placed at the centre of the crucible to increase the length of the graphite-gas-slag contact line. In Table XXI, the results are compared with the results obtained from an experiment using a crucible of almost the same interfacial areas but shorter three-phase contact line.

(vi) Effect of "argon flow rate": The flow rate of purified argon gas was varied to investigate the effect of this parameter on the rate of reaction. The results obtained are summarized in Table XXII.

Table XIX: Effect of "Stirring rate of slag/metal system"

Initial composition of the metal phase: Fe - C - 0.005wt%S
Initial metal weight: 40.00 grams
Initial slag weight: 6.00 grams
Time of reaction: 1 hour
Inside diameter of graphite crucible: 3.0 cm
Temperature of reaction: 1250°C

Experimental Condition	Rate of Stirring	Fe lost to slag, grams	Na lost from slag, grams
Without stirring	0	1.015	0.85
With stirring	40 RPM	1.06	0.87
With stirring	100 RPM	1.095	0.90
With stirring	100 RPM	1.115	0.92

Initial composition of the metal phase: Fe - C - 0.9wt%Cu - 0.005wt%S
Initial metal weight: 40.00 grams
Initial slag weight: 6.00 grams
Time of reaction: 1 hour
Inside diameter of graphite crucible: 3.0 cm
Temperature of reaction: 1250°C

Experimental Condition	Rate of Stirring	Fe lost to slag, grams	Cu lost to slag, grams	Na lost from slag, grams
Without stirring	0	1.00	0.24	0.93
With stirring	100 RPM	1.05	0.27	0.98

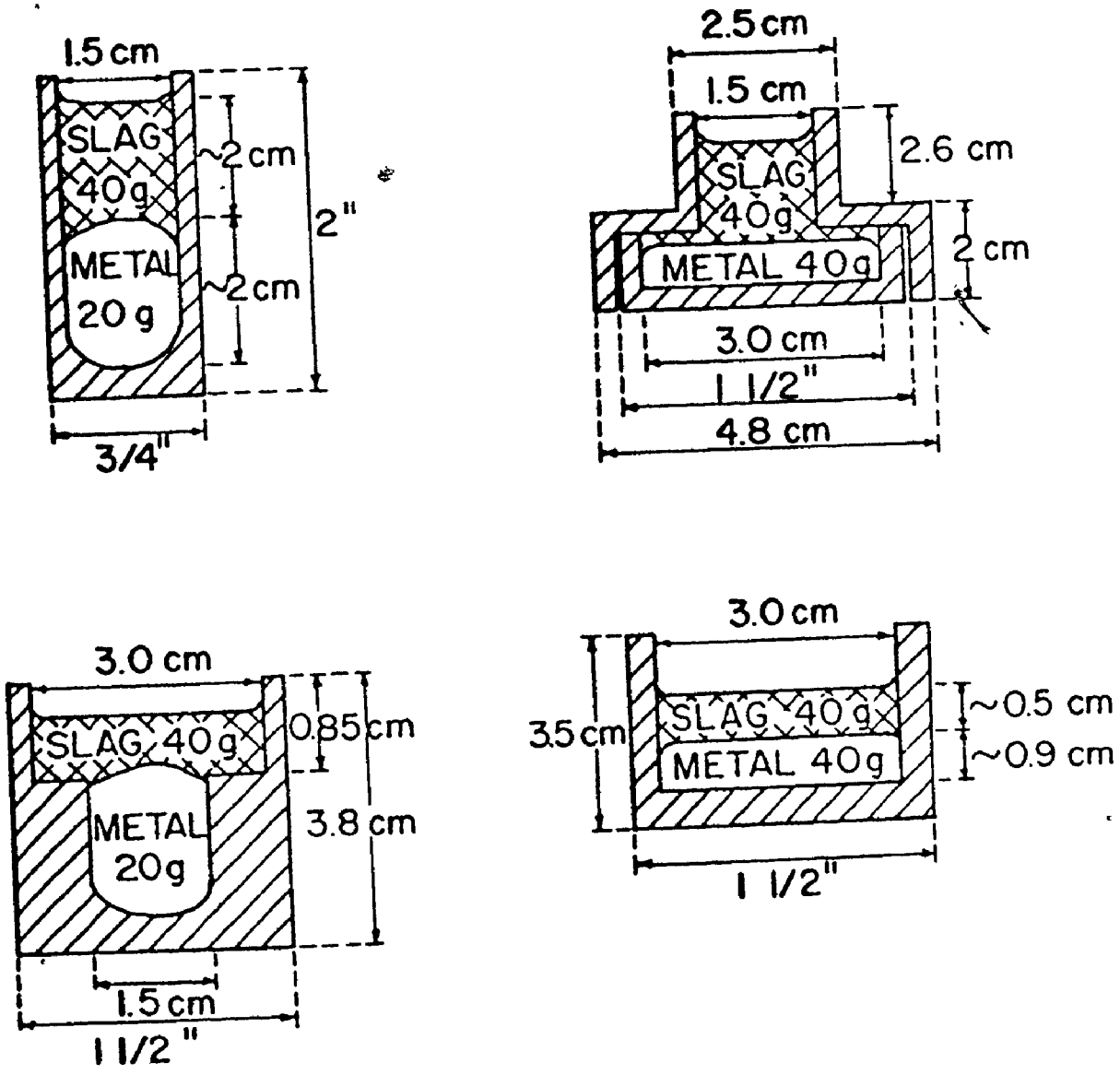

Fig. 27: Dimensions of crucibles used in investigations of effect of interfacial areas (not to scale)

Table XX: Effect of "gas/slag and slag/metal interfacial areas"

Initial metal composition: Fe - C - 0.005wt%S
Reaction Temperature: 1250°C

Time Minutes	Initial metal weight, grams	Initial slag weight, grams	Area of G/S contact, cm^2	Area of M/S contact, cm^2	Fe or Cu lost to slag, g.	Na lost from slag, g.
10	20.00	6.00	1.77	2.55	0.14 Fe	0.115
60	20.00	6.00	1.77	2.55	0.43 "	0.36
10	20.00	6.00	7.07	2.55	0.275 "	0.225
60	20.00	6.00	7.07	2.55	0.86 "	0.715
10	40.00	6.00	1.77	8.30	0.17 "	0.14
60	40.00	6.00	1.77	8.30	0.55 "	0.46
10	40.00	6.00	7.07	8.30	0.35 "	0.285
60	40.00	6.00	7.07	8.30	1.015 "	0.85
			Initial metal composition: Cu- 0.0001wt%C - 0.002wt%S Reaction temperature: 1250°C			
60	40.00	6.00	7.07	8.30	2.81 Cu	1.045

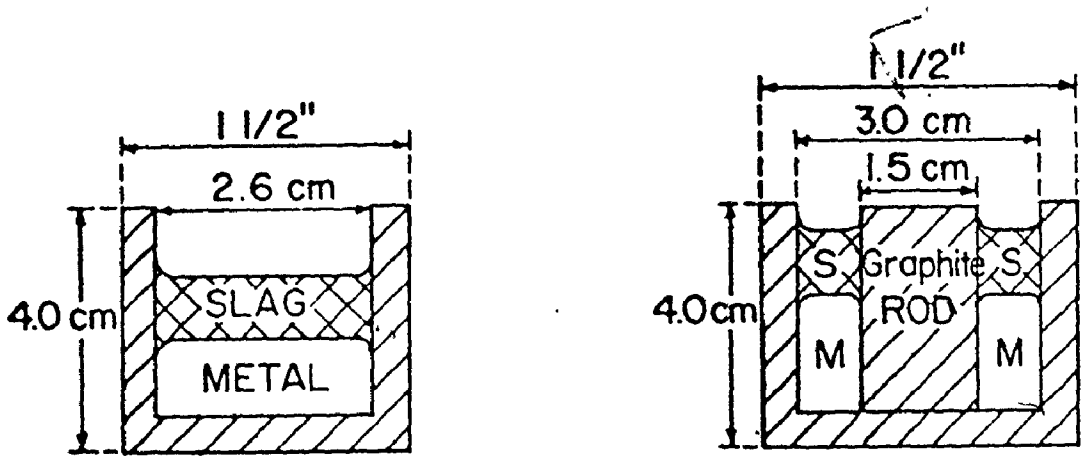

Initial metal composition: Fe - C - 0.005wt%S
Initial metal weight : 40.00 grams
Initial slag weight : 6.00 grams
Time of reaction : 1 hour
Reaction temperature : 1250°C

	G/S interfacial area, cm^2	M/S interfacial area, cm^2	Three-phase contact line length, cm	Fe lost to slag, g	Na lost from slag, g
Crucible 1	6.64	5.31	8.17	0.825	0.68
Crucible 2	6.85	5.31	14.14	0.80	0.70

Fig. 28 and Table XXI: Effect of length of graphite-gas-slag contact line (dimensions of crucibles)

Table XXII: Effect of "argon flow rate"

Initial metal composition: Fe - C - 0.005wt%S
Initial metal weight: 20.00
Initial slag weight: 3.00
Reaction temperature: 1250°C
Reaction time: 1 hour
Crucible diameter: 1.5 cm

Gas flow rate	Fe lost to slag, g.	Na lost from slag, g.
5 cc/min	0.39	0.305
75 cc/min	0.38	0.30
200 cc/min	0.36	0.295
1 lt/min	0.41	0.33
3 lt/min	0.43	0.35

(vii) Effect of "crucible material": Experiments with graphite and recrystallized Al_2O_3 crucibles of the same size were done under identical conditions to find out the effect of crucible material on the rate of reaction. The results are given in Table XXIII.

(viii) Effect of "slag and metal weights": Table XXIV summarizes results obtained for different slag weights with same metal weight as well as for different metal weights with same slag weight, other variables being kept the same.

(ix) Effect of "extremely long times of reaction and high temperature of reaction": As mentioned before, the maximum time of reaction was 48 hours. Beyond this time, the slag was so high in iron sulphide content that the slag and metal phases were more or less a mixture rather than two separate phases sitting one on top of the other. The same type of phenomenonwas observed at shorter times at higher reaction temperatures, e.g., at 1450°C in about 3 hours. So no experimental results have been reported for times beyond 48 hours and for temperatures above 1400°C.

(x) Effect of "initial excess sulphur in the slag phase": Results of experiments with slags containing, initially, different amounts of excess sulphur are given in Table XXV. All the results are for 1 hour experiments at 1250°C. The degree of deviation from stoichiometry is also given as wt%S/wt%Na ratio for each slag.

(xi) Effect of "vacuum": The effect of moderate vacuum on the rate of reaction is summarized in Table XXVI for both carbon-saturated-iron and -copper metallic phases.

Table XXIII: Effect of "crucible material"

Initial metal composition: Fe - C - 0.005wt%S
Initial slag weight: 6.00 grams
Initial metal weight: 40.00 grams
Reaction temperature: 1250°C
Reaction time: 1 hour
Crucible diameter: 3.0 cm

Crucible material	Fe lost to slag, g.	Na lost from slag, g.
Graphite	1.015	0.85
Al_2O_3	0.99	0.80

Table XXIV: Effect of "slag and metal weights"

Initial metal composition: Fe - C - 0.005wt%S
Time of reaction: 1 hour
Reaction temperature: 1250°C
Diameter of graphite crucible: 1.5 cm

Constant slag weight experiments

Metal weight, grams	Slag weight, grams	Fe lost to slag, grams	Na lost from slag, grams
20.00	3.00	0.38	0.30
40.00	3.00	0.38	0.30

Constant metal weight experiments

Metal weight, grams	Slag weight, grams	Fe lost to slag, grams	Na lost from slag, grams
20.00	3.00	0.38	0.30
20.00	6.00	0.43	0.36

Table XXV: Effect of "excess sulphur in the slag phase"

Initial metal composition: Fe - C - 0.005wt%S
Initial metal weight: 20.00 grams
Initial slag weight: 3.00 grams
Reaction time: 1 hour
Reaction temperature: 1250°C
Graphite crucible diameter: 1.5 cm

wt%S in slag	wt%Na in slag	wt%S + wt%Na	Impurities (oxygen + carbon)	S/Na Ratio	Fe lost to slag, g.
41.20	58.55	99.75	0.25	0.705	0.38
41.55	58.25	99.80	0.20	0.713	0.41
41.85	57.75	99.60	0.40	0.725	0.49

Stoichiometric Na_2S: 58.92%Na, 41.08%S, S/Na Ratio = 0.6973

Table XXVI: Effect of "vacuum"

Duration of reaction: 1 hour
Temperature of reaction: 1250°C

Initial Metal composition	Initial metal wt, g.	Initial slag wt, g.	Experimental Conditions	Crucible Diameter cm	Metal lost to slag, g.	Sodium lost from slag, g.
Fe - C - 0.005wt%S	20.00	3.00	with argon flow	1.5	0.38	0.30
"	20.00	3.00	160 mm Hg vacuum	1.5	0.66	0.52
"	40.00	6.00	with argon flow	3.0	1.015	0.85
"	40.00	6.00	135 mm Hg vacuum	3.0	1.35	1.13
Cu - C - 0.002wt%S	20.00	3.00	with argon flow	1.5	1.16	0.43
"	20.00	3.00	150 mm Hg vacuum	1.5	1.83	0.75

5.4 Capillary Experiments

5.4.1 Metal capillary-metal pool

The experimental results obtained for diffusion of sulphur at 1250°C from Fe - C - 0.17wt%S metal capillary to Fe - C - 0.77wt%S metal pool are summarized in Table XXVII. The table also gives the time of diffusion, capillary metal length and final average sulphur content at the end of each experiment.

5.4.2 Slag pool-metal capillary

Table XXVIII summarizes results obtained for different capillary sizes as well as for different slag weights and reaction times. The capillary metal length, capillary metal weight, initial capillary metal composition and final average capillary composition are given for each experimental run.

5.5 Closed-system experiments

The results obtained from the closed-system experiments are presented in Table XXIX. The free-gas volumes which are reported in the table were calculated from the sizes of the crucibles as well as checked by filling the empty space within the crucible with water using a burette. All the results are for reaction temperature of 1250°C and graphite crucibles of 1.5 cm inside diameter.

Table XXVII: Diffusivity of sulphur in carbon-saturated iron at 1250°C

Diameter of capillary	$F*C_o$	$F*\bar{C}$	$F*C_s$	L, cm	Time, sec	D_s cm^2/sec
3 mm	0.28	0.379	1.27	2.38	1800	$2.28*10^{-5}$
3	0.28	0.399	1.27	2.60	3600	$2.06*10^{-5}$
2	0.28	0.415	1.27	2.165	3600	$1.88*10^{-5}$
3	0.28	0.405	1.27	2.60	3600	$2.33*10^{-5}$
3	0.28	0.427	1.27	2.215	3600	$2.35*10^{-5}$
2	0.28	0.430	1.27	2.17	3600	$2.34*10^{-5}$
3	0.28	0.490	1.27	2.15	7200	$2.24*10^{-5}$
2	0.28	0.470	1.27	2.16	7200	$1.87*10^{-5}$
3	0.28	0.500	1.27	2.21	7200	$2.61*10^{-5}$
2	0.28	0.450	1.27	2.215	7200	$1.58*10^{-5}$

where F = Dilution factor used in sulphur analysis = 1.65

Average Diffusivity of sulphur D_s(Average) = $2.15*10^{-5}$ cm^2/sec

Standard Deviation of D_s $\sigma = 0.3*10^{-5}$ cm^2/sec

For method used in evaluating the diffusivities, see discussions

Table XXVIII: Capillary experiments

Slag/Metal reactions
Reaction temperature: 1250°C

Inner capillary diameter, mm	Outer capillary diameter, mm	Time of reaction, seconds	Initial wt of capillary, grams	Final wt of capillary, grams	Capillary wt loss, grams	Final slag weight, grams	l_1 Initial outside length of capillary, cm	l_2 length of inside capillary, cm
1.05	4.25	5400	1.695	1.610	0.085	0.33	3.130	2.925
1.50	4.25	7200	1.857	1.692	0.165	0.762	3.275	3.100
1.50	4.25	5400	1.820	1.705	0.115	0.725	3.200	3.020
1.50	4.25	3600	1.320	1.220	0.100	0.765	2.720	2.48
1.05	4.25	3600	1.535	1.470	0.065	0.32	3.000	2.90
1.50	4.25	3600	1.800	1.690	0.110	0.88	3.170	3.00
1.05	4.25	5400	1.595	1.475	0.120	0.77	2.985	2.865

(continued)

Table XXVIII: Capillary experiments (continued)

Initial F*wt%S in capillary	Final average F*wt%S in capillary	Interface F*wt%S	Final capillary length cm	Diffusivity D_s cm^2/sec *
1.30	1.13	0.06	3.05	$2.55*10^{-5}$
1.30	1.10	0.06	3.135	$2.78*10^{-5}$
1.30	1.07	0.06	3.10	$4.76*10^{-5}$
1.30	1.075	0.06	2.65	$5.04*10^{-5}$
1.30	1.185	0.06	2.96	$1.485*10^{-5}$
1.30	1.14	0.06	3.09	$3.47*10^{-5}$
1.30	1.045	0.06	2.875	$5.04*10^{-5}$

where F = 6.0

For method used in evaluating the diffusivity of sulphur, see discussions

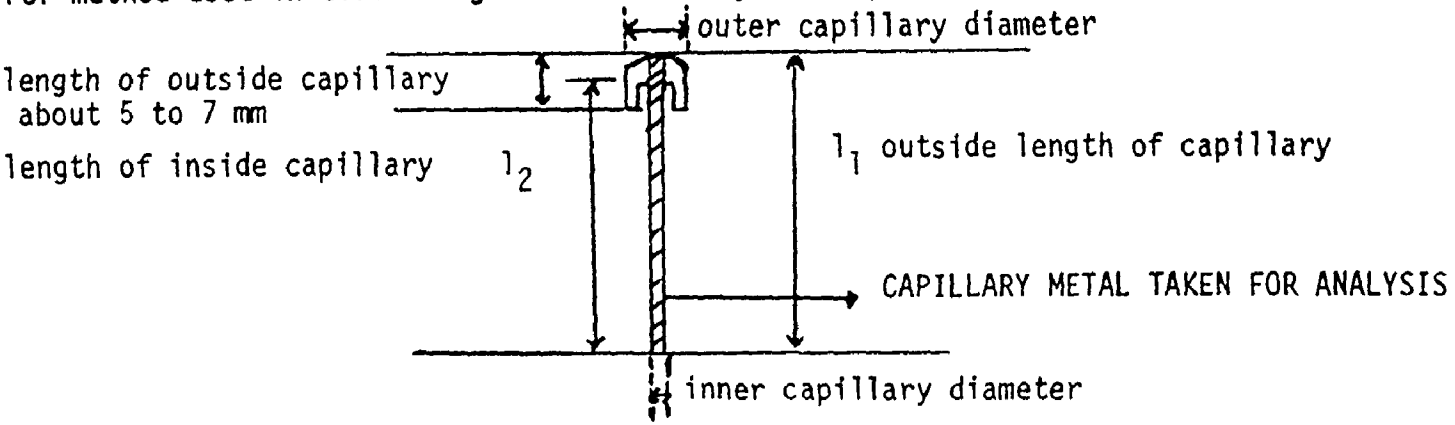

Table XXIX: Closed-system experiments

Reaction temperature: 1250°C
Inside diameter of graphite crucible: 1.5 cm

Initial metal composition	Initial metal wt, g.	Initial slag wt, g.	Reaction time, minutes	Free gas volume, cc	Fe lost to slag, g.	wt lost from S/M system, g.	Final wt%S
Fe - C - 0.005wt%S	20.0154	3.0025	30	6.5	0.030	0.0025	0.004
Fe - C - 0.005wt%S	20.0073	3.0056	60	11.5	0.035	0.0035	0.003
Fe - C - 0.005wt%S	20.0030	2.9975	30	7.0	0.025	0.0002	0.003
Fe - C - 0.75wt%S	20.0096	3.0030	30	17.0	0.260	0.012	0.007

CHAPTER 6

DISCUSSION OF RESULTS

6.1 Introduction

In this chapter, the experimental observations presented in the previous chapter are discussed. The discussions involve the stability of sodium sulphide at high temperatures as well as the thermodynamics and kinetics of the slag/metal reactions under study. An electrochemical explanation of the slag/metal reactions is presented in detail. A reaction mechanism is also proposed for the present study, which is consistent with the experimental observations and results. The assumptions made in the derivation of the mixed-control reaction model are discussed. The discussions of results of the closed-system and capillary experiments are also included in this chapter.

6.2 Thermal stability of sodium sulphide

From the periodic table of sulphides, it can be seen that sodium sulphide will most probably dissociate rather than volatilize at high temperatures, see Table I. There is no reported mass spectrometric or gravimetric study on sodium sulphide because of its hygroscopic nature. However, it is known that in the absence of moisture, sodium sulphide is reasonably stable at high temperatures and does not react with graphite.[37] At 1250°C, the dissociation pressure is quite high, of the order of 10^{-3} atm., (see Appendix I for calculations). In the actual experiments,

since the molten slag was heated under a flow of argon, there was a continuous loss of weight from the slag by decomposition and vaporization. The vapour species from the slag condensed on the colder parts of the alumina reaction tube.

It is known that Na_2S is the most stable form of Na-S compounds at high temperatures. However, other polysulphides, such as $Na_2S_{1.37}$ and $Na_2S_{1.9}$ have also been found to be stable to some degree.[40] The calculated final remaining sulphur and sodium contents in the slag, in the actual experiments, are given in Table XXX. A plot of weight loss from the slag observed against time was assumed to be linear as seen in Fig. 17. However, a slight change in melt properties, i.e., departure from stoichiometry (see Table XXX), should give rise to some non-linearity. Nevertheless, due to the hygroscopic nature of slag, the results reported could have some error.

As approximate calculation for estimating the weight loss expected under vacuum using Knudsen's equation[59] is also given in Appendix II. To calculate the dissociation pressures and the weight loss, it was assumed that the only form of sodium present in gas phase was monatomic Na_1 rather than diatomic Na_2. The second assumption was that the composition of the sulphide slag did not change with time, i.e., remained stoichiometric. The third assumption was related to the condensation coefficient α in the Knudsen equation, the value of which varies in the range 0 and 1. In the calculations $\alpha = 1$ was taken. With these assumptions, the calculations in Appendix II showed that Knudsen's equation was not quite applicable under the present experimental conditions.

Table XXX: Na_2S weight loss from a 1.5 cm ϕ graphite crucible

Initial slag weight = 3.00 grams

Temperature = 1250°C

Furnace atmosphere = Argon

Time (hours)	0	1	3	8
Na_2S wt loss observed, grams	0.03	0.09	0.185	0.52
Wt%S remaining	41.20	41.3	41.9	42.9
Wt%Na remaining	58.55	58.3	57.65	56.7
Final weight of slag, g	2.97	2.91	2.815	2.48
Weight of S remaining, g	1.22	1.20	1.118	1.065
Weight of Na remaining, g	1.74	1.70	1.62	1.41

6.3 Thermodynamic Calculations

6.3.1 For the case of carbon-saturated iron

The desulphurization and sulphurization of Fe-C-S alloys with sodium sulphide slags can be described by the following reaction:

$$(Fe) + [\underline{S}] \rightleftharpoons (\text{"FeS"}) \qquad (6.1)$$

where $[\underline{S}]$ represents sulphur dissolved in iron and ("FeS") means non-stoichiometric liquid iron sulphide in the slag phase.

The solubility limit of sulphur in Fe-C melts can be calculated from the available thermodynamic data (see Appendix III). However, E.T. Turkdogan and A. Hancook[48] have already reported some reliable data on this system by experimental equilibration of "FeS" with Fe-C melts, Fig. 3. From their data, it is known that the solubility of "FeS" in Fe-C melts at 1250°C is 1.8 wt%$\underline{S}$. Taking sulphur-saturated metal in equilibrium with pure molten iron sulphide as the reference state, the activity of iron sulphide in sodium sulphide slag can be calculated using simple proportionality, as proposed for the activity calculations of the binary and ternary oxide systems.[60,61,62]

$$a_{\text{"FeS"}} = \frac{[\text{wt\%}\underline{S}]_{(Na_2S - \text{"FeS" slag})}}{[\text{wt\%}\underline{S}]_{(\text{"FeS"})}} \qquad (6.2)$$

The above relationship is true, if slag and metal are at equilibrium and the diffusion steps in bulk phases are fast. The calculated values of activity of iron sulphide in Na_2S-"FeS" solution are given in Table XXXI for graphite crucibles of different sizes. The deviation of the Na_2S-"FeS" system from ideality has been expressed through the use of the activity coefficient $\gamma_{\text{"FeS"}}$. The calculations demonstrate that the Na_2S-"FeS" system has negative deviation from the ideal law.

Table XXXI: Calculated thermodynamic parameters

$A_{S/G} = 1.77\ cm^2$
$A_{S/M} = 2.55\ cm^2$

Metal Phase: Fe - C - 0.005wt%S

Time, Hours	1/2	1	2	3	4	5	6	7	8
wt%S	0.0135	0.018	0.027	0.036	0.045	0.063	0.090	0.117	0.137
X_{FeS}	0.11	0.175	0.26	0.32	0.37	0.41	0.44	0.47	0.485
$a_{"FeS"}$	0.0075	0.010	0.015	0.020	0.025	0.035	0.050	0.065	0.075
X_{Na_2S}	0.89	0.825	0.74	0.68	0.63	0.59	0.56	0.53	0.515
a_{Na_2S}	0.87	0.80	0.70	0.63	0.57	0.48	0.43	0.37	0.33
$\gamma_{"FeS"}$	0.07	0.06	0.06	0.0625	0.0675	0.085	0.115	0.14	0.155
γ_{Na_2S}	0.98	0.97	0.945	0.925	0.905	0.81	0.77	0.70	0.64
P_{Na}, atm.	0.087	0.0725	0.055	0.0455	0.039	0.030	0.024	0.019	0.017

(continued)

X_{FeS}, X_{Na_2S} = Mole fractions of FeS and Na_2S, respectively

$a_{"FeS"}$, a_{Na_2S} = Activities of "FeS" and Na_2S, respectively

$\gamma_{"FeS"}$, γ_{Na_2S} = Activity coefficients of "FeS" and Na_2S, respectively

wt%S = weight per cent sulphur in metal phase

P_{Na} = Partial pressure of sodium in gas phase

Table XXXI: Calculated thermodynamic parameters (continued)

$A_{S/G}$ = 1.77 cm^2

$A_{S/M}$ = 2.55 cm^2

Metal Phase

Fe - C - 0.7wt%S

Time, Hours	1/2	1	3	8	24	48
wt%S	0.016	0.0215	0.050	0.207	0.57	0.94
X_{FeS}	0.145	0.24	0.39	0.53	0.65	0.75
$a_{"FeS"}$	0.009	0.012	0.028	0.115	0.32	0.52
X_{Na_2S}	0.855	0.76	0.61	0.47	0.35	0.25
a_{Na_2S}	0.82	0.66	0.55	0.26	0.036	0.02
$\gamma_{"FeS"}$	0.062	0.05	0.072	0.217	0.49	0.693
γ_{Na_2S}	0.96	0.87	0.90	0.55	0.103	0.08
P_{Na}, atm.	0.077	0.060	0.036	0.012	0.0027	0.0016

Where, $A_{S/G}$ = slag/gas interfacial area

$A_{S/M}$ = slag/metal interfacial area

(continued)

Table XXXI: Calculated thermodynamic parameters (continued)

$A_{S/G}$ = 7.07 cm^2
$A_{S/M}$ = 8.30 cm^2

Metal Phase
Fe - C - 0.005wt%S

(where $A_{S/G}$ = slag/gas interfacial area, $A_{S/M}$ = slag/metal interfacial area)

Time, Hours	1	2	3	4	5	6	7	8
wt%S	0.027	0.0315	0.036	0.0405	0.045	0.054	0.072	0.090
X_{FeS}	0.235	0.301	0.336	0.360	0.383	0.403	0.422	0.441
$a_{"FeS"}$	0.015	0.0175	0.020	0.0225	0.025	0.03	0.04	0.05
X_{Na_2S}	0.765	0.699	0.664	0.640	0.617	0.597	0.578	0.559
a_{Na_2S}	0.73	0.66	0.61	0.58	0.54	0.505	0.47	0.43
$\gamma_{"FeS"}$	0.064	0.058	0.0595	0.0625	0.065	0.0745	0.095	0.113
γ_{Na_2S}	0.955	0.945	0.92	0.905	0.875	0.845	0.815	0.77
P_{Na}, atm.	0.0566	0.050	0.045	0.041	0.038	0.033	0.028	0.024

$A_{S/G}$ = 7.07 cm^2
$A_{S/M}$ = 2.55 cm^2

Metal Phase
Fe - C - 0.005wt%S

Time, Hours	1	2	3	4	5	6	7	8
wt%S	0.0225	0.0315	0.038	0.0415	0.045	0.0485	0.054	0.063
X_{FeS}	0.200	0.267	0.302	0.327	0.350	0.371	0.390	0.408
$a_{"FeS"}$	0.0125	0.0175	0.0210	0.0230	0.025	0.027	0.030	0.035
X_{Na_2S}	0.800	0.733	0.698	0.673	0.650	0.629	0.610	0.592
a_{Na_2S}	0.77	0.69	0.655	0.625	0.59	0.56	0.53	0.50
$\gamma_{"FeS"}$	0.063	0.066	0.070	0.070	0.0714	0.0728	0.077	0.0857
γ_{Na_2S}	0.96	0.94	0.94	0.93	0.91	0.89	0.87	0.845
P_{Na}, atm.	0.064	0.051	0.045	0.042	0.039	0.037	0.034	0.0305

In fact, inspection of the Na_2S - FeS phase diagram[63] indicates that a negative deviation is to be expected since the phase diagram shows stable solid compounds between Na_2S and FeS, Fig. 29. The activity and activity coefficient of Na_2S have also been calculated through the use of the Gibbs-Duhem equation. The calculations also indicate that γNa_2S is less than unity. An activity diagram for the Na_2S - "FeS" system summarizes the calculated results, Fig. 31.

Now, the overall reaction may be represented by the chemical reaction:

$$(Na_2S) + (Fe) \rightleftharpoons (\text{"FeS"}) + 2\{Na\} \qquad (6.3)$$

where, ( ) brackets represents the liquid state and { } the gaseous state. The thermodynamic properties of the above reaction can be obtained from the data on standard free energy of formation of non-stoichiometric iron sulphide[64] and sodium sulphide.[43]

$$(Fe) + \tfrac{1}{2}\{S_2\} \longrightarrow (\text{"FeS"}) \qquad \Delta G^\circ_{1523^\circ K} = -17938 \text{ cal/mole} \qquad (6.4)$$

$$2\{Na\} + \tfrac{1}{2}\{S_2\} \longrightarrow (Na_2S) \qquad \Delta G^\circ_{1523^\circ K} = -45886 \text{ cal/mole} \qquad (6.5)$$

Therefore, the standard free energy change for reaction (6.3) is the sum of the corresponding values of the reactions (6.4) and (6.5) at 1250°C (1523°K).

Then,

$$\Delta G^\circ_{1523^\circ K} = 27948 = -RT\ln K = -RT\ln \frac{a_{\text{"FeS"}} \cdot P^2_{Na}}{a_{Na_2S} \cdot a_{Fe}} \qquad (6.6)$$

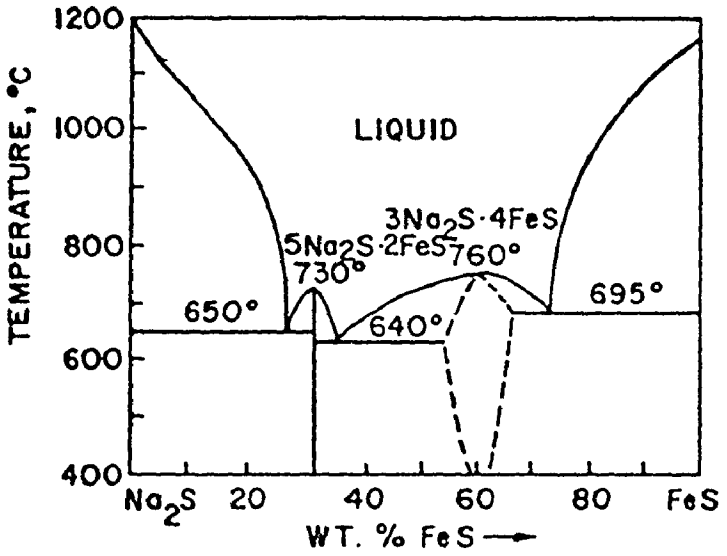

Fig. 29: System Na_2S - FeS[63]

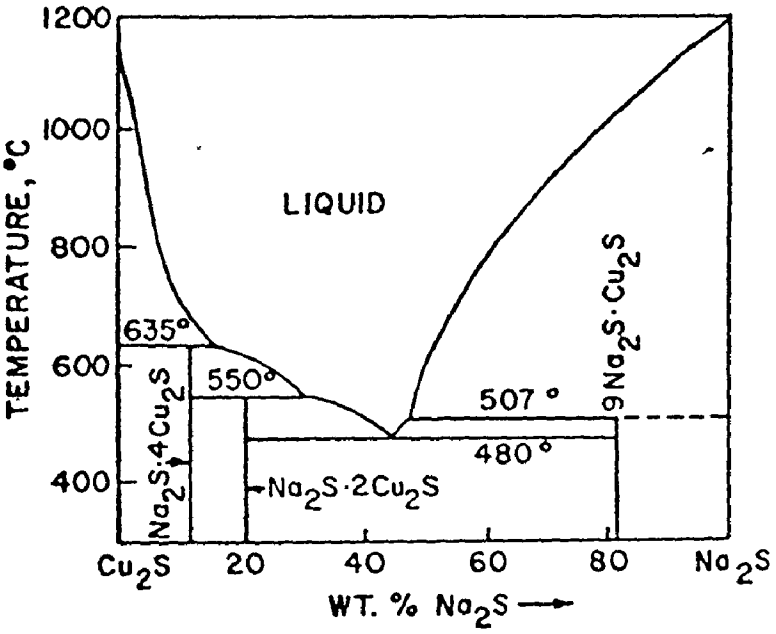

Fig. 30: System Cu_2S - Na_2S[65]

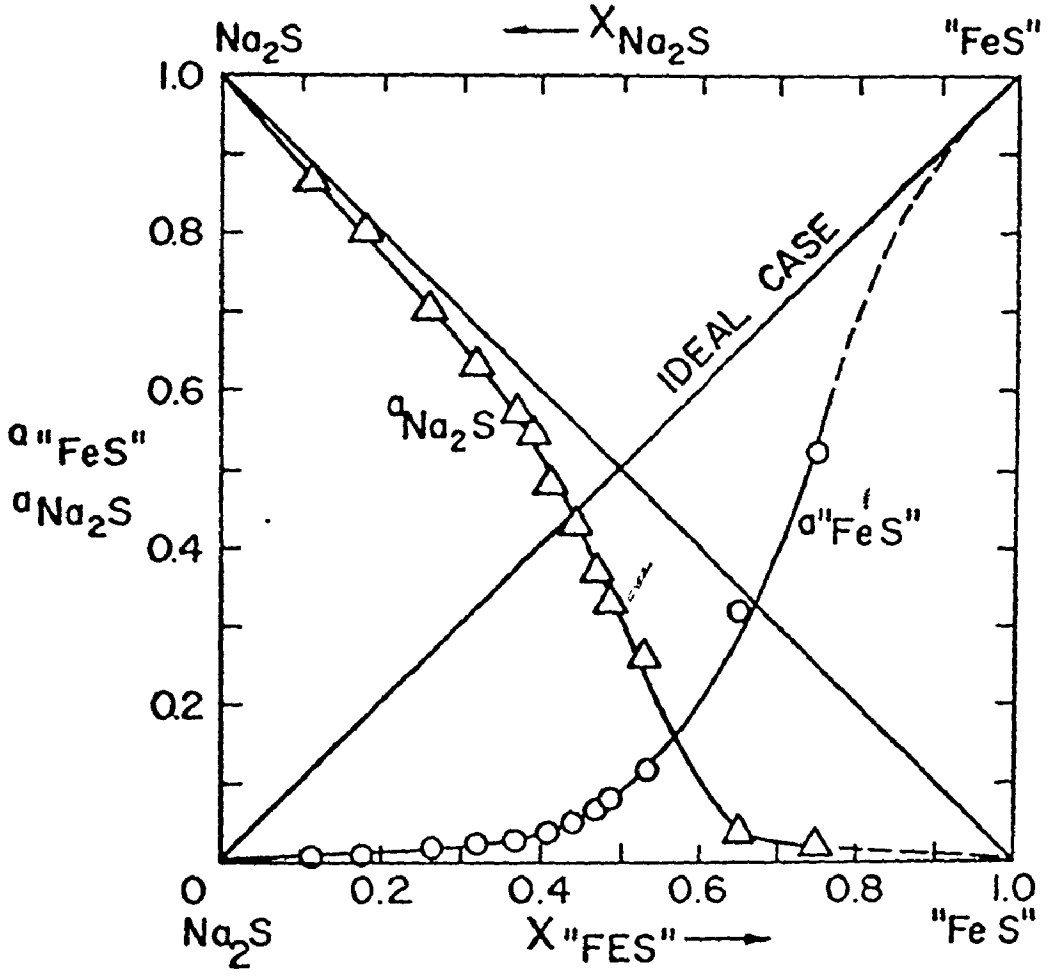

Fig. 31: "FeS" - Na_2S Activity diagram at 1250°C

Reference state: Activity of pure liquid "FeS" = 1.0

Rearranging the above equation and substituting the calculated values of activities of "FeS" and Na_2S and taking the value of the activity of iron, containing about 4.5 wt%C, equal to 0.675[34], Fig. 32, the partial pressure of sodium above the melt can be calculated for different reaction times, Table XXXI.

Thus, these calculations indicate that in the Na_2S - "FeS" system, there is a strong interaction between the two sulphides in the slag phase.

In Appendices IV and V, detailed calculations of activities of Cu_2S, Na_2S, FeS and MnS in ternary Na_2S - FeS - Cu_2S and Na_2S - FeS - MnS slags are given. In these calculations, a behaviour similar to that of binary was assumed, i.e., observed sulphur levels in the metal phase were related to FeS activity in ternary slags.

6.3.2 For the case of carbon-saturated copper

A similar approach to the one described for carbon-saturated iron can be used for the case of carbon-saturated copper. The solubility limit of sulphur in copper has been reported[47] to be 1.65 wt% at 1250°C, (see Cu-S binary diagram, Fig. 5). Although in the actual experiments, there was 0.0001 wt% carbon present in the copper phase, it was assumed that the effect of small amount of carbon on the solubility of sulphur in copper was negligible. Again, taking as a reference state the system in which sulphur-saturated metal is in equilibrium with pure molten Cu_2S, the activity of copper sulphide in sodium sulphide was calculated using the relationship,

$$a_{Cu_2S} = \frac{[wt\%\underline{S}]_{(Na_2S - Cu_2S\ Slag)}}{[wt\%\underline{S}]_{(Cu_2S)}} \qquad (6.7)$$

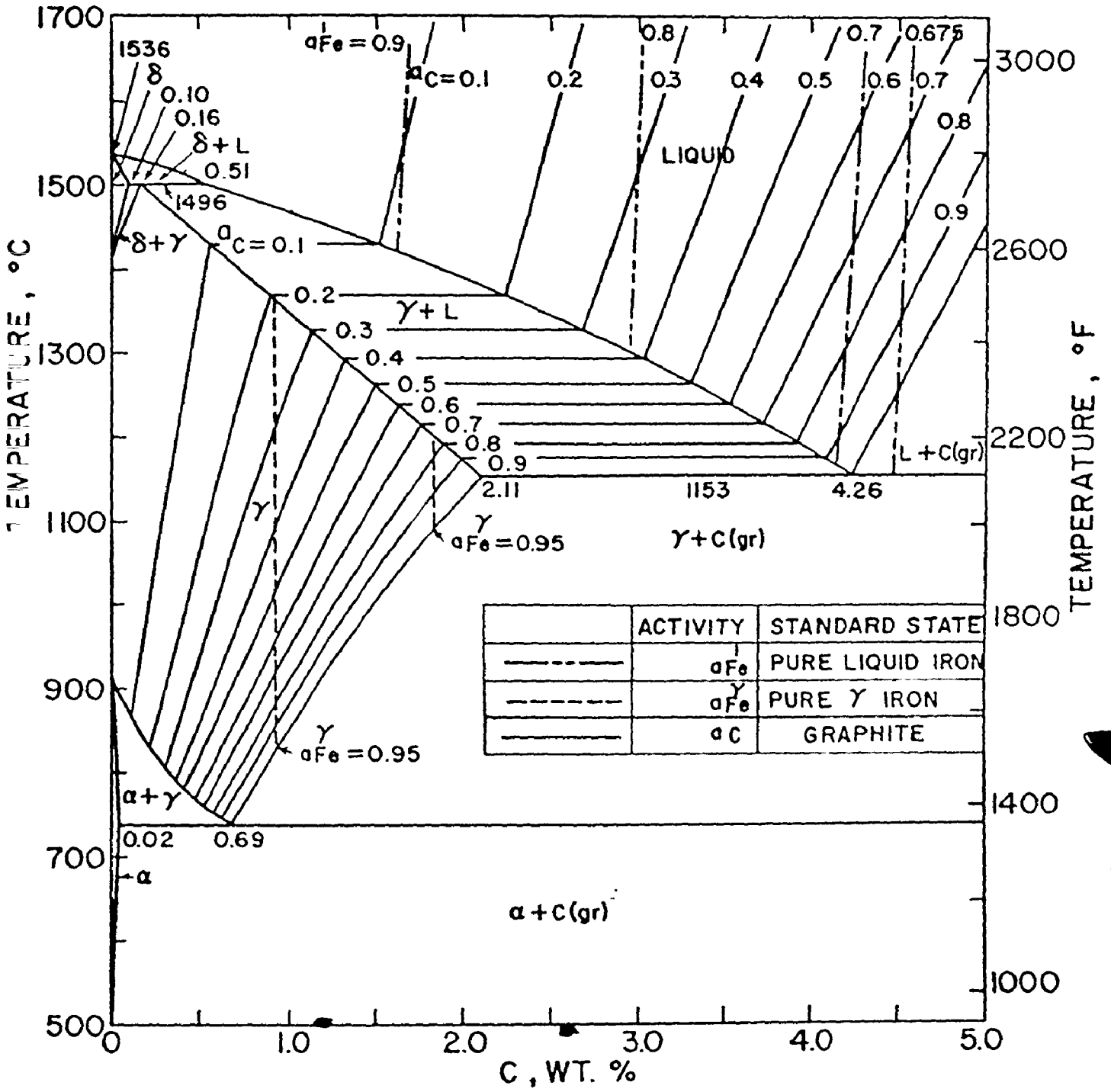

Fig. 32: Iso-activity curves for iron and carbon in the liquid and the γ-phase regions of the stable iron-graphite system

The calculated values of activities of copper sulphide in Na_2S - Cu_2S solution are given in Table XXXII for graphite crucibles of different size. Calculations show that the Na_2S - Cu_2S system has a negative deviation from ideality like the Na_2S - "FeS" system but not as strong. Figure 33 summarizes calculated activities of copper sulphide and sodium sulphide and indicates a negative deviation from ideality in both cases. The work of Richardson et al.[24] also reported negative deviation from ideality at lower temperatures. Figure 30 shows the binary Na_2S - Cu_2S diagram.[65]

The overall reaction for the case of copper can be represented by the chemical reaction,

$$(Na_2S) + 2(Cu) \rightleftharpoons (Cu_2S) + 2\{Na\} \qquad (6.8)$$

The thermodynamic properties of the above reaction were obtained from the data on the standard free energy of formation of copper sulphide[34,66] and sodium sulphide,[43]

$$2(Cu) + \frac{1}{2}\{S_2\} \longrightarrow (Cu_2S) \qquad \Delta G^\circ_{1523^\circ K} = -20200 \text{ cal/mole} \qquad (6.9)$$

$$2\{Na\} + \frac{1}{2}\{S_2\} \longrightarrow (Na_2S) \qquad \Delta G^\circ_{1523^\circ K} = -45886 \text{ cal/mole} \qquad (6.10)$$

Therefore, the standard free energy charge for reaction (6.8) given above is the sum of the corresponding values for the reactions (6.9) and (6.10) at 1250°C.

Then,

$$\Delta G^\circ = 25686 = -RT\ln \frac{a_{Cu_2S} \cdot P_{Na}^2}{a_{Na_2S} \cdot a_{Cu}^2} \qquad (6.11)$$

Table XXXII: Calculated thermodynamic parameters

$A_{S/G} = 1.77\ cm^2$

$A_{S/M} = 2.55\ cm^2$

Metal Phase: Cu - 0.0001 wt%C - 0.002 wt%S

Time, Hours	1	2	3	4	5	6	7	8
wt%S	0.035	0.063	0.096	0.145	0.200	0.240	0.295	0.340
X_{Cu_2S}	0.238	0.321	0.38	0.427	0.486	0.523	0.566	0.603
a_{Cu_2S}	0.021	0.038	0.058	0.088	0.121	0.145	0.179	0.206
X_{Na_2S}	0.762	0.679	0.62	0.573	0.514	0.477	0.434	0.397
a_{Na_2S}	0.67	0.532	0.424	0.321	0.247	0.205	0.16	0.130
γ_{Cu_2S}	0.089	0.119	0.153	0.206	0.249	0.278	0.315	0.342
γ_{Na_2S}	0.88	0.784	0.684	0.56	0.481	0.43	0.368	0.328
$P_{Na,atm.}$	0.081	0.054	0.039	0.0275	0.0205	0.017	0.0135	0.0115

continued

Table XXXII: Calculated thermodynamic parameters (continued)

$A_{S/G} = 7.07\ cm^2$

$A_{S/M} = 8.30\ cm^2$

Metal Phase: Cu - 0.0001 wt%C - 0.002 wt%S

Time, Hours	1	2	3	4	5	6	7	8
wt%S	0.0495	0.0907	0.1155	0.140	0.173	0.198	0.2145	0.231
X_{Cu_2S}	0.287	0.352	0.387	0.416	0.445	0.467	0.488	0.506
a_{Cu_2S}	0.03	0.055	0.07	0.085	0.105	0.12	0.13	0.14
X_{Na_2S}	0.713	0.648	0.613	0.583	0.555	0.533	0.512	0.494
a_{Na_2S}	0.58	0.46	0.40	0.35	0.30	0.27	0.25	0.225
γ_{Cu_2S}	0.104	0.156	0.181	0.204	0.236	0.257	0.266	0.276
γ_{Na_2S}	0.814	0.709	0.652	0.60	0.5405	0.507	0.488	0.456
$P_{Na,atm.}$	0.063	0.0415	0.034	0.029	0.024	0.0215	0.020	0.018

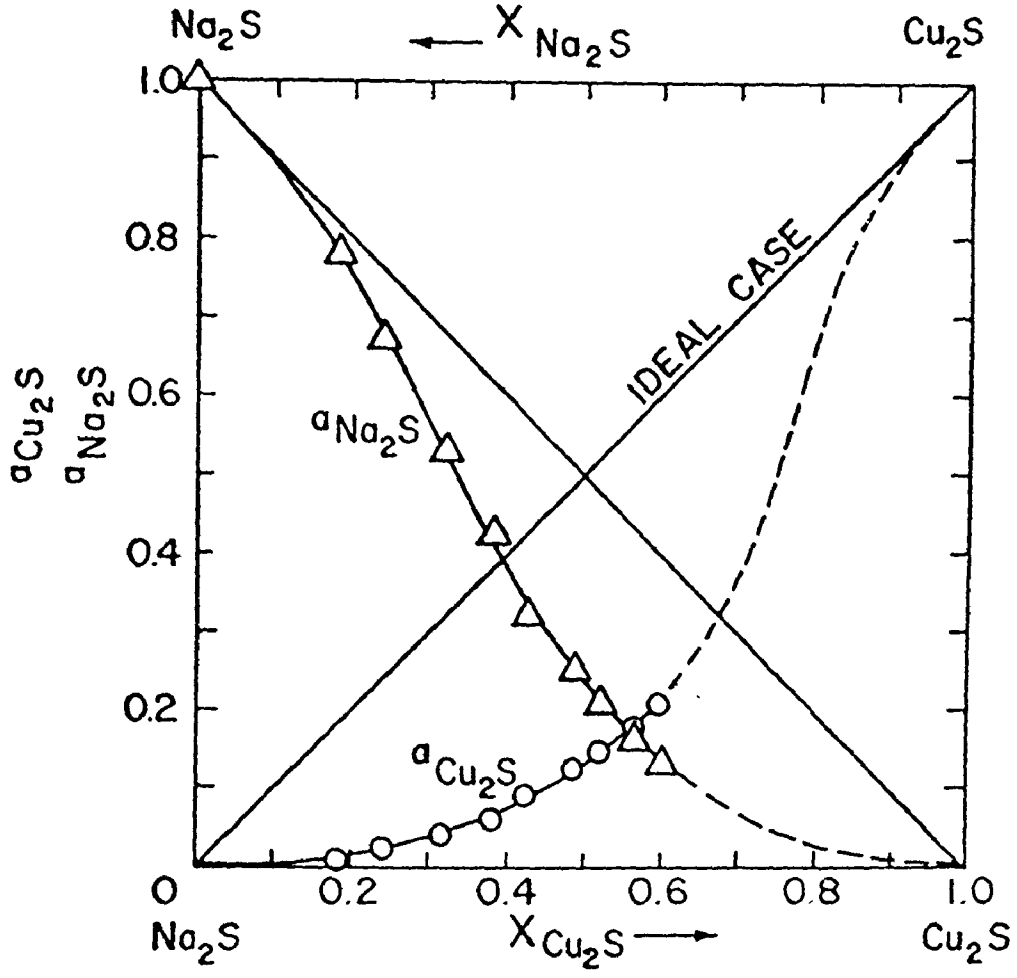

Fig. 33: Cu_2S - Na_2S Activity diagram at 1250°C

Reference state: Activity of pure copper sulphide = 1.0

Rearranging Eq. (6.11) and substituting the calculated values of activities of Cu_2S and Na_2S and taking the value of activity of copper equal to 1.0, the partial pressure of sodium above the melt was calculated for different reaction times. A plot of P_{Na} against time for the case of iron and copper metallic phases shows the fast decrease in the sodium partial pressure, above the melt, with increasing time. In the case of copper, the initial decrease was found to be faster than in the case of iron, Fig. 34.

6.4 Electrochemical explanation of slag/metal reactions

As summarized by Fig.19 to 26, there was always a decrease in the sodium and corresponding increases in iron, copper and manganese contents of the slag during the course of the slag/metal reactions. The initial rate of loss of sodium was relatively high but decreased as time passed. The rapid decrease in the rate of sodium loss in the early stages of the slag/metal reaction was most probably due to the decrease in the driving force as well as the decrease in the area of slag/metal interface caused by the decay of turbulence, created by addition of liquid metal to the slag phase. As it can be seen from Fig. 35, the amount of sodium loss was higher in the cases of manganese-and copper-containing melts. Figure 35 also shows, for comparison, the total weight loss from Na_2S at 1250°C in the absence of a metal phase. The presence of the metal phase enhances the rate of loss of sodium. Figure 24 illustrates that the high rate of loss of manganese to the slag phase substantially suppressed the transfer of iron to the slag. As the metal phase became depleted in manganese the

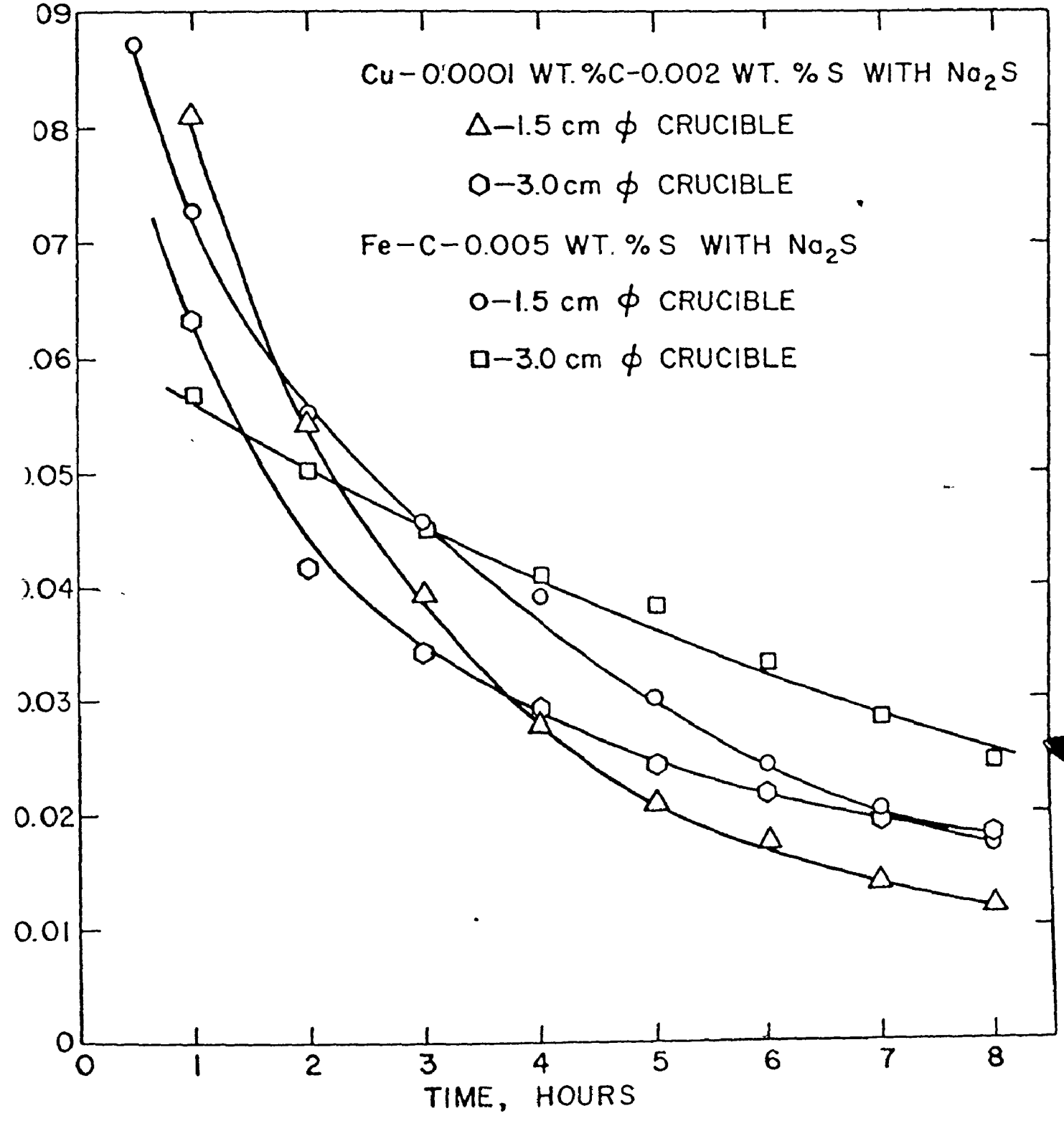

Fig. 34: Change of partial pressure of sodium vapour with time

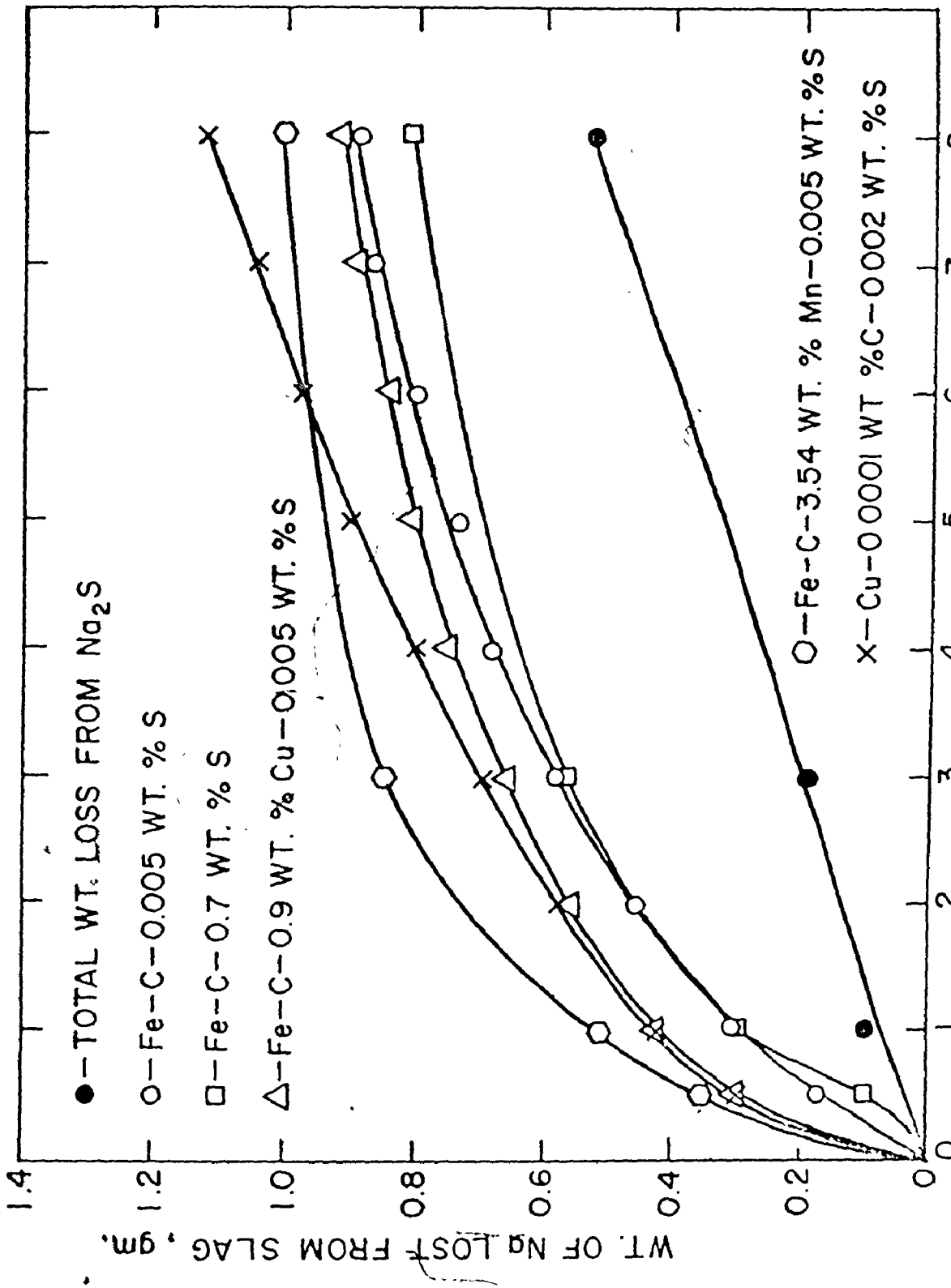

Fig. 35: Sodium lost from slag (grams) against time (hours) (For 1.5 cm ϕ crucibles)

rate of iron transfer increased substantially at longer times of reaction.

The relationship between the transfer of various elements is shown in Figs. 36 to 43. The quantity plotted is the number of chemical equivalents of S, Fe, Mn and Cu transferred to the slag, or the number of equivalents of Na evolved against reaction time. It is evident that the sum of the equivalents of Fe, Mn, Cu and S corresponds very closely at all times with the equivalents of sodium lost from the slag. An exact correspondence is not expected in view of the experimental and analytical errors as well as errors due to assumptions about the valence state of the ions present in the slag phase. For simplicity, it was assumed that the slag contained only Fe^{++}, Mn^{++} and Cu^{+} ions. However, it is known that Mn, Fe and Cu may have mixed valence states.

If $\dot{n}$ represents the rate of transfer or evolution, in moles per second, the positive sign being used for metal to slag transfer and the negative for the reverse reactions and sodium loss from the slag phase,

$$-2\dot{n}_S + 2\dot{n}_{Fe} + 2\dot{n}_{Mn} + \dot{n}_{Cu} = \dot{n}_{Na} \qquad (6.12)$$

This relationship was satisfactorily confirmed in all experiments whether sulphur transfer was from slag to metal or metal to slag, with the correct sign being inserted in the equation above.

These observations are more readily understood if transfers from the metallic phase to the ionic slag phase or vice versa are considered as electrochemical partial reactions. Sulphur, at the oxygen potential of carbon-saturated iron, must exist in the slag as sulphide ions.[67]

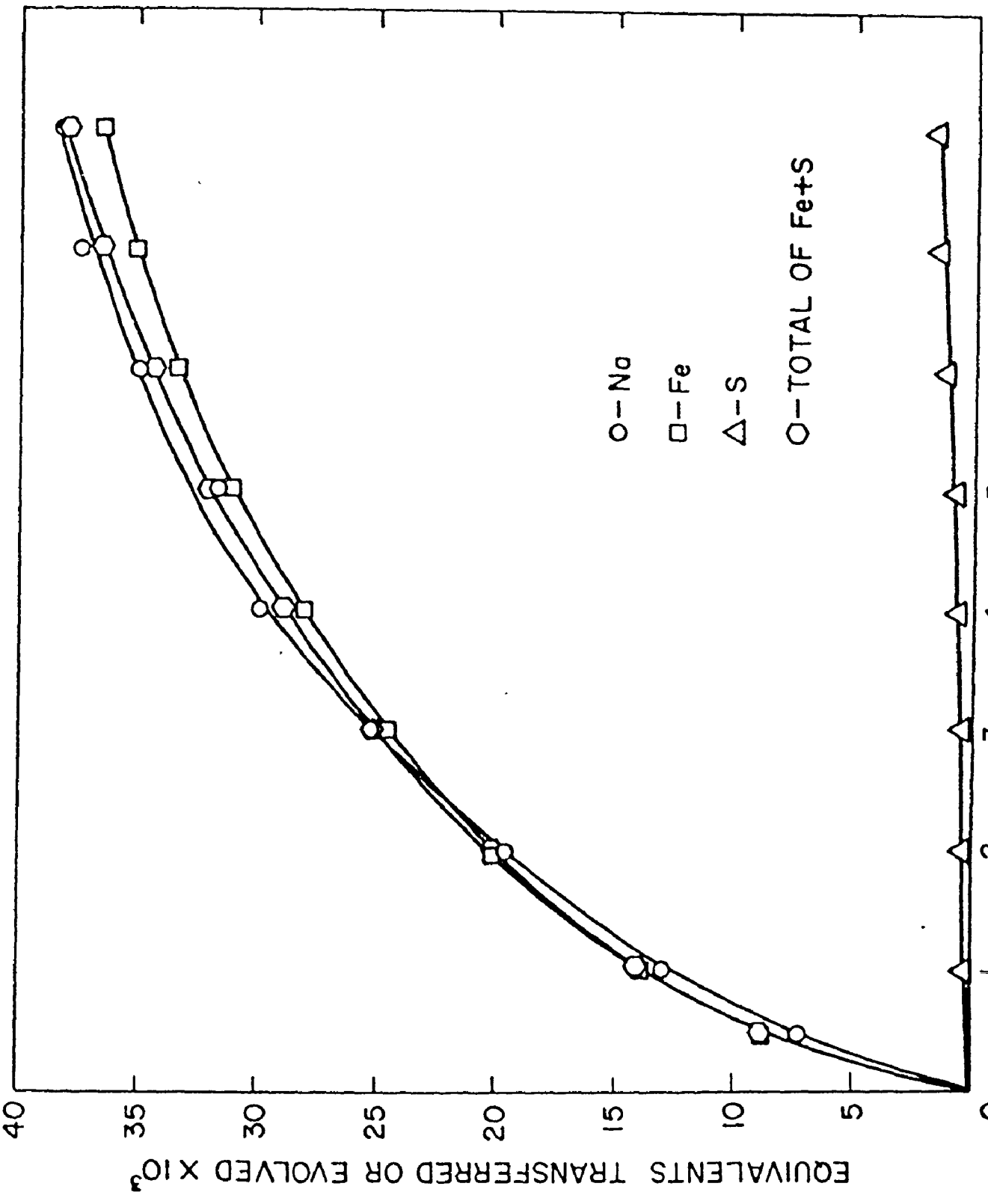

Fig. 36: Equivalent transferred or evolved against time (For Fe - C - 0.005wt%S alloy with dehydrated Na_2S, 1.5 cm ϕ crucible)

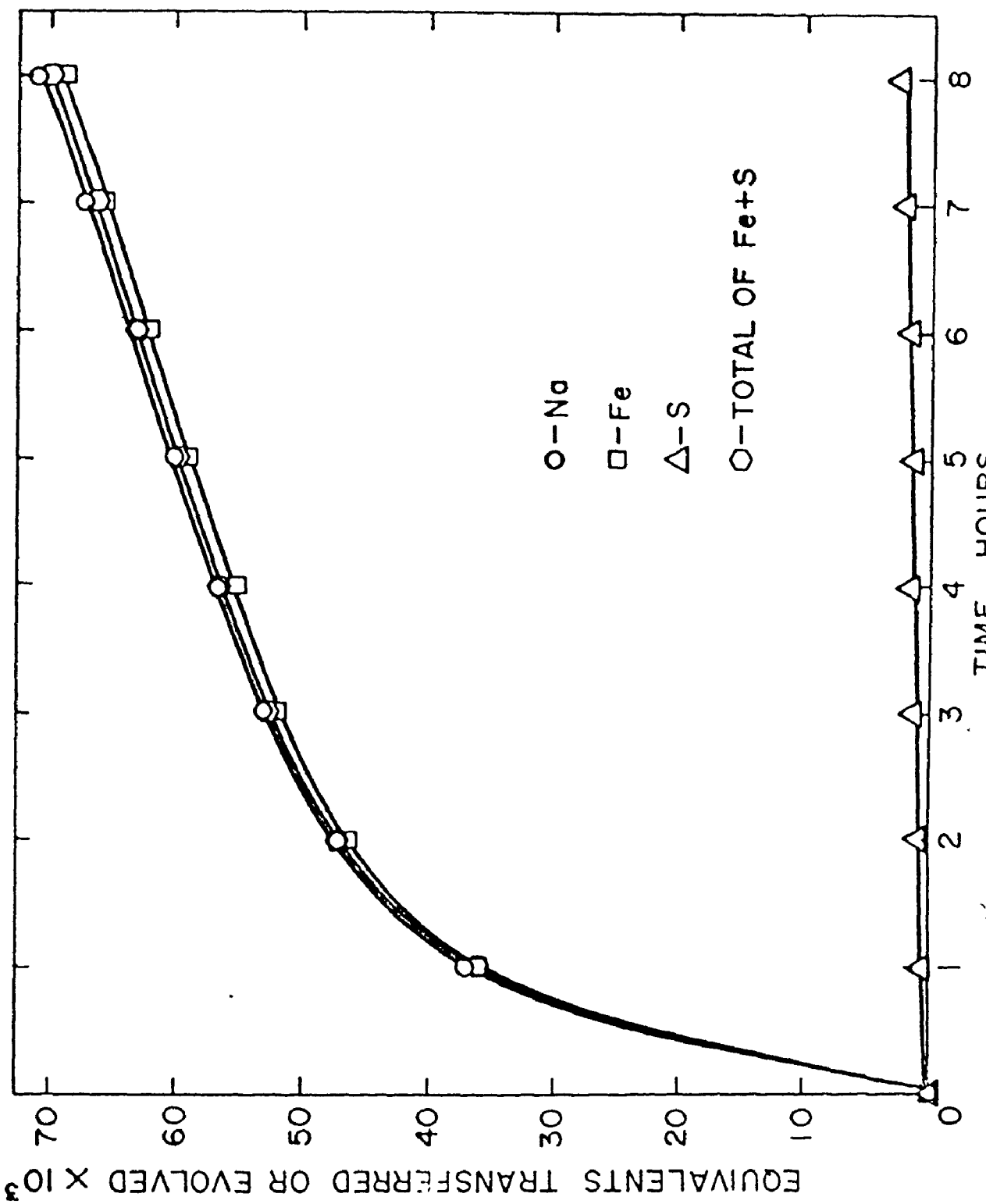

Fig. 37: Equivalent transferred or evolved against time (For Fe - C - 0.005wt%S with dehydrated Na_2S, 3.0 cm ϕ crucible)

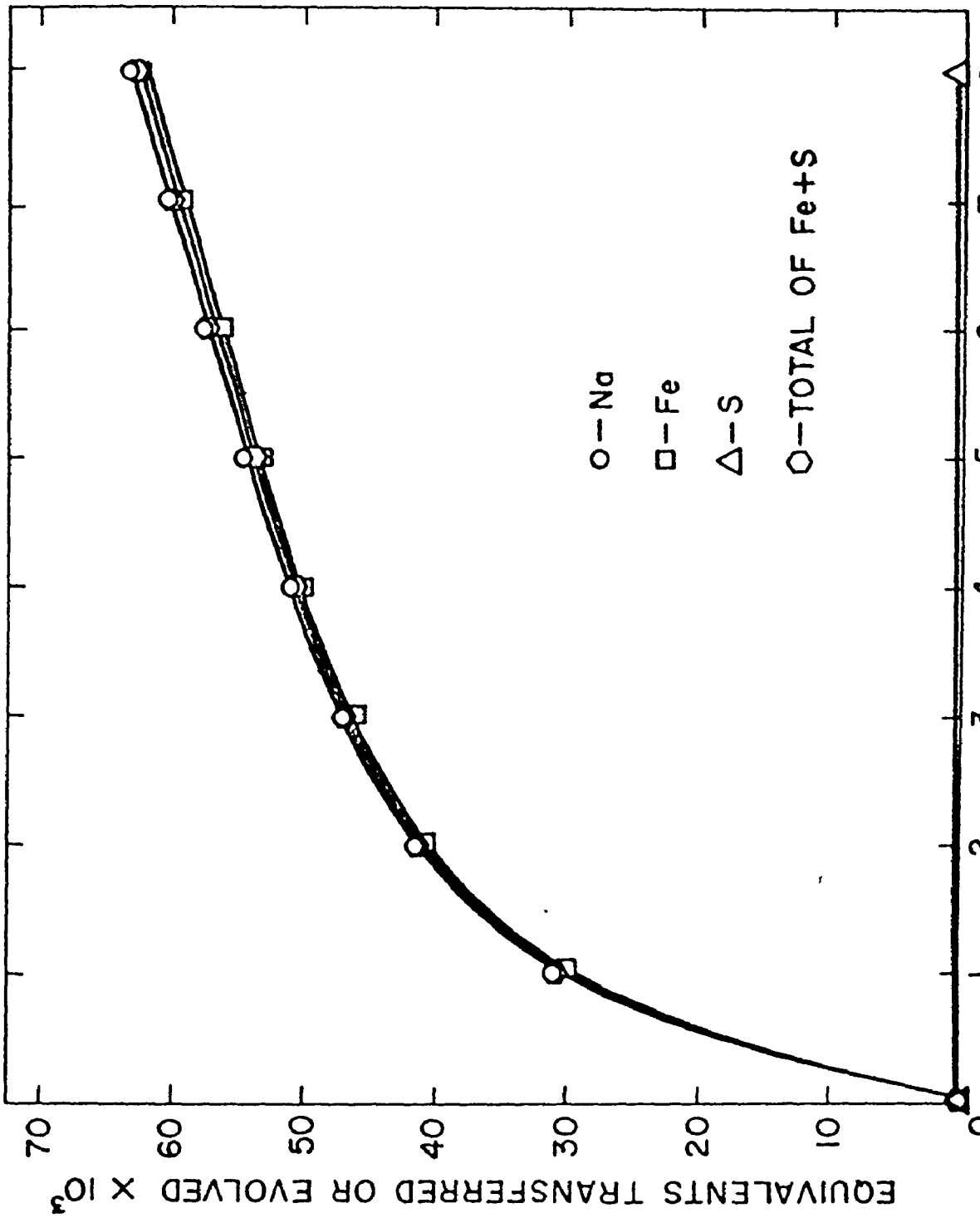

Fig. 38: Equivalents transferred or evolved against time (For Fe - C - 0.005wt%S with dehydrated Na_2S, 3.0/1.5 cm ϕ crucible)

Fig. 39: [illegible] (Na_2S, 1.5 cm ϕ crucible)

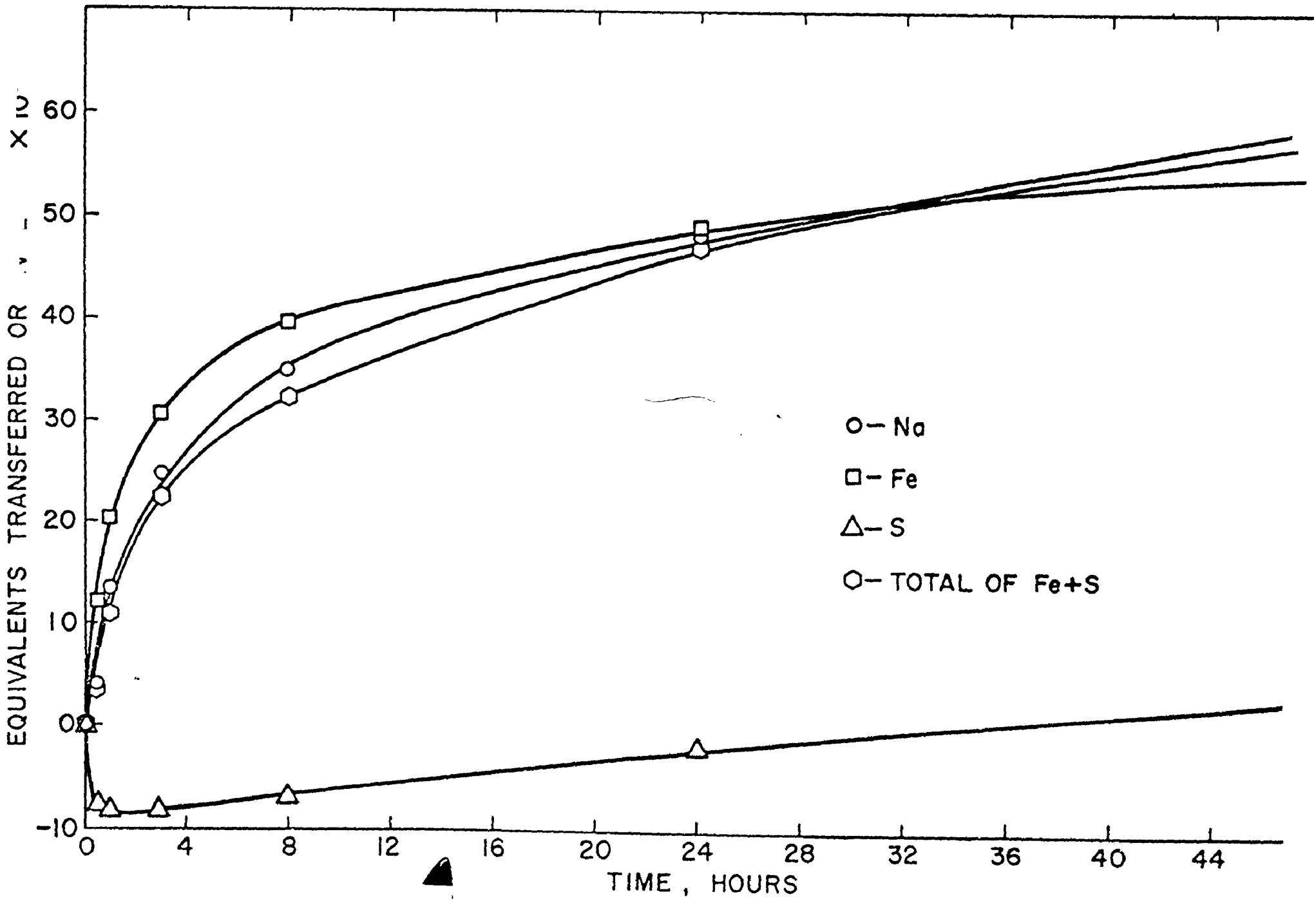

[illegible] TIME , HOURS

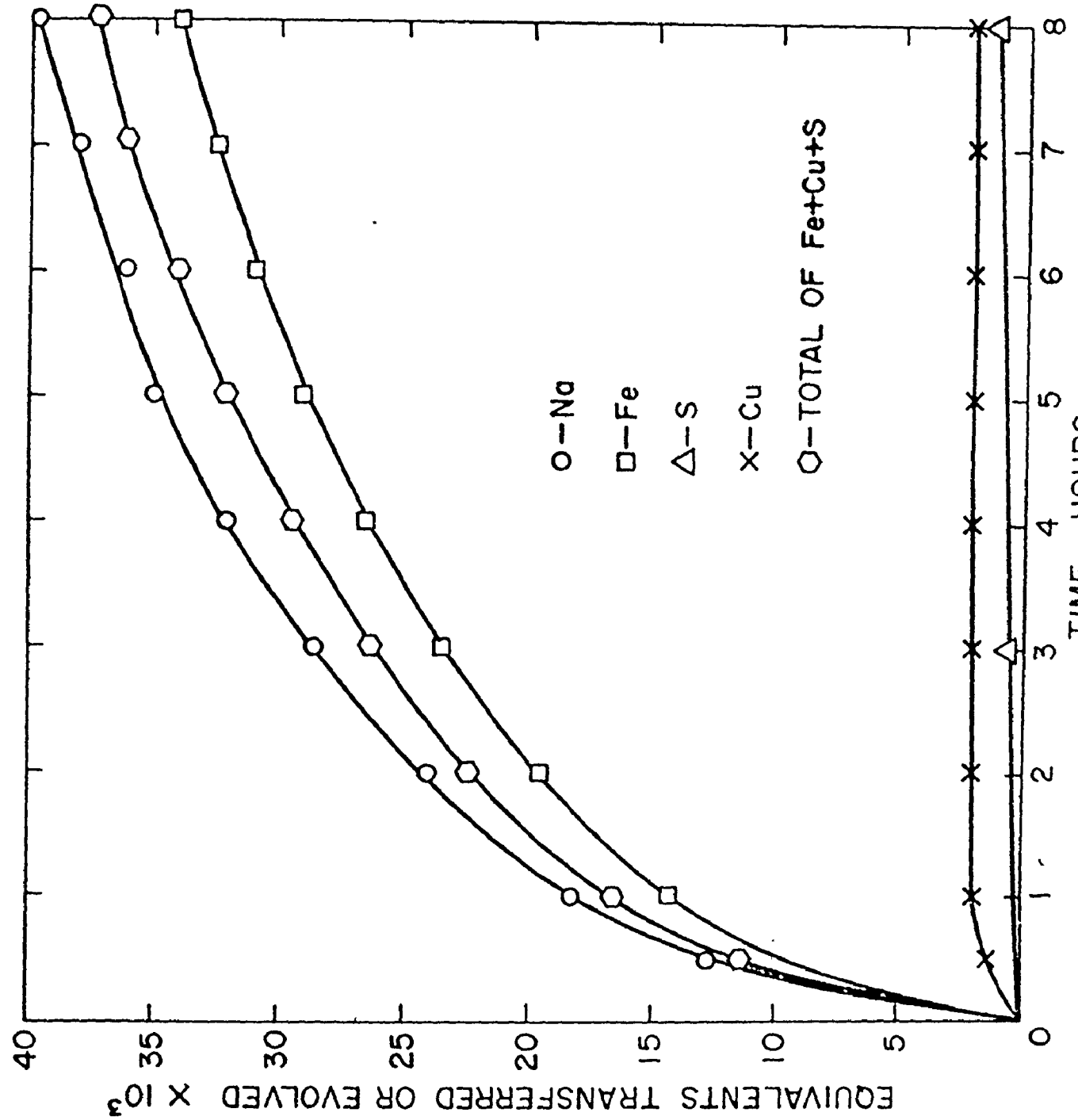

dehydrated Na_2S, 1.5 cm ϕ crucible)

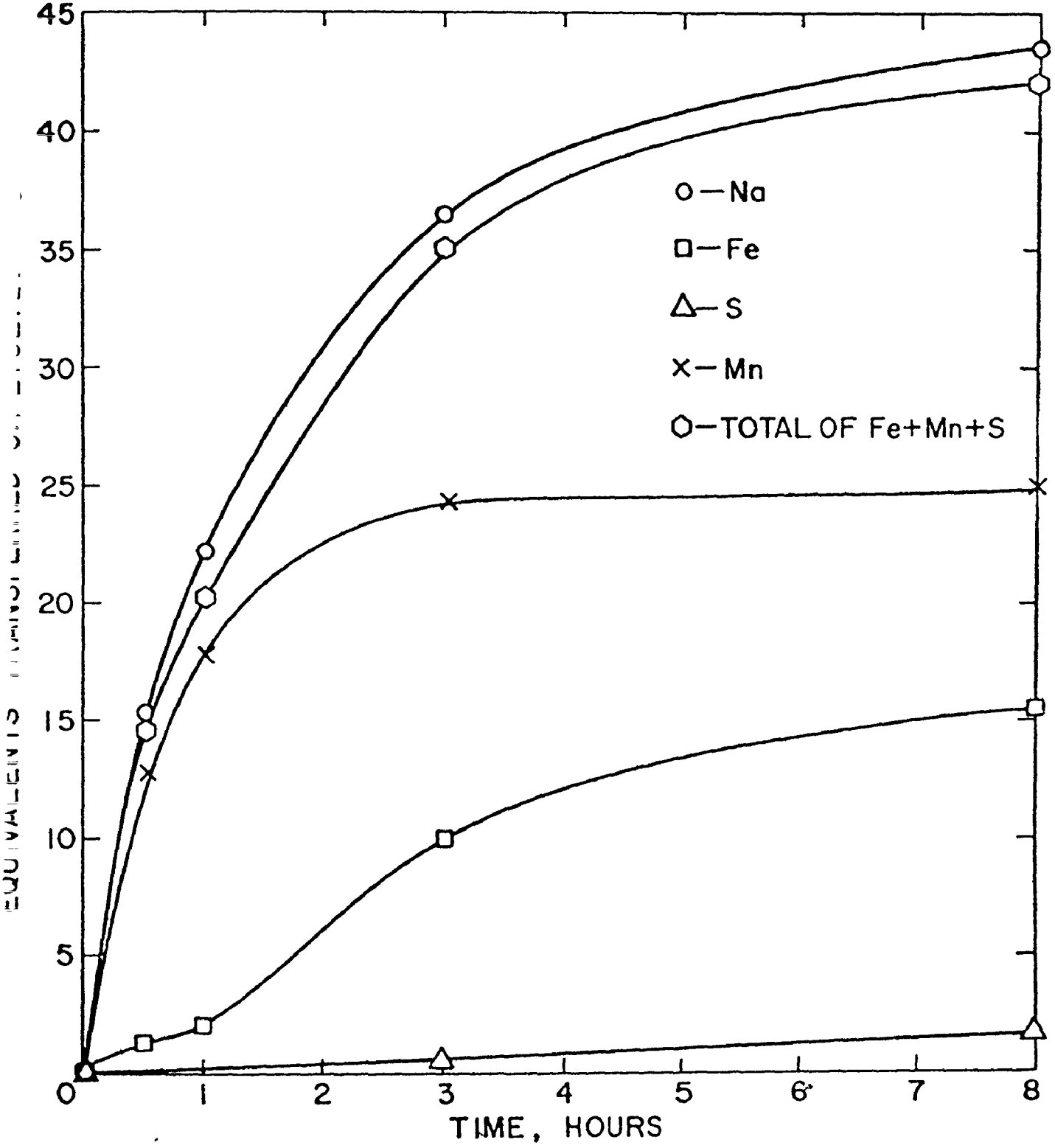

Fig. 41: Equivalents transferred or evolved against time (For Fe - C - 3.54wt%Mn - 0.005wt%S with dehydrated Na_2S, 1.5 cm ϕ crucible)

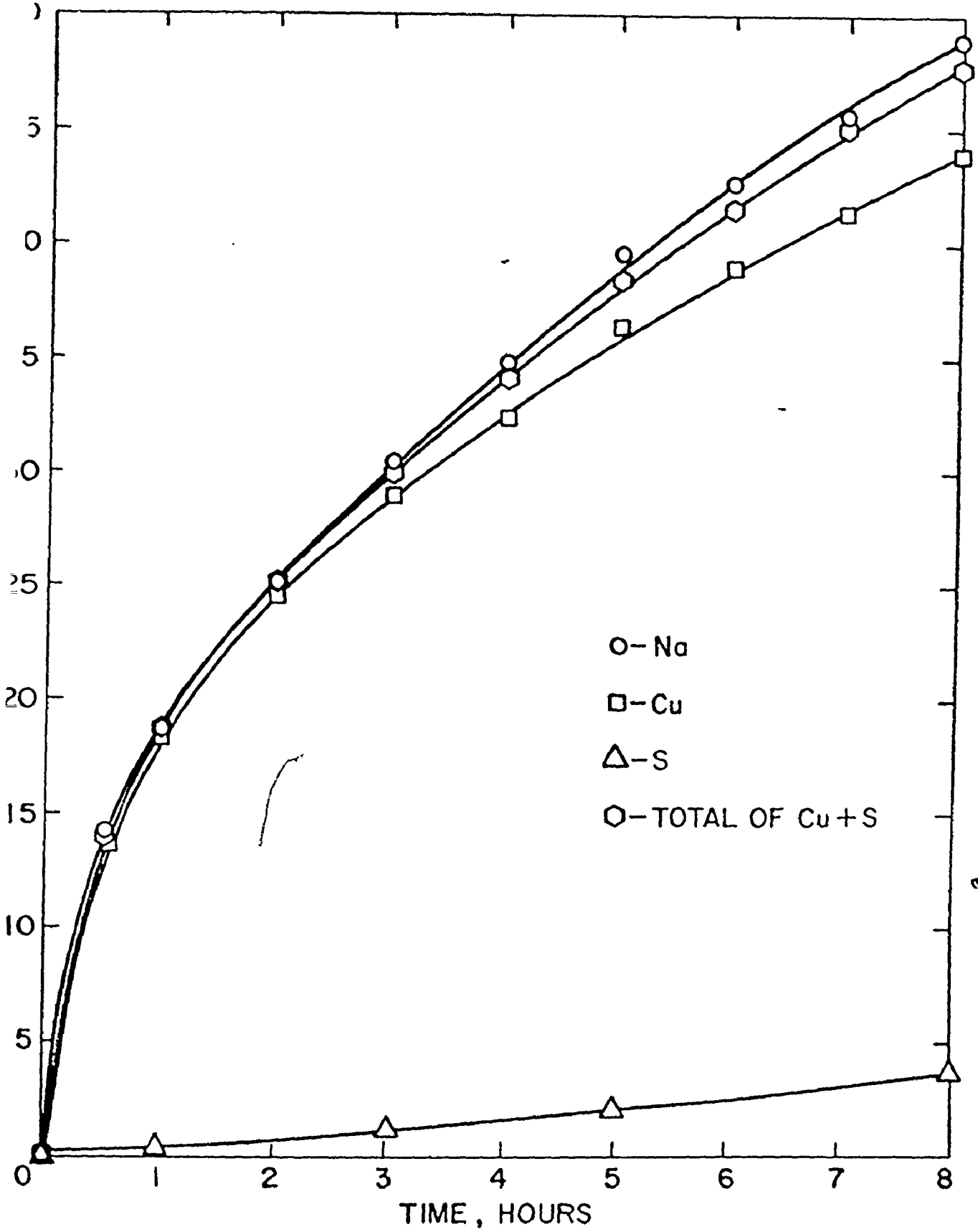

Fig. 42: Equivalents transferred or evolved against time (For Cu -0.0001wt%C - 0.002wt%S with dehydrated Na_2S, 1.5 cm ϕ crucible)

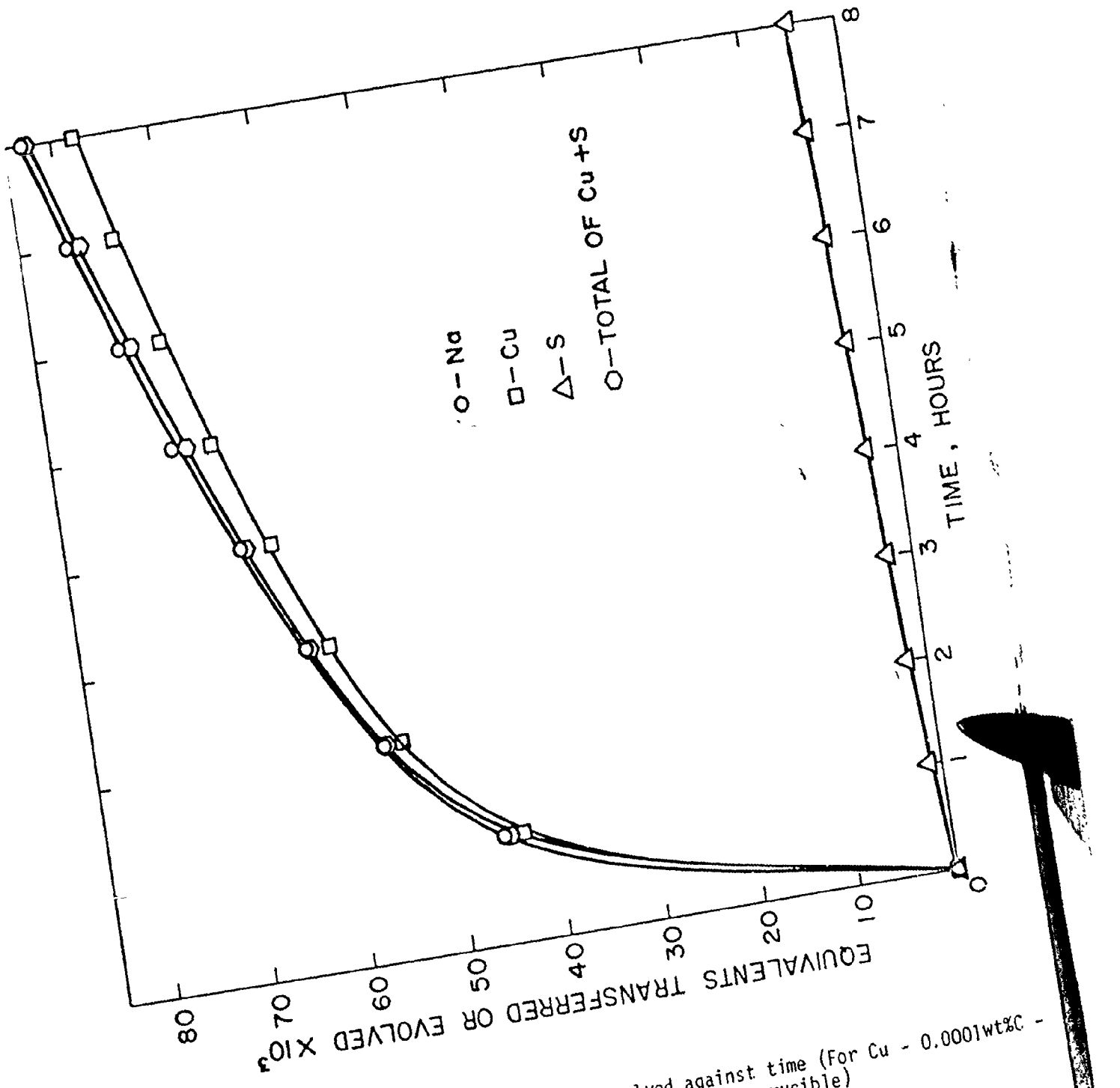

Fig. 43: Equivalent transferred or evolved against time (For Cu - 0.0001wt%C - 0.002wt%S with dehydrated Na_2S, 3.0 cm ϕ crucible)

$$\begin{aligned} \text{Anodic} \quad & Fe \longrightarrow Fe^{++} + 2e^{-} \\ & Mn \longrightarrow Mn^{++} + 2e^{-} \\ & Cu \longrightarrow Cu^{+} + e^{-} \\ & S^{=} \longrightarrow S + 2e^{-} \text{ (initially cathodic)} \\ \text{Cathodic} \quad & Na^{+} + e^{-} \longrightarrow \{Na\}_{gas} \end{aligned} \tag{6.13}$$

Therefore, each atom of copper, manganese or iron which transfers to the slag must give up its electrons at the phase-boundary. To preserve electroneutrality, sodium must pick-up the electrons produced by anodic reactions. Conversely, the loss of sodium from the slag may induce the anodic reactions to take place. In the case of high sulphur melts, initially sulphur transfer from the metal phase to the slag phase will neutralize some of the electrons produced by anodic reactions. Therefore, the sodium loss will be less drastic as compared to, initially, low sulphur-containing melts, Fig. 35.

The presence of alloying elements like Mn and Cu in the metal phase results in increased loss of sodium from the slag due to the anodic reaction of these elements at the slag/metal phase boundary, Fig. 35. Although this has been observed experimentally, there was also a substantial reduction in the amount of iron lost to the slag which is not due to the lack of opportunity for iron atoms in the case of manganese containing melts. This is thought to be due to simultaneous displacement reaction

$$(Fe^{++}) + [Mn] \longrightarrow (Mn^{++}) + [Fe] \tag{6.14}$$

which explains the decrease in iron loss initially. The above reaction

becomes insignificant when the melt becomes depleted, or reaches near equilibrium ratio, in manganese content. Then, there is further loss of iron to the slag as expected, Fig. 24. In molecular terms,

$$[\underline{Mn}]_{1wt\%} + (FeS) \longrightarrow (MnS) + (Fe) \quad \Delta G^\circ_{1523^\circ K} = -8160 \text{ cal/mole} \quad (6.15)$$

The calculated driving force (ΔG°) for this reaction indicates that it is favourable at 1250°C, when the components are at their standard states (see Appendix V).

Analysis of the copper-containing melts was more difficult. Limited solubility of copper in Fe - C melts made additions of copper above a few wt% impossible. With limited additions of copper, there was an increased loss of sodium from the slag as the anodic oxidation of copper occurred but the loss of iron to the slag was hardly affected by the presence of copper in the metal phase, Fig. 35. This might imply that there were two parallel reactions taking place,

$$(Fe) + (Na_2S) \rightleftharpoons 2\{Na\} + (FeS) \quad (6.16)$$

$$2[\underline{Cu}]_{1wt\%} + (Na_2S) \rightleftharpoons 2\{Na\} + (Cu_2S) \quad (6.17)$$

and the exchange reaction,

$$2[\underline{Cu}]_{1wt\%} + (FeS) \longrightarrow (Cu_2S) + (Fe) \quad \Delta G^\circ_{1523^\circ K} = 10370 \text{ cal/mole} \quad (6.18)$$

in comparison with the main reactions (6.16) and (6.17) was not important, (see Appendix IV).

In all the experiments reported, even after 48 hours, equilibrium

state was not reached, in principle, because of the continuing transfers of Fe, S, etc., between slag and metal phases and the removal of Na vapour by the flowing inert gas. However, the distribution of Mn and Cu seemed to approach a partial equilibrium under the experimental conditions studied, Figs. 23 and 24. So at partial equilibrium it is possible to represent the partitioning of the alloying element between the slag and metal by a distribution ratio. The distribution ratios obtained for Cu and Mn are given in Appendix IV - V.

The results obtained from the slag/metal reactions gave further information about the stability of slag phase. Since the amount of Na lost from the slag was balanced electrochemically by the flux of Fe, Cu, Mn and S, the final weight of slag calculated from the composition of the slag should be the same as that determined by weighing. This would be true if there wereno loss by volatilization. The data given in Table XXXIII indicate that there was up to 3% weight loss due to volatilization as well as due to initial loss of weight before the slag/metal reaction started, i.e., during thermal equilibration. Some discrepancy was also introduced by the water content of the slag which was picked up during weighing and subsequent handling before and after experimentation. The results tabulated were a further proof of the fact that sodium sulphide decomposed rather than volatilized at high temperatures. In the absence of a metal phase both sulphur and sodium were lost from the molten sulphide. But, when the metal phase was present, the sulphur in the slag was tied up by the Fe, Mn and Cu which transferred to the slag phase as a result of sodium loss. This conclusion was also evident from the sulphur analysis of the

Table XXXIII: The difference between calculated and observed final slag weights
Initial metal weight = 20.00 grams
Initial slag weight = 3.00 grams
Reaction temperature = 1250°C
Diameter of graphite crucible = 1.5 cm

For Fe - C - 0.005 wt%S

Time Hours	1/2	1	2	3	4	5	6	7	8
Final slag wt. observed, g.	3.03	3.04	3.05	3.04	3.04	3.07	3.08	3.05	3.075
Calculated, g.	3.036	3.06	3.09	3.105	3.12	3.125	3.12	3.12	3.12
Difference, g.	0.006	0.02	0.04	0.065	0.08	0.055	0.04	0.07	0.045

For Cu - C - 0.002 wt%S

Time,Hours	1/2	1	2	3	4	5	6	7	8
Final slag wt. observed, g.	3.53	3.69	3.94	4.08	4.20	4.33	4.42	4.53	4.62
Calculated, g.	3.55	3.72	3.96	4.125	4.245	4.39	4.475	4.565	4.645
Difference, g.	0.02	0.03	0.02	0.045	0.045	0.04	0.055	0.035	0.025

The differences between calculated and observed final slag weights of other systems

Time, Hours	1/2	1	3	8
Systems				
Fe - C - 0.7 wt%S	0.04 g	0.01	0.06	0.07
Fe - C - 0.9 wt%Cu	0.01	0.03	0.080	0.10
Fe - C - 3.54 wt%Mn	0.045	0.035	0.080	0.075

slag phase. In the slag/metal experiments, the total amount of sulphur in the slag remained almost constant, while the sodium content of the slag decreased substantially with increasing time. Any decrease in wt% sulphur content of slag was due to conversion of Na_2S to FeS and Cu_2S which have higher molecular weights.

6.5 Reversion of sulphur transfer

The minimum point in the metal sulphur content vs. time plot, in the case of high initial sulphur containing melts, was due to partial reversion of sulphur, at longer times, from slag to the metal phase, Fig. 44. The reversion of sulphur was due to increasing FeS activity of the slag, due to iron transfer, with increasing time. Initially, the slag phase contained no FeS, but the metal phase had a finite activity of FeS. So the transfer of FeS to the slag phase was very fast. But once the minimum sulphur content in the metal phase was reached, the FeS content of the slag continued to increase as iron replaced sodium in sulphide slag. Therefore,

$$\text{Initially } (Fe) + [\underline{S}] \longrightarrow (\text{"FeS"}) \qquad (6.19)$$

$$\text{Later } (Na_2S) + (Fe) \longrightarrow (\text{"FeS"}) + 2\{Na\} \qquad (6.20)$$

$$\text{and } (\text{"FeS"}) \longrightarrow (Fe) + [\underline{S}] \qquad (6.21)$$

This increase in the iron sulphide content of the slag resulted in reversion of reaction (6.19) as represented by (6.21), so resulting in steady increase of sulphur content of the metal phase.

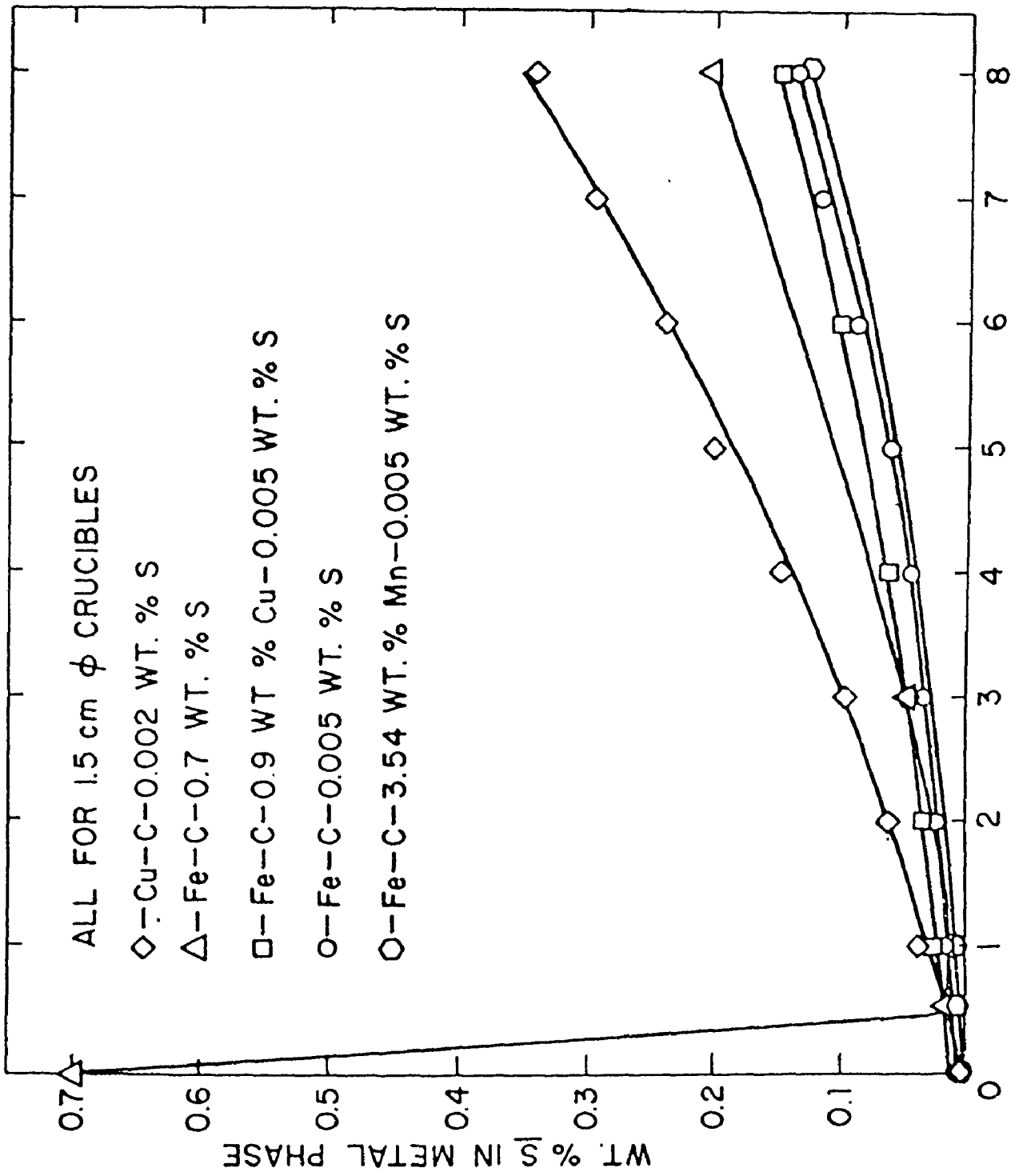

Fig. 44: wt%S in the metal phase against time (hours)

However, in the case of melts containing low initial sulpur, there was a continuous increase in the sulphur content of the metal phase. This was due to reduction of Na_2S by iron alone, Eq. (6.20). Probably, there was a minimum as before but it was not detected because it was reached in too short a period of time and involved a very small change in sulphur concentration.

In the case of alloy-containing melts, manganese additions resulted in slightly lower pick-up of sulphur in the early stages. However, after the manganese was depleted in the metal phase, the reversion of sulphur greatly accelerated and so did the rate of increase of FeS content of the slag. The effect of copper on short-and long-time sulphur pick-up by the metal phase was not very substantial; probably it was overshadowed by the effect of iron.

Finally, it was found that carbon-saturated copper behaved more or less like carbon-saturated iron. The only difference was that the sulphur pick-up by the metal phase was higher in the case of carbon-saturated copper, Fig. 44.

6.6 Theoretical Considerations

6.6.1 Rate-controlling steps

For a three-phase slag/metal reaction, such as

$$x(M) + (Na_2S) \rightleftharpoons (M_xS) + 2\{Na\} \qquad (6.22)$$

where, M represents Fe, Cu, Cu (in Fe) or Mn (in Fe), and x is equal to one for Fe and Mn, two for Cu, the reaction can be broken down into the

following elementary steps:

1. Transport of the reactants from the bulk phasesto the slag/metal interface;
2. The reactions at the slag/metal interface, which itself may involve several steps;
3. Transport of the reaction products from the slag/metal interface into the bulk phases;
4. Transport of the reactants to the slag/gas interface;
5. The reactions at the slag/gas interface;
6. Transport of the gaseous reaction products away from the slag/gas interface into the bulk gas phase;
7. Migration of electrons from the slag/metal interface to the gas/slag interface.

Under most conditions, significant concentration differences, induced by interfacial reactions, are found only in the vicinity of an interface. Therefore, according to Wagner,[3] the theoretical analysis could be confined to the concentration distribution in the boundary layer, and the proper choice of the thickness of the boundary layer(δ) would essentially eliminate the error introduced by this approximation.

The possible rate-controlling step can be ascribed either to diffusion or chemical reaction or both. If the chemical reaction step is the slow step, then the concentration gradients through the bulk phases will be negligibly small and the rate of the process will be determined by the rate of the phase-boundary reaction. If, on the other hand, the chemical reaction step is much faster than one or more of the diffusion steps, partial equilibrium may be considered to be approached at the interfaces, and the overall rate of the process will be essentially determined by the diffusion of one or more of the reacting species to

or from the interfaces. Unfortunately, the actual reactions may be much more complex than the cases mentioned above. Two or more steps may have similar rates, making it difficult to single-out any one as the sole rate-determining step. Under these circumstances, the reaction is said to be mixed-controlled.

In order to determine the rate-limiting steps for the reaction, the effects of several variables on the system were studied. These variables included chemical composition of the metal phase, stirring rate, temperature, crucible geometry, crucible material, gas flow rate, length of graphite-gas-slag contact line, slag-to-metal ratio and total pressure of the system.

6.6.2 Experimental findings

(i) Effect of "stirring rate"

The rate of stirring had a small effect on this reaction as summarized in Table XIX. The results are given for no stirring and stirring with a graphite rod at 40 RPM and 100 RPM. Since the observed rate did not change significantly due to speeding up of the mass transport by stirring, it can be deduced that the overall reaction was mainly controlled by interfacial chemical reactions, rather than by a diffusion step in the slag or metal phase.

(ii) Effect of "temperature"

Temperature changes had a very marked effect on the reaction rate, Table XXXIV. The effect of temperature can be examined quantitatively by calculating the energy of activation for the process. Let us assume

that the temperature dependence in this system may be expressed as follows:

$$\text{Rate} = A \exp(-Q/RT)$$

As the overall rate may not be controlled by an elementary step, the quantity Q may be called "apparent activation energy". In this Arrhenius-type relationship, the pre-exponential factor A could be taken as a constant. Taking the logarithm of both sides of this equation and then by plotting -log(rate) against 1/T°K as shown in Fig. 45, the resulting slope will have the value Q/2.3R, giving the apparent energy of activation for the reaction under consideration. A regression analysis of data gives a value of about 17.5 Kcal/mole with a standard error of estimate of ± 1.5 Kcal/mole. This value is too high for the diffusion of the components in the metal, but, on the other hand, it is lower than one would expect for diffusion in the slag or for the chemical reactions. However, there has been no work done in the latter areas. So the value of apparent activation energy cannot be used to reach a definite conclusion concerning the rate-controlling step.

(iii) Effect of "slag-to-metal ratio" with constant interfacial areas

A series of experiments in which the slag-to-metal ratio was varied, have been carried out to indicate the characteristics of the controlling step. It was found that the rate of reaction was little affected by changes in metal weight. Conversely, when the slag weight was altered there was a corresponding change in the rate of reaction. This experimental result showed the importance of the slag phase in

Table XXXIV: The effect of "temperature"

Metal phase: Fe - C - 0.005 wt%S

Crucible size: 1.5 cm ϕ

Time of reaction: 1 hour

Initial metal weight = 20.00 grams

Initial slag weight = 3.00 grams

T°C	T°K	$\frac{1}{T}°K^{-1}$	wt of Fe in slag, g	rate, gram/ min.	log rate
1200°C	1473°K	$6.788*10^{-4}$	0.305	$5.08*10^{-3}$	-2.294
1250	1523	$6.565*10^{-4}$	0.38	$6.16*10^{-3}$	-2.21
1300	1573	$6.357*10^{-4}$	0.43	$7.16*10^{-3}$	-2.144
1350	1623	$6.161*10^{-4}$	0.53	$8.83*10^{-3}$	-2.054
1400	1673	$5.977*10^{-4}$	0.62	$10.33*10^{-3}$	-1.986

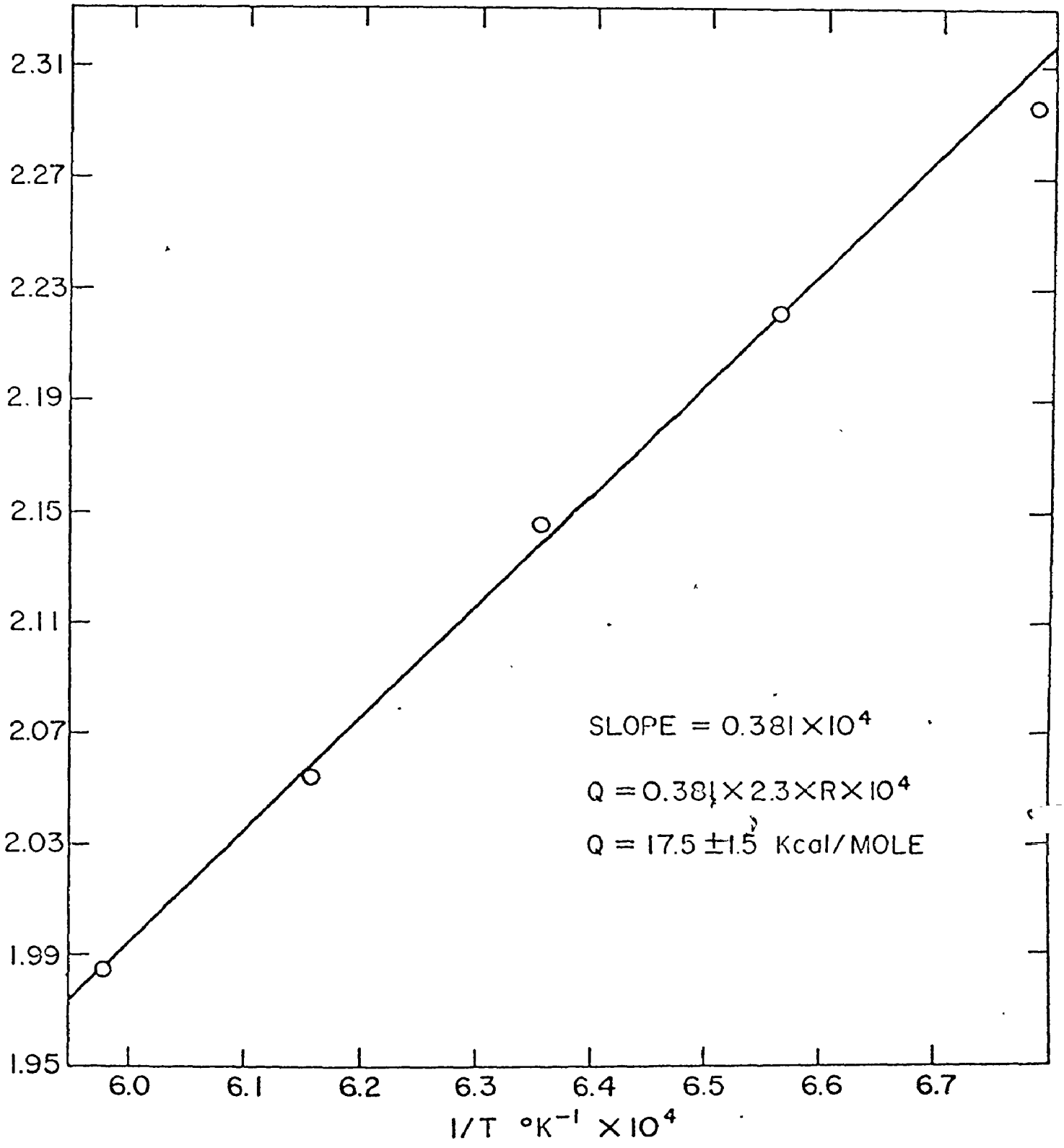

Fig. 45: -log (rate) vs. $\frac{1}{T}$ °K^{-1}

controlling the rate of reactions, Table XXIV.

(iv) Effect of "crucible material"

When the slag/metal reaction was investigated in a graphite crucible, it was possible that anodic reactions took place at the slag/metal interface and cathodic reaction at the gas/slag interface. The electrons most probably migrated in the graphite crucible and the slag. this is illustrated schematically in Fig. 46 for the present case.

However, when the slag/metal reaction was investigated in an alumina crucible the electrons had to migrate through the slag only, since the alumina crucible is not a good conductor by electrons.

Experimental results indicated no definite effect of crucible material on the rate of reaction in this study, Table XXIII. This would indicate that the"FeS"- Na_2S sulphide mixture behaved like an electronic conductor. It is well known that an overwhelming number of sulphides are electronic semiconductors.[68] In fact, the measurements of electrical conductivity on Cu_2S - FeS sulphide melts have been reported in literature.[69] From the results, partial electronic conduction seems possible when FeS is present. A study of electrical conductance in molten Cu - Fe sulphide mattes has shown that pure molten Cu_2S behaves like a semiconductor in that it is an electronic conductor.[70,71] On the other hand, pure molten FeS, another electronic conductor, behaves like a metallic conductor in that its specific conductance decreases with increase in temperature. There is no reported information on molten sodium sulphide but it is expected to be similar to other sulphides. Sodium sulphide usually contains an excess of sulphur or other impurities

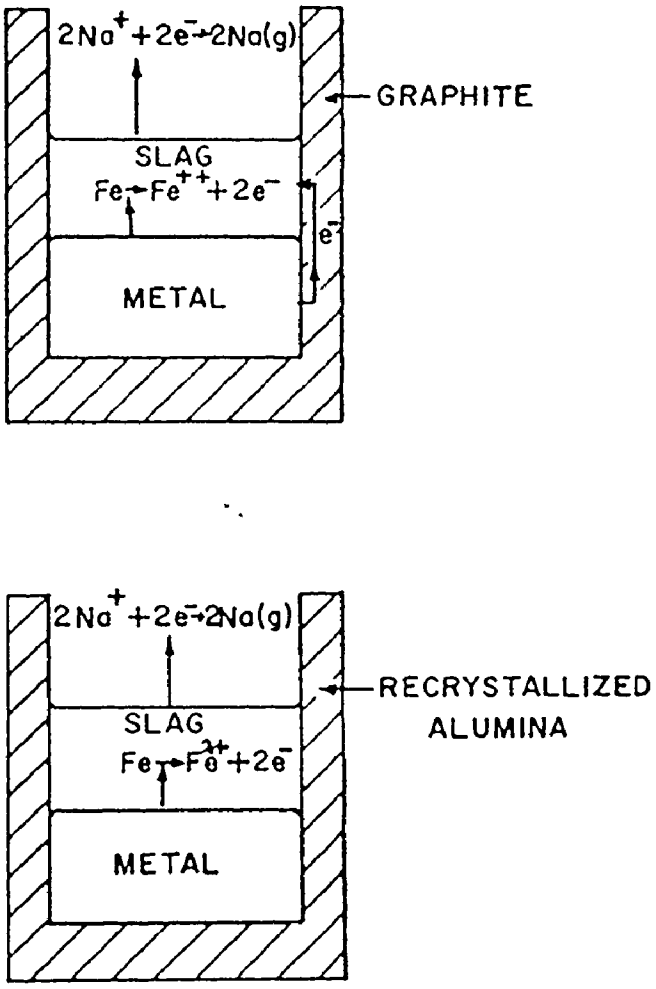

Fig. 46: Effect of "crucible material"

*Alternate mechanisms are fully described in Appendix VIII

which may act as an electron acceptor, providing a component of positive hole conduction as in the case of impure or non-stoichiometric FeS (see two-dimensional arrangement, Fig. 47).

(v) Effect of "gas flow rate"

Relative insensitivity of the reaction rate to changes in inert gas flow rate indicated that the forced convection of sodium vapour in the gas phase was not important within the range of experimental study, Table XXII.

(vi) Effect of "changes in graphite-gas-slag contact line length"

The results summarized in Table XXIshow that the reaction rate was little affected by an increase in graphite-gas-slag contact line length. In these experiments, the slag/metal and gas/slag contact areas were kept constant. Insensitivity of results to the changes of three-phase contact line length meant that the loss of sodium was essentially from the whole slag surface. In other words, the sodium vapour nucleation at the three-phase contact line was relatively unimportant for present considerations.

(vii) Calculated partial pressure of sodium vapour

The calculated partial pressure of sodium vapour in equilibrium with the slag phase is tabulated in Tables XXXI and XXXII. The calculated value was less than 1 atmosphere for all reaction times. This indicated that the sodium vapour could not nucleate at the slag/metal interface. A bubble formation inside the slag itself would have required the pressure to be greater than 1 atmosphere. From the calculated values, it can be concluded that sodium was lost from the slag/gas interface as a result

Non-metal Excess: p-type conductor

Na^+ $S^=$ Na^+ $S^=$ Na^+ $S^=$

$S^=$ Na^+ S^- Na^+ $S^=$ Na^+

Na^+ $S^=$ Na^+ S^- Na^+ $S^=$

$S^=$

$S^=$ Na^+ $S^=$ Na^+ $S^=$ Na^+

S^- Representing positive electron holes

$S^=$ Non-metal excess

Fig. 47: Two-dimensional arrangement for expected non-stoichiometry in Sodium Sulphide

of evaporation.

(viii) Effect of "crucible geometry"

The effect of crucible geometry on the observed rate of reaction also illustrated the importance of the slag/metal and gas/slag interfacial areas. When the slag/metal contact area was kept constant and the slag/gas interfacial area was increased there was more rapid transfer of iron to the slag as well as correspondingly higher amount of sodium loss from the slag. The same was true for the case in which the gas/slag contact area was unaltered and the slag/metal contact area was increased. But the increase was not as substantial as in the previous case. The most drastic increase was observed when both the slag/metal and slag/gas interfacial areas were increased compared to the original experiments. In all cases, the rate increase, however, was not proportional to the increase in areas, Table XX.

(ix) Effect of "chemical composition of metal phase"

As mentioned before the presence of manganese and copper in the metal phase as alloying elements accelerated the rate of loss of sodium from the slag phase. This fact indicated the relative importance of the slag/metal interface. The rate of loss of sodium was already accelerated by the presence of a metal phase containing no manganese or copper. These alloying elements increased this rate further thus indicating the controlling effect of the phase-boundary reactions at the slag/metal interface. Also the nature of the metal phase, i.e., whether it was iron or copper alloy was very important.

(x) Effect of "initial excess sulphur in slag phase"

The increase in iron loss to the slag phase, as the excess sulphur increased in the slag phase, was thought to be due to the reaction of this excess sulphur. The excess sulphur would induce more iron transfer, in addition to the corresponding effect due to sodium loss, to form"FeS"- Na_2S solutions, Table XXV.

(xi) Effect of "vacuum"

Substantial increase in the rate of reaction even under moderate vacuum conditions indicated the importance of diffusion in the gas phase. Since the gaseous diffusion coefficient is inversely proportional to total pressure, at lower pressures the diffusivity of sodium vapour was increased. Such a change led to increased overall rate of reaction, Table XXVI.

6.6.3 Conclusion from experimental findings

The slag/metal reaction under study appeared to be slow and after 48 hours non-equilibrium conditions were still present. The small influence of stirring and large influence of temperature, i.e., relatively high apparent activation energy, as well as the influence of vacuum led to the conclusion that the overall rate of reaction was mainly controlled by the chemical reaction at the gas/slag and slag/metal boundaries and diffusion of sodium in the gas phase. The relative insensitivity of the overall rate of reaction to variations of metal weight, crucible material, argon flow rate and length of graphite-gas-slag contact line also strengthened this conclusion. This conclusion is also consistent with the

dependence of the overall rate on interfacial areas and chemical composition of the metal phase.

6.7 Mixed-Control Models

6.7.1 Mixed-control model for cases of carbon-saturated-iron and -copper alloys

The mixed-control model which has been developed for the present system takes into consideration the phase-boundary reactions and diffusion in gas phase as the important rate controlling steps.

(i) Phase-Boundary reactions: The rates of chemical reactions at the gas/slag and slag/metal phase boundaries may be assumed to be first order. Based on the law of mass action the following expressions can be written:

For $Na^+ + e^- \longrightarrow (Na)_{gas}$

$$-\frac{d(C_{Na^+}.V_S/A_1)}{dt} = k_1 C_{Na^+} - k_1' P^*_{Na} \qquad (6.23)$$

For $Fe \longrightarrow Fe^{++} + 2e^-$

$$\frac{d(C_{Fe^{++}}.V_S/A_2)}{dt} = k_2 C_{Fe} - k_2' C_{Fe^{++}} \qquad (6.24)$$

where, C_{Na^+} = concentration of sodium ions in slag phase, moles/cm^3

$C_{Fe^{++}}$ = concentration of iron ions in slag phase, moles/cm^3

k_1 = forward rate constant for sodium, cm/sec

k_2 = forward rate constant for iron, cm/sec

k_1' = backward rate constant for sodium, moles/cm^2.sec.atm

k_2' = backward rate constant for iron, cm/sec

V_S = volume of slag, cm^3

P^*_{Na} = partial pressure of sodium at gas/slag interface

t = time, sec

C_{Fe} = concentration of iron in metal phase

A_1 = slag/gas interfacial area, cm^2

A_2 = slag/metal interfacial area, cm^2

The above equations are for variable slag volume. The concentration terms in the above equations (6.23) and (6.24) can be replaced by the following expressions,

$$\begin{aligned} C_{Na^+} &= N_{Na^+}/V_S \\ C_{Fe^{++}} &= N_{Fe^{++}}/V_S \\ C_{Fe} &= N_{Fe}/V_M \end{aligned} \qquad (6.25)$$

where, N_{Na^+} = No. of moles of sodium ions in slag phase

$N_{Fe^{++}}$ = No. of moles of iron ions in slag phase

N_{Fe} = No. of moles of iron in metal phase

V_M = Volume of metal

Then, assuming A_1 and A_2 to be constant,

$$-\frac{dN_{Na^+}}{dt} = k_1 A_1 \frac{N_{Na^+}}{V_S} - k_1' A_1 P^*_{Na} \qquad (6.26)$$

$$\frac{dN_{Fe^{++}}}{dt} = k_2 A_2 \frac{N_{Fe}}{V_M} - k_2' A_2 \frac{N_{Fe^{++}}}{V_S} \qquad (6.27)$$

(ii) Diffusion in gas phase: The flux of sodium vapour from the gas/slag boundary to the bulk can be expressed as,

$$J_{Na} = k_g A_1 (P^*_{Na} - P^B_{Na}) \qquad (6.28)$$

where, P^{*}_{Na} = Partial pressure of sodium at the gas/slag boundary

P^{B}_{Na} = Partial pressure of sodium in bulk gas

k_g = Gas transfer coefficient

under quasi-steady state conditions,

$$J_{Na} = - \frac{dN_{Na^+}}{dt} \tag{6.29}$$

then, the flux Eq. (6.28) becomes,

$$- \frac{dN_{Na^+}}{dt} = k_g A_1 (P^{*}_{Na} - P^{B}_{Na}) \tag{6.30}$$

(iii) Addition of resistances: Since the two chemical resistances at the boundaries and the diffusional resistance are in series in the present system, the three resistances can be added to obtain the overall expression.

From Eqs. (6.26) and (6.30),

$$k_1 A_1 \frac{N_{Na^+}}{V_S} - k_1' A_1 P^{*}_{Na} = k_g A_1 (P^{*}_{Na} - P^{B}_{Na}) \tag{6.31}$$

Rearranging,

$$P^{*}_{Na} = \frac{(k_1 N_{Na^+}/V_S) + (k_g \cdot P^{B}_{Na})}{k_g + k_1'} \tag{6.32}$$

Substituting value of P^{*}_{Na} in Eq. (6.26),

$$- \frac{dN_{Na^+}}{dt} = A_1 k_1 \frac{N_{Na^+}}{V_S} - A_1 k_1' \left(\frac{k_1 \frac{N_{Na^+}}{V_S} + k_g P^{B}_{Na}}{k_g + k_1'} \right) \tag{6.33}$$

after collecting terms,

$$-\frac{dN_{Na^+}}{dt} = \frac{A_1 k_1 k_g}{k_g + k_1'} \frac{N_{Na^+}}{V_S} - A_1 \frac{k_1' k_g}{k_g + k_1'} P^B_{Na} \qquad (6.34)$$

If we redefine,

$$k^* = \frac{k_1 k_g}{k_g + k_1'} \text{ and } k^{**} = \frac{k_1' k_g}{k_g + k_1'}$$

we get two equations and four unknown rate constants, i.e.,

$$-\frac{dN_{Na^+}}{dt} = k^* A_1 \frac{N_{Na^+}}{V_S} - k^{**} A_1 P^B_{Na} \qquad (6.35)$$

$$\frac{dN_{Fe^{++}}}{dt} = k_2 A_2 \frac{N_{Fe}}{V_M} - k_2' A_2 \frac{N_{Fe^{++}}}{V_S} \qquad (6.36)$$

Now, the volume of the slag may be replaced by an expression of the type,

$$V_S = \frac{1}{2} N_{Na^+} V_{Na_2S} + N_{Fe^{++}} V_{FeS} \qquad (6.37)$$

where, V_{Na_2S} = molar volume of sodium sulphide[35]

V_{FeS} = molar volume of iron sulphide[35]

The expression of the variation of volume of slag with composition changes as given above means that the slag has a network of sulphur ions and the volume is only affected by the incoming Fe to the slag phase and the loss of sodium from the slag.

(iv) Solution of rate equations: Equations (6.35) and (6.36) are related by the appearance, in both expressions, of V_S which is a

function of slag composition, and hence time. This relation has been already defined by the adoption of the definition of V_S. It should be pointed out that Eqs (6.35) and (6.36) are related through another very important and necessary constraint of the system. It is that the ionic melt, i.e., slag phase, must maintain electrical neutrality. One way to express this constraint is as follows:

$$\frac{d}{dt}\left(N_{Na^+} + 2N_{Fe^{++}}\right) = 0 \tag{6.38}$$

and

$$N_{Na^+} + 2N_{Fe^{++}} = N^{\circ}_{Na^+} = 2N^{\circ}_{S^=} \tag{6.39}$$

where, $N^{\circ}_{Na^+}$ = No. of moles of sodium ions initially present in slag phase

$N^{\circ}_{S^=}$ = No. of moles of sulphur ions initially present in slag phase

The choice of the integration constant in terms of the initial state is certainly justified. It has been observed that with low sulphur alloys, the amount of sulphur in the slag phase remained constant with increasing time within the experimental error limits.

In order to separate variables in Eqs. (6.35) and (6.36) the relation

$$N^{\circ}_{Na^+} = N_{Na^+} + 2N_{Fe^{++}}$$

is applied in the definition of V_S, then, we have

$$V_S = \frac{1}{2} N_{Na^+} \left(V_{Na_2S} - V_{FeS}\right) + \frac{1}{2} N^{\circ}_{Na^+} V_{FeS} \tag{6.40}$$

or

$$V_S = \frac{1}{2} N^{\circ}_{Na^+} V_{Na_2S} + N_{Fe^{++}} (V_{FeS} - V_{Na_2S}) \qquad (6.41)$$

Equation (6.35) and (6.36) may now be written in the following form:

$$-\frac{dN_{Na^+}}{dt} = k^* A_1 \frac{N_{Na^+}}{\frac{1}{2} N_{Na^+}(V_{Na_2S} - V_{FeS}) + \frac{1}{2} N^{\circ}_{Na^+} V_{FeS}} - k^{**} A_1 P^B_{Na} \qquad (6.42)$$

$$\frac{dN_{Fe^{++}}}{dt} = k_2 A_2 \frac{N_{Fe}}{V_M} - k_2' A_2 \frac{N_{Fe^{++}}}{N_{Fe^{++}}(V_{FeS} - V_{Na_2S}) + \frac{1}{2} N^{\circ}_{Na^+} V_{Na_2S}} \qquad (6.43)$$

(v) Numerical Solutions: Equations (6.42) and (6.43) were solved with a CDC 6400 computer using "Rosenbrock optimization programs",[74] (see Appendix VI for details). A number of assumptions were made in order to solve the above equations. Since the sodium vapour which was lost from the slag deposited on the colder parts of the furnace reaction tube, it was assumed that the partial pressure of sodium in the bulk gas phase, P^B_{Na}, was constant but unknown. The slag/metal interfacial area, A_2, was calculated from the shape of the solidified metal phase. The slag/gas interfacial area, A_1, was calculated from the diameter of the crucible used.

Equations (6.42) and (6.43) were solved separately for k*, k** and k_2, k_2', respectively. First, the values of k* and k** were optimized by feeding into the computer, experimentally observed values of rate of loss of sodium with Eq. (6.42). Later, the best values of k_2 and k_2' were found using the experimentally determined iron concentrations in

the slag phase with equation (6.43). Tables XXXV and XXXVI summarize the values of parameters used and rate constants calculated for graphite crucibles of different sizes.

The accuracy of the electroneutrality assumption was checked by solving Eqs. (6.35) and (6.36) simultaneously, using Eq. (6.37), for four unknown rate constants using the experimentally determined values. The results obtained were found to be in good agreement with the rate constants determined thus making the above mentioned neutrality assumption valid.

As can be seen from Tables XXXV and XXXVI that the agreement between the calculated rate constants for graphite crucibles of different sizes is also good.

A similar type of approach was taken for the case of carbon-saturated copper. The corresponding equations were

$$-\frac{dN_{Na^+}}{dt} = k^* A_1 \frac{N_{Na^+}}{V_S} - k^{**} A_1 P^B_{Na} \qquad (6.44)$$

$$\frac{dN_{Cu^+}}{dt} = k_3 A_2 \frac{N_{Cu}}{V_M} - k_3' A_2 \frac{N_{Cu^+}}{V_S} \qquad (6.45)$$

$$V_S = \frac{1}{2} N_{Na^+} V_{Na_2S} + \frac{1}{2} N_{Cu^+} V_{Cu_2S} \qquad (6.46)$$

where, k_3 = forward rate constant for copper

k_3' = backward rate constant for copper

V_{Cu_2S} = molar volume of copper sulphide

with the electrical neutrality assumption that $N^\circ_{Na^+} = N_{Na^+} + N_{Cu^+}$, Eqs. (6.44) and (6.45) reduced to,

Table XXXV: Calculated rate constants for Fe - C - 0.005wt%S - Na_2S systems (1.5 cm ϕ crucible)

Time, Hours	1	2	3	4	5	6	7	8
Na lost, g.	0.30	0.45	0.58	0.68	0.73	0.80	0.86	0.88
Na remaining, g.	1.47	1.32	1.19	1.09	1.04	0.97	0.91	0.89
Fe lost, g.	0.38	0.56	0.69	0.79	0.87	0.93	0.98	1.02
N_{Na^+}	0.0639	0.0574	0.0517	0.0474	0.0452	0.0422	0.0396	0.0387
$N_{Fe^{++}}$	0.0068	0.0100	0.0123	0.0141	0.0155	0.0166	0.0175	0.0182

$A_1 = 1.77\ cm^2$ $\quad V_{FeS} = 18.565$

$A_2 = 2.55\ cm^2$ $\quad V_{Na_2S} = 42.026$

$N^{\circ}_{Na^+} = 0.0769$

$$P = \frac{N_{Fe}}{V_M} = \frac{(20.00 * 0.955)/56}{20.00/6.4} = 0.1091$$

Calculated values: (i) Assuming $N^{\circ}_{Na^+} = N_{Na^+} + 2N_{Fe^{++}}$ and solving Eqs. (6.42) and (6.43) separately for the unknown rate constants,

$k^* = 0.14 * 10^{-3}$ cm/sec $\quad k^{**} P^B_{Na} = 0.47 * 10^{-5}$ moles/cm^2.sec

$k_2 = 0.62 * 10^{-5}$ cm/sec $\quad k'_2 = 0.44 * 10^{-4}$ cm/sec

(ii) Solving Eqs. (6.35) and (6.36) for four unknown rate constants without the electroneutrality assumption,

$k^* = 0.12 * 10^{-3}$ cm/sec $\quad k^{**} P^B_{Na} = 0.41 * 10^{-5}$ moles/cm^2.sec

$k_2 = 0.63 * 10^{-5}$ cm/sec $\quad k'_2 = 0.43 * 10^{-4}$ cm/sec

Table XXXVI: Calculated rate constants for Fe - C - 0.005wt%S - Na_2S system (3.0 cm ϕ crucible)

Time, Hours	1	2	3	4	5	6	7	8
Na lost, g.	0.85	1.08	1.21	1.30	1.38	1.46	1.55	1.63
Na remaining, g.	2.69	2.46	2.33	2.24	2.16	2.08	1.99	1.91
Fe lost, g.	1.015	1.29	1.45	1.555	1.65	1.74	1.835	1.925
N_{Na^+}	0.1170	0.1070	0.1012	0.0974	0.0938	0.0904	0.0866	0.0829
$N_{Fe^{++}}$	0.0181	0.0231	0.0259	0.0278	0.0295	0.0311	0.0327	0.0344

$A_1 = 7.07\ cm^2$ $V_{FeS} = 18.565$ $N_{Fe}/V_M = 0.1091$

$A_2 = 8.30\ cm^2$ $V_{Na_2S} = 42.026$ $N^{\circ}_{Na^+} = 0.1539$

Calculated values: (i) Assuming $N^{\circ}_{Na^+} = N_{Na^+} + 2N_{Fe^{++}}$ and solving Eqs. (6.42) and (6.43) separately for the unknown rate constants,

$k^* = 0.13 * 10^{-3}$ cm/sec $\quad k^{**}p^B_{Na} = 0.46 * 10^{-5}$ moles/cm^2.sec

$k_2 = 0.58 * 10^{-5}$ cm/sec $\quad k'_2 = 0.50 * 10^{-4}$ cm/sec

(ii) Solving Eqs. (6.35) and (6.36) for four unknown rate constants without the electroneutrality assumption,

$k^* = 0.12 * 10^{-3}$ cm/sec $\quad k^{**}p^B_{Na} = 0.41 * 10^{-5}$ moles/cm^2.sec

$k_2 = 0.57 * 10^{-5}$ cm/sec $\quad k'_2 = 0.47 * 10^{-4}$ cm/sec

$$-\frac{dN_{Na^+}}{dt} = k^*A_1 \frac{N_{Na^+}}{\frac{1}{2} N_{Na^+}(V_{Na_2S} - V_{Cu_2S}) + \frac{1}{2} N^\circ_{Na^+} V_{Cu_2S}} - k^{**}A_1 P^B_{Na} \qquad (6.47)$$

$$\frac{dN_{Cu^+}}{dt} = k_3A_2 \frac{N_{Cu}}{V_M} - k_3'A_2 \frac{N_{Cu^+}}{\frac{1}{2} N_{Cu^+}(V_{Cu_2S} - V_{Na_2S}) + \frac{1}{2} N^\circ_{Na^+} V_{Na_2S}} \qquad (6.48)$$

As before, each equation has two unknown rate constants. Each equation was solved for the rate constants and the values obtained summarized in Tables XXXVII and XXXVIII. Equations (6.44) and (6.45) were also solved without making the electroneutrality assumption. Tables XXXVII and XXXVIII also give the values obtained in this manner. It can be seen that, as before, the agreement between rate constants calculated with and without the neutrality assumption is good. Also there is good agreement between values calculated for graphite crucibles of different sizes.

It is apparent from Tables XXXV, XXXVI, XXXVII and XXXVIII that the k* and k** values are about the same for carbon-saturated-iron and -copper. This is to be expected since the gas/slag boundary is not drastically affected by changing the metal phase. However, the rate constants k_2, k_3 and k_2', k_3' are different for carbon-saturated-iron and -copper because of the different nature of metal in contact with the slag phase.

6.7.2 Mixed-control model for iron-carbon-copper alloy

A model similar to the one developed for iron-carbon and copper-carbon alloys can be developed for the case of iron-carbon-copper alloy.

Now, the rates of chemical reactions at the boundaries and the

Table XXXVII: Calculated rate constants for Cu- 0.0001wt%C - 0.002wt%S - Na_2S system (1.5 cm ϕ crucible)

Time, Hours	1	2	3	4	5	6	7	8
Na lost, g.	0.43	0.58	0.69	0.78	0.885	0.955	1.03	1.10
Na remaining, g.	1.34	1.19	1.08	0.99	0.885	0.815	0.74	0.67
Cu lost, g.	1.16	1.56	1.83	2.05	2.31	2.47	2.65	2.80
N_{Na^+}	0.0583	0.0517	0.0471	0.0431	0.0384	0.0355	0.0321	0.0292
N_{Cu^+}	0.0182	0.0245	0.0288	0.0322	0.0363	0.0389	0.0417	0.0441

$A_1 = 1.77\ cm^2$ $\quad V_{Cu_2S} = 28.418$ $\quad N_{Cu}/V_M = 0.1227$

$A_2 = 2.55\ cm^2$ $\quad V_{Na_2S} = 42.026$ $\quad N^{\circ}_{Na^+} = 0.0769$

Calculated Values: (i) Assuming $N^{\circ}_{Na^+} = N_{Na^+} + N_{Cu^+}$ and solving Eqs. (6.47) and (6.48) separately for the unknown rate constants,

$k^* = 0.11 * 10^{-3}$ cm/sec $\quad k^{**}P^B_{Na} = 0.24 * 10^{-5}$ moles/cm^2.sec

$k_3 = 0.14 * 10^{-4}$ cm/sec $\quad k'_3 = 0.54 * 10^{-4}$ cm/sec

(ii) Solving Eqs. (6.44) and (6.45) for four unknown rate constants without the electroneutrality assumption,

$k^* = 0.13 * 10^{-3}$ cm/sec $\quad k^{**}P^B_{Na} = 0.35 * 10^{-5}$ moles/cm^2.sec

$k_3 = 0.15 * 10^{-4}$ cm/sec $\quad k'_3 = 0.58 * 10^{-4}$ cm/sec

Table XXXVIII: Calculated rate constants for Cu - 0.0001wt%C - 0.002wt%S - Na_2S system (3.0 cm ϕ crucible)

Time, Hours	1	2	3	4	5	6	7	8
Na lost, g.	1.045	1.29	1.43	1.545	1.665	1.755	1.835	1.91
Na remaining, g.	2.495	2.25	2.11	1.995	1.875	1.785	1.705	1.63
Cu lost, g.	2.81	3.43	3.78	4.07	4.35	4.57	4.77	4.95
N_{Na^+}	0.1085	0.0978	0.0918	0.0867	0.0815	0.0776	0.0741	0.0709
N_{Cu^+}	0.0442	0.0540	0.0595	0.0641	0.0685	0.0720	0.0751	0.0779

$A_1 = 7.07\ cm^2$ $\quad V_{Cu_2S} = 28.418$ $\quad N_{Cu}/V_M = 0.1227$

$A_2 = 8.30\ cm^2$ $\quad V_{Na_2S} = 42.026$ $\quad N^{\circ}_{Na^+} = 0.1539$

Calculated values: (i) Assuming $N^{\circ}_{Na^+} = N_{Na^+} + N_{Cu^+}$ and solving Eqs. (6.47) and (6.48) separately for the unknown rate constants,

$k^* = 0.99 * 10^{-4}$ cm/sec $\quad k^{**}P^B_{Na} = 0.28 * 10^{-5}$ moles/cm^2.sec

$k_3 = 0.13 * 10^{-4}$ cm/sec $\quad k'_3 = 0.63 * 10^{-4}$ cm/sec

(ii) Solving Eqs. (6.44) and (6.45) for four unknown rate constants without the electroneutrality assumption,

$k^* = 0.12 * 10^{-3}$ cm/sec $\quad k^{**}P^B_{Na} = 0.36 * 10^{-5}$ moles/cm^2.sec

$k_3 = 0.15 * 10^{-4}$ cm/sec $\quad k'_3 = 0.69 * 10^{-4}$ cm/sec

rate of gaseous diffusion can be expressed as,

$$-\frac{dN_{Na^+}}{dt} = k_1 A_1 \frac{N_{Na^+}}{V_S} - k_1' A_1 P_{Na}^* \tag{6.49}$$

$$\frac{dN_{Fe^{++}}}{dt} = k_2 A_2 \frac{N_{Fe}}{V_M} - k_2' A_2 \frac{N_{Fe^{++}}}{V_S} \tag{6.50}$$

$$\frac{dN_{Cu^+}}{dt} = k_3 A_2 \gamma_{Cu} \frac{N_{Cu}}{V_M} - k_3' A_2 \frac{N_{Cu^+}}{V_S} \tag{6.51}$$

$$J_{Na} = -\frac{dN_{Na^+}}{dt} = A_1 k_g (P_{Na}^* - P_{Na}^B) \tag{6.52}$$

where $V_S = \frac{1}{2} N_{Na^+} \quad V_{Na_2S} + N_{Fe^{++}} V_{FeS} + \frac{1}{2} N_{Cu^+} V_{Cu_2S}$

γ_{Cu} = activity coefficient of copper in iron[72,73]

As before, addition of above equations results in three equations with six unknown rate constants, i.e.,

$$-\frac{dN_{Na^+}}{dt} = k^* A_1 \frac{N_{Na^+}}{V_S} - k^{**} A_1 P_{Na}^B \tag{6.53}$$

$$\frac{dN_{Fe^{++}}}{dt} = k_2 A_2 \frac{N_{Fe}}{V_M} - k_2' A_2 \frac{N_{Fe^{++}}}{V_S} \tag{6.54}$$

$$\frac{dN_{Cu^+}}{dt} = k_3 A_2 \gamma_{Cu} \frac{N_{Cu}}{V_M} - k_3' A_2 \frac{N_{Cu^+}}{V_S} \tag{6.55}$$

The above equations were solved with a computer using "Rosenbrock optimization program". Table XXXIX summarizes the experimental data used and the rate constants determined. It can be seen from the comparison of rate constants for the binary (Fe - C, Cu - C) and ternary (Fe - C - Cu) systems that there is reasonable agreement.

Table XXXIX: Calculated rate constants for Fe - C - 0.9wt%Cu - 0.005wt%S - Na_2S system (1.5 cm ϕ crucible)

Time, Hours	1	2	3	4	5	6	7	8
Na lost, g.	0.42	0.55	0.655	0.74	0.80	0.83	0.88	0.91
Na remaining, g.	1.35	1.22	1.115	1.03	0.97	0.94	0.89	0.86
Fe gained, g.	0.40	0.55	0.66	0.74	0.805	0.86	0.91	0.95
Cu gained, g.	0.125	0.138	0.142	0.142	0.142	0.141	0.141	0.140
N_{Na^+}	0.0587	0.0530	0.0485	0.0448	0.0422	0.0409	0.0387	0.0374
$N_{Fe^{++}}$	0.00715	0.0098	0.0118	0.0132	0.0144	0.0154	0.0163	0.0170
N_{Cu^+}	0.00197	0.00217	0.00224	0.00224	0.00224	0.00222	0.00222	0.00220

$A_1 = 1.77\ cm^2$ $\quad V_{FeS} = 18.565$ $\quad N_{Fe}/V_M = \frac{(20.00 * 0.945)/56}{20.00/6.5} = 0.1097$

$A_2 = 2.55\ cm^2$ $\quad V_{Na_2S} = 42.026$ $\quad N_{Cu}/V_M = \frac{(20.00 * 0.009)/63.5}{20.00/6.5} = 0.00092$

$N^{\circ}_{Na^+} = 0.0769$ $\quad V_{Cu_2S} = 28.418$

$$\log \gamma_{Cu} = \log \gamma^{\circ}_{Cu} + \frac{1}{2.303}(\epsilon^{Cu}_{Cu}X_{Cu} + \epsilon^{C}_{Cu}X_C) = \log 8.5 + \frac{1}{2.303}[(-5.5 * X_{Cu}) + (4.2 * X_C)]$$

where, ϵ = interaction coefficient, X_i = mole fraction of elementi, γ° = activity coefficient at infinite dilution

Therefore, for 4.5 wt%C and 0.2 wt%Cu

$$\log \gamma_{Cu} = 0.9294 + \frac{1}{2.303}[(-5.5 * 0.00152) + (4.2 * 0.1808)] = 1.255$$

$$\gamma_{Cu} = 18$$

Calculated values: Solving Eqs. (6.53), (6.54) and (6.55) for six unknowns,

$k^* = 0.15 * 10^{-3}$ cm/sec $\quad k^{**}p^B_{Na} = 0.49 * 10^{-5}$ moles/cm^2.sec

$k_2 = 0.64 * 10^{-5}$ cm/sec $\quad k'_2 = 0.48 * 10^{-5}$ cm/sec

$k_3 = 0.14 * 10^{-4}$ cm/sec $\quad k'_3 = 0.94 \times 10^{-4}$ cm/sec

6.7.3 Accuracy of calculated rate constants

The Rosenbrock search program described in Appendix VI was used for obtaining a local mininum of a function of several variables.[74] The mathematical models proposed in this study contained unknown rate constants which were determined by comparing the experimental and theoretical values of N's. The computation was terminated when the sum of squares of deviations between the calculated and experimental values was less than 10^{-5} $(mole)^2$. The program printed out, at the end of each pattern-search, the "best" values of the variables and the number of function evaluations. It was clear from the print-out that the agreement between the calculated and experimental values was good as long as the above criterion was satisfied.

6.8 Discussion of assumptions made in the calculations and development of mixed-control model

In the calculation of rate constants a number of assumptions were made, the significance of which is discussed below.

(1) The slag/metal contact area was calculated from the shape of the solidifed metal. It was assumed that the area was the same in the liquid state. The lack of information with respect to interfacial tension forces in the present system made this assumption necessary.

(2) The gas/slag contact interface was assumed to remain flat during the experiments. However, it was observed that the solidified gas/slag interfaceswere not quite flat. As the experimental time increased the interface became concave. This was due to changing interfacial tension as the FeS and Cu_2S content of the slag increased

steadily. The slag started to climb the graphite crucible walls and the gas/slag contact area increased with time. This effect was substantial with the small size graphite crucibles. It is expected that the error introduced by this assumption for the case of 3.0 cm diameter graphite crucibles was small.

(3) The penetration of slag between graphite crucible wall and the metal phase due to wetting conditions at long times was not taken into consideration in the calculations. It was assumed that the thin layer of slag which penetrated in between was very limited in amount.

(4) When the plug from the upper graphite crucible was removed in the double crucible experiments, the metal ran into the lower crucible in a few seconds. During this period, the area terms were quite different and changing. However, in the calculations the area terms were assumed to be constant during the whole duration of experiments. The error coming from this assumption was not substantial due to the short time required for the pouring of the metal. In some experiments, the metal and slag phases were placed in the same crucible from the beginning and the start of the reaction was timed from the moment the slag became molten. It was found that the rate of reaction was not affected to an appreciable degree by the double crucible arrangement. This also meant that the initial stirring resulting from falling metal into the slag phase was not very important.

(5) Partial pressure of sodium in the bulk gas phase was assumed to be constant. The sodium which was lost from the slag condensed on the colder parts of the furnace tube and lids. Since, the deposit was always

at constant temperature, it is expected that this assumption is reasonable.

(6) The molar volumes of sulphides used in calculations were calculated using the reported room temperature densities of these sulphides.[35]

$$\rho_{Na_2S} = 1.856 \text{ g/cc}$$
$$\rho_{FeS} = 4.74 \text{ g/cc}$$
$$\rho_{Cu_2S} = 5.6 \text{ g/cc}$$

The densities of carbon-saturated-iron and -copper were taken to be

$$\rho_{Fe - C} = 6.4 \text{ g/cc}^{(34)}$$
$$\rho_{Cu - C} = 7.8 \text{ g/cc}$$
$$\text{and } \rho_{Fe - C - Cu} = 6.5 \text{ g/cc}$$

(7) The volume of slag was calculated using the following expressions:

$$\text{For } Na_2S - FeS \qquad V_S = \tfrac{1}{2} N_{Na^+} V_{Na_2S} + N_{Fe^{++}} V_{FeS}$$
$$Na_2S - Cu_2S \qquad V_S = \tfrac{1}{2} N_{Na^+} V_{Na_2S} + \tfrac{1}{2} N_{Cu^+} V_{Cu_2S}$$
$$Na_2S - FeS - Cu_2S \qquad V_S = \tfrac{1}{2} N_{Na^+} V_{Na_2S} + N_{Fe^{++}} V_{FeS} + \tfrac{1}{2} N_{Cu^+} V_{Cu_2S}$$

This meant that the slag had a network of sulphur ions and the volume was only affected by the incoming iron and copper to the slag phase and the loss of sodium from the slag. This assumption is reasonable since there was little loss of sulphur from the slag to the metal phase or gas phase.

(8) In the calculations, the concentrations rather than the

activities were used, except in the case of copper in iron. Concentrations being more fundamental statistical quantities than activities led to their use. Also, the activities of sulphides were not as reliable as the concentrations since they were calculated using the sulphur content of the metal phase.

Only in the case of Fe - C - Cu alloy, the activity coefficient of copper, γ_{Cu}, was introduced into the equations because of extreme positive deviation from Raoult's Law as well as availability of information in calculation of this coefficient.[72,73]

(9) It was assumed that the sodium in the gas phase was monatomic sodium, although a certain percentage was probably diatomic sodium gas. Lack of information led to this assumption. However, it is known that sodium gas in equilibrium with pure liquid sodium at 1250°C contains only small amount of diatomic sodium.

(10) Iron and copper ions in the slag were assumed to be all Fe^{++} and Cu^{+}. Small error was thought to be introduced by this assumption since the relation $\dot{n}_{Na} = 2\dot{n}_{Fe} + \dot{n}_{Cu}$ was shown to hold to a good degree.

(11) In the calculations, the initial composition of sodium sulphide slag was assumed to be stoichiometric. The error introduced was negligible since the initial slag compositions were always close to stoichiometry.

(12) The model did not take into consideration the contributions to the overall resistance of diffusion of species in metal and slag and the transfer of electrons through graphite and the slag from the slag/metal interface to the gas/slag interface. As mentioned before, the

experimental observations showed these resistances to be small compared to the resistances of interfacial reactions and gaseous diffusion.

(13) The application of the law of mass action to the following interfacial reaction

$$Na^+ + e^- \longrightarrow \{Na\}_{gas}$$

should give,

$$-\frac{d(C_{Na^+} V_S/A_1)}{dt} = \bar{k}_1 C_{Na^+} C_{e^-} - k_1' P^*_{Na} \qquad (6.56)$$

However, in the model discussed, the concentration of electrons, C_{e^-}, was assumed to be constant, Eq. (6.23). In fact, the forward rate constant in the original equation was $\bar{k}_1 C_{e^-}$. Similarly, k_2 and k_3 were products of $\bar{k}_2 C_{e^-}$ and $\bar{k}_3 C_{e^-}$, respectively.

6.9 Discussions of the Results of the Closed-System Experiments

6.9.1 Theoretical considerations

In a closed-system of 4 phases and 5 components, the degrees of freedom predicted by the phase rule[75] is 3. The system under study has four phases (metal, slag, gas and graphite), and five components (Fe, Na, S, C and Ar). The three degrees of freedom are temperature, initial %S and the total pressure which is determined by the argon in the closed system in combination with the other gaseous species at equilibrium under the imposed temperature. Then the P_{Na} is uniquely determined.

For the simplest case of the reaction of carbon-saturated iron with pure sodium sulphide,

$$(Fe) + (Na_2S) \rightleftharpoons (FeS) + 2\{Na\} \tag{6.57}$$

If we let V be equal to the free gas volume within the closed-system and M_m and M_s be the initial amounts of iron and Na_2S in moles, respectively, and assuming no sulphur transfer to simplify the calculations, we can calculate the partial pressure of sodium in equilibrium with the slag/metal system.

First, we let the experimentally determined extent of reaction be equal to x, i.e., x moles of iron is transferred to the slag. Then, the corresponding sodium loss expected, from Eq. (6.57) is 2x moles. Assuming ideal gas behaviour, the partial pressure of sodium will be,

$$P_{Na} = 2x \frac{RT}{V} \tag{6.58}$$

since the number of moles of iron sulphide in the slag is equal to x and the number of moles of sodium sulphide is equal to $M_s - x$, the mole fractions of FeS and Na_2S will be,

$$X_{FeS} = x/M_s \tag{6.59}$$

$$X_{Na_2S} = \frac{M_s - x}{M_s} \tag{6.60}$$

The equilibrium relationship for the reaction under consideration may be expressed in terms of the properties defined above.

$$K = \frac{P_{Na}^2 \cdot a_{FeS}}{a_{Fe} \cdot a_{Na_2S}} = \frac{(2x \frac{RT}{V})^2 (\frac{x}{M_s}) \gamma_{FeS}}{a_{Fe} (\frac{M_s - x}{M_s}) \gamma_{Na_2S}} \tag{6.61}$$

where, γ_{FeS} and γ_{Na_2S} are activity coefficients of iron sulphide and sodium sulphide, respectively.

$$a_{Fe} = 0.675 \text{ for carbon-saturated iron at } 1250°C$$

The values of γ_{FeS} and γ_{Na_2S} are already calculated in the thermodynamics section (6.3). Substituting the values for these, at a known mole fraction of FeS, it is theoretically possible to calculate the equilibrium constant at a known temperature. The calculated value can then be compared with the value of K obtained from the free energy change associated with the reaction.

6.9.2 Discussion of experimental results

It was found very difficult to apply the theoretical model developed above, to the present system. The reason was mainly the deviation of the slag composition from stoichiometry. Slight variations in initial slag composition resulted in large variations in the amount of metal lost to the slag phase, Table XXXX. Furthermore, since weight changes were small, the presence of small amount of water in the slag affected the results substantially. The weight change determinations were also influenced by absorption of sodium into the graphite pores by capillary action.

However, the experimental results confirmed qualitatively the expected behaviour of the system that the reaction would stop when a certain vapor pressure of sodium had built up in the closed-system. The amount of iron lost to the slag and the amount of sodium lost from the slag were extremely small compared to the open system, Table XXIX.

Table XXXX: Calculations for the closed-system experiments

For Fe - C - 0.005wt%S alloy with dehydrated Na_2S

Initial metal wt, g.	Initial slag wt, g.	Free gas volume, cc	Fe lost to slag, g.	Na loss expected, g	Expected net decrease in total system wt, g.	Actual decrease in total system wt, g.	Final wt%S
20.0154	3.0025	6.5	0.030	0.025	0.025	0.0025	0.004
20.0073	3.0056	11.5	0.035	0.029	0.029	0.0035	0.003
20.0030	2.9975	7.0	0.025	0.020	0.020	0.0002	0.003

For initial slag weight of three grams

For initial slag Composition	Excess sulphur, g.	Amount of Fe that balances excess S, g.
41.08%S	0.	0.
41.18%S	0.003	0.005
41.58%S	0.015	0.026

Stoichiometric sodium sulphide: 58.92%Na, 41.08%S

In the case of melts containing high initial sulphur, it was found that the sulphur was lost to the slag as iron sulphide as in the open system,

$$(Fe) + [\underline{S}] \longrightarrow (\text{"FeS"}) \qquad (6.62)$$

But, in contrast to the open system, after the loss of sulphur, there was no further loss of iron to the slag phase, resulting in considerably smaller loss of iron to the slag. As a result, the final sulphur content of the metal phase was lower.

These experiments showed that a closed-system would be much more efficient in eliminating undesirable elements such as copper and sulphur from the melt, without losing substantial amounts of iron to the slag, provided that sufficient sulphur was present in the metal phase before the start of the slag/metal reaction.

6.10 Capillary Experiments

6.10.1 Principle of measurement

The capillary-reservoir method has been applied, in the present work, to the measurement of diffusion coefficients. In this method, a capillary tube of uniform diameter, with one end sealed, is filled with an alloy of an initial concentration C_o. The capillary is then immersed in a large reservoir melt of the same type of alloy of different concentration C_s. After a given period of time, the capillary is taken out of the reservoir and the diffusion coefficient is determined as follows:

Fick's second law for unidirectional diffusion may be written,

$$\frac{\partial C}{\partial t} = D \cdot \frac{\partial^2 C}{\partial x^2} \tag{6.63}$$

It may be assumed that the variation of diffusion coefficient D with concentration C can be neglected. If the boundary value at the open-end of the capillary is assumed to be C_s and the diffusion time t and the capillary length l are selected so that the concentration changes in the capillary, resulting from diffusion, should not penetrate the full length of the capillary, i.e., semi-infinite system, the initial and boundary conditions will be as follows:

$$\begin{aligned} &\text{I.C.} \quad C = C_o \;,\; t = 0 \;,\; x \geq 0 \\ &\text{B.C.1} \quad C = C_s \;,\; t > 0 \;,\; x = 0 \\ &\text{B.C.2} \quad C = C_o \;,\; t > 0 \;,\; x = \infty \end{aligned} \tag{6.64}$$

under these conditions, the solution of Eq. (6.63) is written as,[76,77]

$$\frac{C - C_o}{C_s - C_o} = 1 - \text{erf}\left(\frac{x}{2\sqrt{Dt}}\right) \tag{6.65}$$

in which erf refers to Gauss' error integral. Under the same conditions, the average concentration $\bar{C}$ in the capillary, after some short time t, is related to the diffusion coefficient through the following approximate equation.[78,79]

$$\frac{\bar{C} - C_s}{C_o - C_s} = \frac{8}{\pi^2}\left(e^{-\theta} + \frac{1}{9}e^{-9\theta} + \frac{1}{25}e^{-25\theta}\right) \tag{6.66}$$

where $\theta = \pi^2 Dt/4l^2$

The diffusion coefficient can be evaluated either from Eq. (6.65) by measuring the concentration distribution along the longitudinal direction of the capillary or from Eq. (6.66) by measuring the average concentration in the capillary. In the present work, the latter method was chosen because this is simpler with respect to experimental technique and also is believed to yield more reliable results in liquid diffusion. However, a precision of only ± 10% is considered quite good for measurements with liquid metal systems. The hydrodynamic problems of capillary entrance into the reservoir and turbulent mixing at the capillary mouth are of major concern to any improvement that may be obtained with the capillary-reservoir method.[80]

6.10.2 Macrosegregation on solidification of capillary metal

In order to evaluate the extent of macrosegregation attending solidification, a homogeneous alloy was held in the capillary and quenched. Chemical analysis of the sections of the capillary metal for sulphur confirmed that no macrosegregation was brought about by the quenching technique. The average sulphur content of the capillary was found to be 0.28 ± 0.01wt%S.

6.10.3 Concentration profile in capillary metal

The concentration profile of sulphur was measured to test whether the boundary conditions chosen for Eqs. (6.65) and (6.66) were satisfactory. A quenched capillary specimen was sectioned after an experimental diffusion run into several slices of pre-determined length by a micro-cutter and

each slice was chemically analyzed. An example of the concentration profile measured is shown in Fig. 48. In this figure, the concentration of sulphur is plotted against the distance from the capillary-reservoir interface and each point represents the average concentration of the slice cut out of the indicated location. The curve in the figure represents the concentration profile calculated from Eq. (6.65) using the value of the diffusion coefficient given in the following section. As is seen from the figure, the observed concentration profile is in fairly good agreement with that calculated and no evidence of convection was found during the diffusion process or of the disturbance of the interface during solidification. The concentration changes in the capillary did indicate that it was an semi-infinite system. So facts mentioned above may be taken as evidence that the experimental technique used and the method of calculation using Eq. (6.66) are appropriate.

6.10.4 Experimental diffusion coefficient obtained

Diffusion coefficient of sulphur in molten carbon-saturated iron has been measured at 1250°C by the method described above. The results are presented in tabular form in Table XXVII. The average D_s value was calculated to be $2.15 * 10^{-5}$ cm^2/sec. The standard deviation in D_s values was found to be $0.3 * 10^{-5}$ cm^2/sec. The reported interdiffusivity values for sulphur in carbon-saturated iron by other workers[81,82,83] are also summarized in Table XXXXI. Although there is no reported value at 1250°C the extrapolations of the reported equations, to the lower temperature range, gave reasonably close agreement with the experimentally obtained

Fig. 48: Concentration of sulphur (wt%) against distance from interface (cm)

For metal capillary - metal pool

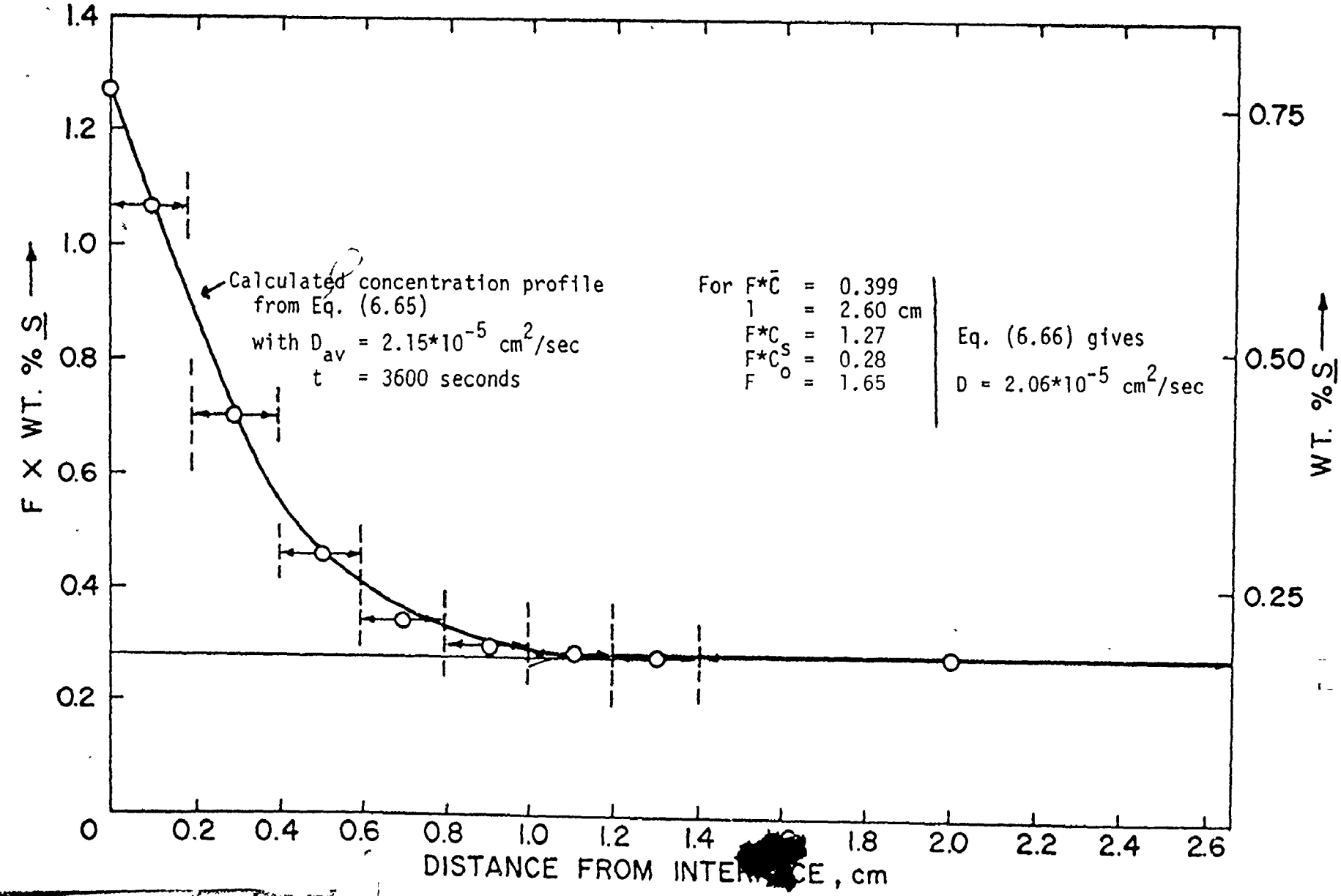

Table XXXXI: Interdiffusivity of sulphur in carbon-saturated iron at 1250°C, estimated by extrapolation to lower temperature range

Temperature Range Investigated	D_o cm^2/sec	Q Cal/mole	D cm^2/sec (at 1250°C)	Worker
1300 - 1431°C	$7.4 * 10^{-3}$	21000	$0.7 * 10^{-5}$	Grace, Derge[81]
1390 - 1560°C	$2.8 * 10^{-4}$	7500	$2.3 * 10^{-5}$	Kawai, Saito[82]
1350 - 1450°C	$1.63 * 10^{-2}$	28500	$1.3 * 10^{-5}$	Majdic, Schenck[83]

where, $D = D_o \exp(- Q/RT)$

value of the diffusion coefficient D_s.

6.11 Capillary slag/metal reactions

The results of the capillary slag/metal reactions were treated as described in the previous section. Now, the experimentally determined average sulphur concentration $\bar{C}$ was substituted in Eq. (6.66) and the diffusivity of sulphur in the capillary metal phase was calculated for short-time experiments. In the calculations, it was assumed that the equilibrium sulphur content at the slag/metal phase boundary, C_s, was equal to 0.010wt%S. This sulphur level was about the minimum reached with different initial sulphur-containing melts in the double-crucible experiments (section 5.3). The rate of loss of sulphur from the capillary metal of initial composition Fe - C - 0.215wt%S to the sulphide slag pool was found to be diffusion controlled, Table XXVIII. The calculated diffusivity of sulphur for the capillary metal-slag pool system agreed well with that evaluated in the absence of slag. This fact indicated that diffusion in metal was the rate limiting-step for sulphur transfer from the metal to the slag phase, Fig. 49. The rate of diffusion in unmixed systems is of metallurgical importance in slag/metal reactions. In the present study, since the slag phase had certain extent of convective mixing and in the metal phase there was little convection, the rate limiting effect of diffusion of sulphur in the metal phase is to be expected

The agreement between the diffusivity of sulphur obtained from metal capillary-metal pool experiments and metal capillary-slag pool

Fig. 49: Concentration of sulphur (wt%) against distance from interface (cm)

For metal capillary - slag pool

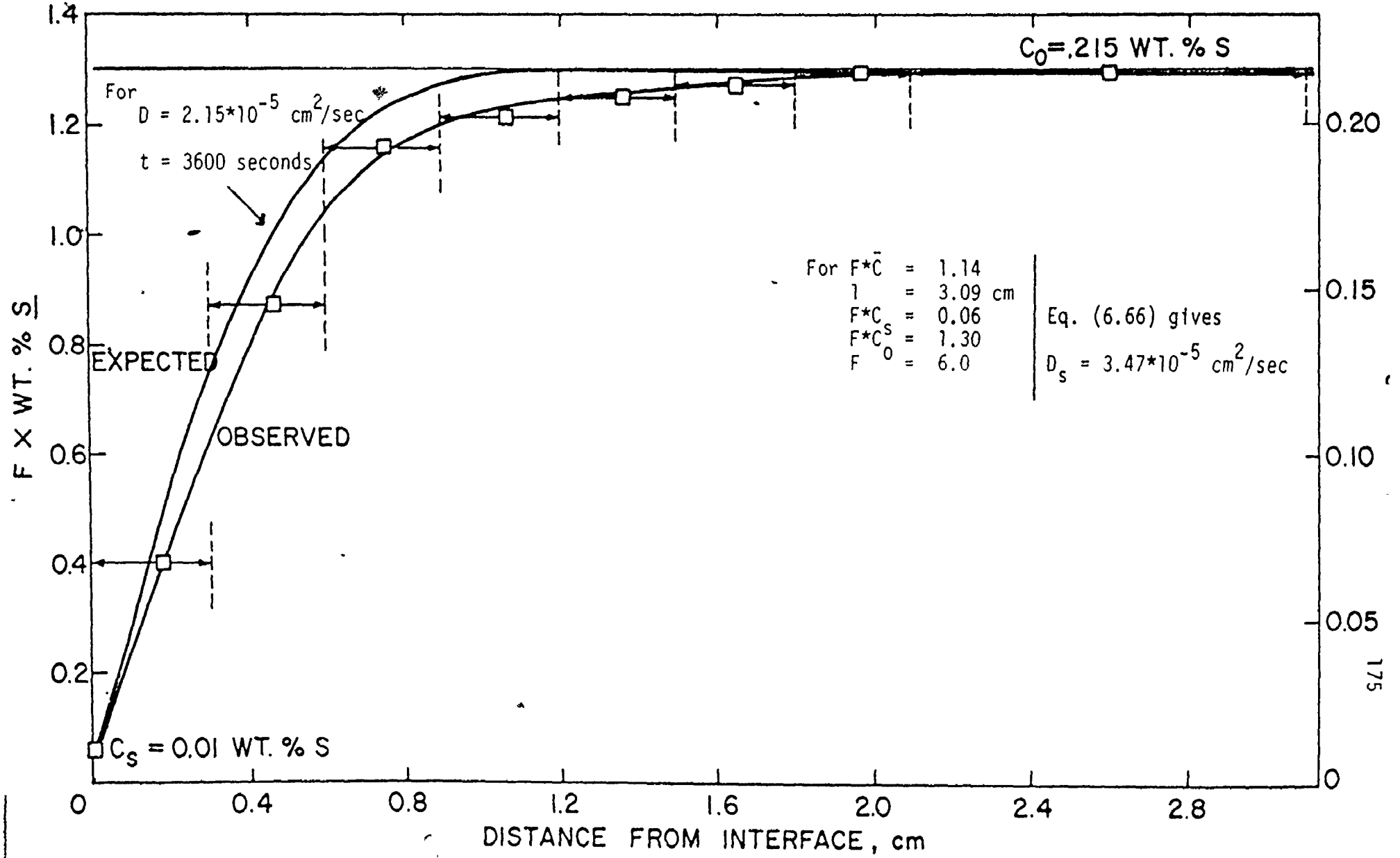

experiments is reasonable considering the various assumptions made. In the case of the slag/metal experiments, it was assumed that the slag/metal boundary was stationary, whereas due to iron loss to the slag, the length of the capillary metal decreased leading to moving boundary conditions. Next, it was assumed that the sulphur content at the slag/metal boundary was constant throughout the experiments. From previous results, we know that as the FeS content of the slag increases with time, the sulfurizing ability of the slag also increases, leading to higher sulphur values at the slag/metal boundary. As mentioned in the experimental procedure, for analysis only the inner capillary metal was taken and it was assumed that the slag penetration between the graphite and outer capillary metal did not affect the gradient of sulphur in the inner metal capillary. An error was introduced by this assumption since the diffusion of sulphur was also affected by the sulphur level in the outer capillary. Apart from the assumptions made, the capillary metal-slag pool system is more likely to have convective mixing due to addition of slag on top the capillary as well as the use of a larger capillary diameter.

Some experiments, in which the slag phase was placed in a graphite capillary and the metal was present as a pool, failed to give satisfactory results due to the slag creeping out of the capillary. The ultimate aim of these capillary experiments would have been to place both metal and slag phases in capillaries. Then, a knowledge of the concentration profiles and interface concentrations would have enhanced the understanding of the kinetics of the slag/metal reaction under study. Due to the difficulties experienced with the slag phase, the capillary type experiments were discontinued.

CHAPTER 7

SUMMARY AND CONCLUSIONS

The reactions between sodium sulphide base slags and carbon-saturated iron alloys and carbon-saturated copper alloys have been studied extensively at 1250°C and many experiments were carried out at even higher temperatures. The nature of reactions may be generalized in the following form:

For melts containing low initial sulphur

$$X(M) + (Na_2S) \longrightarrow (M_xS) + 2\{Na\} \qquad (7.1)$$

$$(M_xS) \longrightarrow X(M) + [\underline{S}] \qquad (7.2)$$

For melts containing high initial sulphur same as above, except initially

$$X(M) + [\underline{S}] \longrightarrow (M_xS) \qquad (7.3)$$

where, M stands for Fe, Cu, $\underline{Cu}$ (in Fe) and $\underline{Mn}$ (in Fe)

X is equal to one for Fe and Mn, two for Cu.

The double-crucible technique was utilized under a flowing argon atmosphere in a vertical, resistance-heated, tubular furnace.

The effects of changes in various experimental parameters on the observed rate of reaction were studied to identify the rate-controlling steps. It has been concluded that mass transport processes, except the gaseous diffusion of sodium vapour, did not contribute significant

resistance to the overall reaction. The interfacial reactions, namely, vapourization of sodium at gas/slag interface and oxidation of metals at slag/metal boundary, were related by the requirement of electroneutrality of the slag. A theoretical model based on mixed-control mechanism was developed. The experimental data have been analyzed in terms of the proposed model with a CDC 6400 computer using the "Rosenbrock optimization" in search of the best kinetic parameters. Interpretations given were supported by other experiments carried out in the present study; such as closed-system experiments for testing the reversibility of reaction, capillary experiments for investigating the contribution of diffusion in the metal phase, study of thermal stability of dehydrated sodium sulphide at high temperatures, etc. Calculations were also extended to cover evaluation of activities in the sulphide mixtures under study. Negative deviations from ideality in the cases of "FeS" - Na_2S and Cu_2S - Na_2S were apparent.

With regards to the practical aspects of the present study, it can be mentioned that sodium sulphide slags are capable of removing Cu, Mn and S from hot-metal efficiently. An electrochemical interpretation was given for the mechanism of removal of these elements. The reversion of sulphur at extended reaction times was also clarified. The distribution ratios for copper and manganese were found to be about 24 and 175, respectively. Under the present experimental conditions, the distribution ratios obtained were larger than those obtained in pilot plant scale experimental runs. The difference was most probably due to better controlled experimental conditions and better quality of slag material used in the experiments.

It was found that sulphide slags with better high temperature stability need to be developed for use under steelmaking conditions. It was also clear from the closed-system experiments that the best results of desulphurization and decopperization could be obtained in a closed-system. With such a system, the iron loss to the slag phase and sulphur reversion could be minimized.

APPENDIX I

Partial Pressure of Sodium and Sulphur in Equilibrium with pure Na_2S at 1250°C

The decomposition reaction can be represented as,

$$(Na_2S) \rightleftharpoons 2\{Na\} + \frac{1}{2}\{S_2\}$$

the standard free energy of decomposition can be obtained from "The JANAF Tables", at 1250°C, (Table II).

$$\Delta G^\circ_{1523^\circ K} = + 45886 \text{ cal/mole}$$

since, at equilibrium

$$\Delta G^\circ = - RT\ln K = - RT\ln \frac{P_{S_2}^{\frac{1}{2}} P_{N_a}^{2}}{a_{Na_2S}}$$

for pure Na_2S, $a_{Na_2S} = 1.0$

Therefore,

$$45886 = - 4.575*1523*\log P_{S_2}^{\frac{1}{2}} P_{Na}^{2}$$

Condition of stoichiometry is that $P_{Na} = 4P_{S_2}$

Substituting above condition and solving for P_{Na} and P_{S_2} one obtains,

$$P_{S_2} = 7.65*10^{-4} \text{ atm.}$$

$$P_{Na} = 30.6*10^{-4} \text{ atm.}$$

The above calculation assumes that the sulphide stays stoichiometric as well as the presence of only monatomic sodium in the gas phase.

APPENDIX II

Expected Weight Loss in Vacuum from Knudsen's Equation

The weight of each constituent leaving unit area in unit time is given by Knudsen's equation[59]

$$P(atm) = 0.02256 \frac{\alpha\ \omega\ (grams)}{A(cm^2)\ t(sec)} \sqrt{\frac{T°K}{M}}$$

where, M = molecular weight or atomic weight

Assuming, α = condensation coefficient = 1.0

Substituting the calculated equilibrium partial pressure of sodium at 1250°C, one can estimate the weight loss expected due to sodium evaporation for A = 1.77 cm^2 and t = 3600 sec.

$$30.6*10^{-4} = 0.02256 \frac{\omega}{1.77*3600} \sqrt{\frac{1523}{23}}$$

$$\omega_{Na}(calculated) = 106 \text{ grams}$$

Similarly for sulphur,

$$\omega_S(calculated) = 26.5 \text{ grams}$$

These are the weight losses expected due to sodium and sulphur loss from a 1.5 cm ϕ crucible in one hour at 1250°C. The actual total weight loss observed under argon atmosphere was only 0.10 grams, indicating that the Knudsen's equation is not quite applicable under present conditions with the assumptions made above and the use of calculated equilibrium partial pressure of sodium.

APPENDIX III

Solubility of Sulphur in Fe - C Melts at 1250°C

$$(Fe) + [\underline{S}]_{1wt\%} \rightleftharpoons (\text{"FeS"}) \quad \Delta G_1^\circ \qquad (1)$$

Thermodynamic properties of reaction (1) can be obtained from the data on standard free energy of formation of non-stoichiometric iron sulphide in the presence of iron and the free energy of solution of sulphur in iron.[64,84]

$$(Fe) + \frac{1}{2}\{S_2\} \longrightarrow (\text{"FeS"}) \quad \Delta G_2^\circ = -29970 + 7.90\ T \qquad (2)$$

$$[\underline{S}]_{1wt\%} \longrightarrow \frac{1}{2}\{S_2\} \quad \Delta G_3^\circ = +32280 - 5.60\ T \qquad (3)$$

Although the value of free energy for reaction (2), given above, is valid in the temperature range 1809 to 2000°K, since the line for the above reaction in the Ellingham diagram, see Fig. 1, is more or less a straight line, it is assumed that the same equation is valid down to 1523°K.

The standard free energy change of reaction (1) is the sum of the corresponding values of the reactions (2) and (3) at 1523°K.

$$\Delta G_1^\circ = +5813$$

$$\text{Then} \quad 5813 = -RT\ln \frac{a_{\text{"FeS"}}}{h_{\underline{S}}\, a_{Fe}} \qquad (4)$$

Taking, as a reference state, the system in which sulphur saturated metal is in equilibrium with a pure "FeS" slag and assuming a value of unit activity for the "FeS" in that system, the following equation can be

written;

$$5813 = -4.575 * 1523 \log \frac{1}{h_{\underline{S}} \cdot a_{Fe}} \qquad (5)$$

Since the activity of iron containing 4.5wt%C is 0.675, see Fig. 32, the saturation sulphur at 1250°C can be calculated:

$$\log(0.675\ h_{\underline{S}}) = 0.84 \qquad (6)$$

$$\text{Therefore, } f_S \text{wt\%}\underline{S} = 10.3 \qquad (7)$$

The Henrian activity coefficient of sulphur f_S, in Fe - 4.5wt%C - S alloy, can be estimated from the data reported by J.P. Morris and R.C. Buehl[85] and Shiro Banya and J. Chipman.[86] The equation given above is then simplified to:

$$\text{wt\%}\underline{S} = \frac{10.3}{4.85} = 2.12$$

Considering the various assumptions made in the above calculations and the presence of possible errors in the estimation of f_S, the calculated value agrees reasonably well with the reported 1.8wt%$\underline{S}$ used in the actual calculations. The data reported by Turkdogan et al.[48] is thought to be more reliable than the value obtained through thermodynamic calculations.

APPENDIX IV

Calculation of the Activities in the Ternary FeS - Cu_2S - Na_2S System

In this Appendix, the activity of Cu_2S is evaluated based on the calculated activity of "FeS" in the slag and the equilibrium constant of the exchange reaction to be defined below. In Fig. 50, the ternary phase diagram of Na_2S - FeS - Cu_2S has been reproduced for reference.(65)

From thermodynamic data at 1250°C,(64,34)

$$(Fe) + \tfrac{1}{2}\{S_2\} \longrightarrow (FeS") \qquad \Delta G^\circ_{1523°K} = -17938 \text{ cal/mole}$$

$$2(Cu) + \tfrac{1}{2}\{S_2\} \longrightarrow (Cu_2S) \qquad \Delta G^\circ_{1523°K} = -20200 \text{ cal/mole}$$

Subtracting

$$2(Cu) + ("FeS") \longrightarrow (Cu_2S) + (Fe) \quad \Delta G^\circ = -2262 \text{ cal/mole}$$

$$2(Cu) + ("FeS") \longrightarrow (Cu_2S) + (Fe) \quad \Delta G^\circ = -2262 \text{ cal/mole}$$

$$2(Cu) \longrightarrow 2[\underline{Cu}]1wt\% \qquad \Delta G^\circ = -12632 \text{ cal/mole}$$

Subtracting

$$2[\underline{Cu}]1wt\% + ("FeS") \longrightarrow (Cu_2S) + (Fe) \quad \Delta G^\circ = 10370 \text{ cal/mole}$$

Since, $\Delta G^\circ = -RT\ln K$ at equilibrium,

$$10370 = -4.575*1523*\log \frac{a_{Fe}\, a_{Cu_2S}}{h^2_{\underline{Cu}}\, a_{"FeS"}}$$

Therefore,

$$\frac{a_{Fe}\, a_{Cu_2S}}{h^2_{\underline{Cu}}\, a_{"FeS"}} = 0.0325$$

where, $h_{\underline{Cu}}$ is the Henrian activity of Cu in the metal phase. Since the activity of iron is little affected by the presence of small amount of Cu in the metal phase, the activity of iron is mainly determined by carbon, i.e., at 4.5wt%C

$$a_{Fe} = 0.675$$

Henrian activity of Cu in metal is given by $h_{\underline{Cu}} = f_{Cu} wt\%\underline{Cu}$

where, $\log f_{Cu} = \log f_{Cu}^{Cu} + \log f_{Cu}^{C} + \log f_{Cu}^{S}$

$$= e_{Cu}^{Cu}\ wt\%Cu + e_{Cu}^{C}\ wt\%C + e_{Cu}^{S}\ wt\%S$$

$$= [-\ 2.1\ wt\%Cu + 8.5\ wt\%C - 2.4\ wt\%S] * 10^{-2}$$

$$= (-\ 2.1*0.2 + 8.5*4.5 - 2.4*0.02) * 10^{-2}$$

$$= (-\ 0.42 + 38.25 - 0.05) * 10^{-2}$$

$$= 0.378$$

Therefore, $f_{Cu} = 2.4$

Henrian activity coefficient is mainly determined by carbon, therefore, it may be assumed that its variation with time due to changes in S and Cu may be neglected.

Time, Hours	1/2	1	2	3	4	5	6	7	8
wt%Cu	0.37	0.275	0.21	0.19	0.19	0.19	0.195	0.195	0.20
$h_{Cu} = f_{Cu}$ wt%Cu	0.89	0.66	0.50	0.455	0.455	0.455	0.465	0.465	0.48

Activity of iron sulphide in the slag phase can be calculated in the same way as it was done for the binary "FeS" - Na_2S system.

Time, Hours	1/2	1	2	3	4	5	6	7	8
wt%S	0.014	0.020	0.032	0.045	0.059	0.078	0.099	0.120	0.147
[S] saturation	1.8	1.8	1.8	1.8	1.8	1.8	1.8	1.8	1.8
$a_{"FeS"}$ in slag	0.0078	0.011	0.018	0.025	0.033	0.043	0.055	0.067	0.082
wt of Fe in slag, g.	0.32	0.40	0.55	0.66	0.74	0.805	0.86	0.91	0.95
wt of "FeS" in slag, g.	0.50	0.63	0.865	1.04	1.16	1.265	1.35	1.43	1.49
wt of Cu in slag, g.	0.106	0.125	0.138	0.142	0.142	0.142	0.141	0.141	0.140
wt of Cu_2S in slag, g.	0.133	0.156	0.173	0.178	0.178	0.178	0.176	0.176	0.175
wt of Na_2S in slag, g.	2.47	2.30	2.04	1.86	1.74	1.63	1.55	1.45	1.38
$X_{"FeS"}$	0.15	0.19	0.26	0.31	0.35	0.38	0.405	0.43	0.46

Subsituting the calculated values of a_{Fe}, $h_{\underline{Cu}}$ and $a_{"FeS"}$ in the equilibrium relationship:

$$a_{Cu_2S} = 0.048 \quad a_{"FeS"} \quad h^2_{\underline{Cu}}$$

The activity of Cu_2S in the slag was calculated and tabulated as follows:

Time, Hours	1/2	1	2	3	4	5	6	7	8
a_{Cu_2S}	0.0003	0.00023	0.00022	0.00025	0.00033	0.00043	0.00057	0.00070	0.00091
X_{Cu_2S}	0.022	0.026	0.0285	0.0295	0.0295	0.0295	0.029	0.029	0.029
γ_{Cu_2S}	0.013	0.009	0.0075	0.0085	0.011	0.0145	0.020	0.024	0.031

The distribution ratios of Cu, in terms of wt%, are also listed below as a function of the reaction time.

Time, Hours	1/2	1	2	3	4	5	6	7	8
[wt%Cu] metal	0.37	0.275	0.21	0.19	0.19	0.19	0.195	0.195	0.20
(wt%Cu)slag	3.4	4.05	4.5	4.6	4.6	4.6	4.6	4.6	4.6
Distribution ratio $n = \frac{(Cu\%)slag}{[\underline{Cu}]\ metal}$	9.2	14.7	21.4	24.2	24.2	24.2	23.6	23.6	23.0

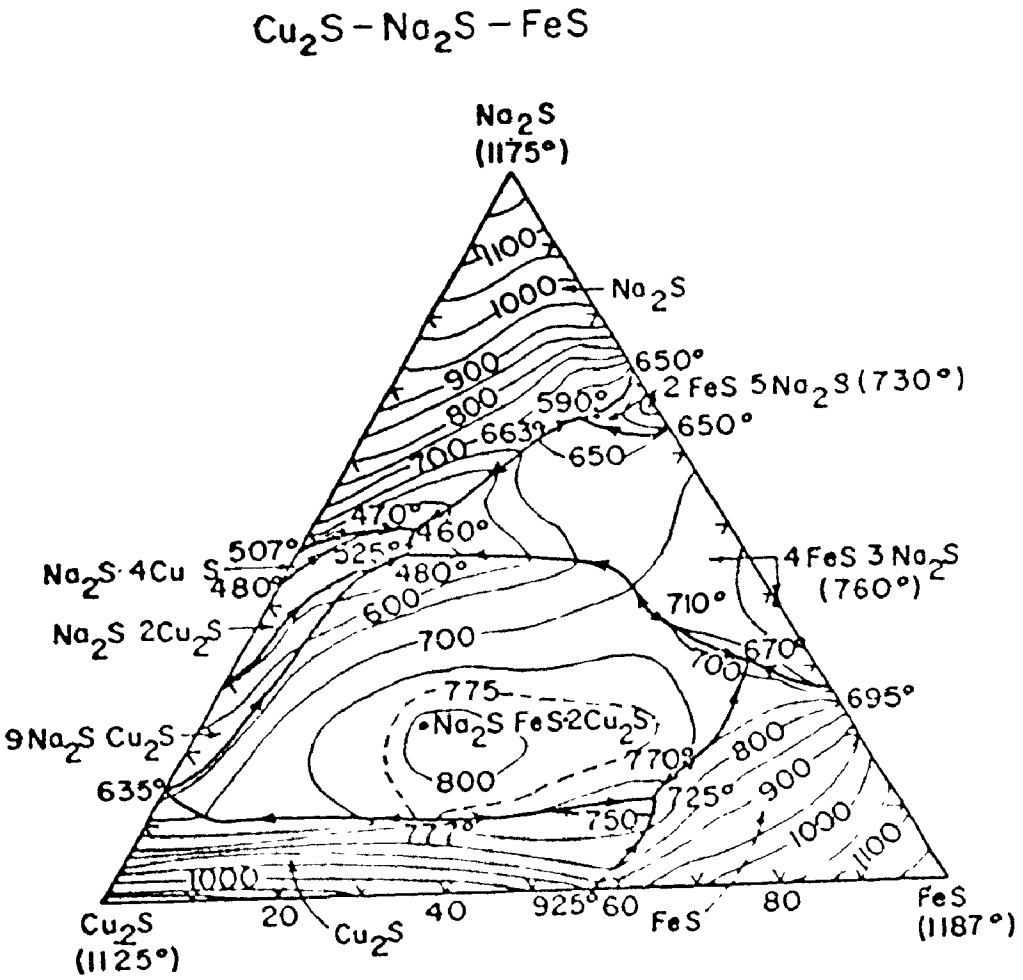

Fig. 50: System Cu_2S - Na_2S - FeS

APPENDIX V

Calculation of the activities in ternary FeS - MnS - Na_2S system

In this Appendix, the activity of MnS is evaluated based on the calculated activity of "FeS" in the slag and the equilibrium constant of the exchange reaction to be defined below:

From thermodynamic data at 1250°C[34,64]

$$(Fe) + \frac{1}{2}\{S_2\} \longrightarrow (\text{"FeS"}) \quad \Delta G^\circ_{1523°K} = -17938 \text{ cal/mole}$$

$$(Mn) + \frac{1}{2}\{S_2\} \longrightarrow \langle MnS\rangle_s \quad \Delta G^\circ_{1523°K} = -40000 \text{ cal/mole}$$

Subtracting

$$(Mn) + (\text{"FeS"}) \longrightarrow \langle MnS\rangle_s + (Fe) \quad \Delta G^\circ = -22062 \text{ cal/mole}$$

$$(Mn) \longrightarrow [\underline{Mn}]_{1wt\%} \quad \Delta G^\circ = -13900 \text{ cal/mole}$$

Subtracting

$$(\underline{Mn})_{1wt\%} + (\text{"FeS"}) \longrightarrow \langle MnS\rangle_s + (Fe) \quad \Delta G^\circ = -8160 \text{ cal/mole}$$

Therefore,

$$-8160 = -4.575*1523 \log \frac{a_{MnS}\, a_{Fe}}{h_{\underline{Mn}}\, a_{\text{"FeS"}}}$$

$$\frac{a_{MnS}\, a_{Fe}}{h_{\underline{Mn}}\, a_{\text{"FeS"}}} = 14.8$$

As before,

$$a_{Fe} = 0.675$$

Henrian activity of manganese $h_{\underline{Mn}} = f_{Mn}\ wt\%\underline{Mn}$

where,

$$\log f_{Mn} = \log f^{Mn}_{Mn} + \log f^{C}_{Mn} + \log f^{S}_{Mn}$$

$$\log f_{Mn} = e^{Mn}_{Mn}\ wt\%Mn + e^{C}_{Mn}\ wt\%C + e^{S}_{Mn}\ wt\%S$$

For wt%S = 0.01 $\qquad \log f_{Mn} = (-4.3*10^{-2})*0.01$

Therefore $f_{Mn} \simeq 1$

$h_{\underline{Mn}} \simeq wt\%\underline{Mn}$

Time, Hours	1/2	1	3	8
$h_{\underline{Mn}}$	1.82	1.12	0.193	0.128

Similarly, the activity of iron sulphide in the slag can be calculated from the S level of the melt

Time, Hours	1/2	1	3	8
wt%S	0.007	0.0115	0.0525	0.124
$a_{"FeS"}$	0.0039	0.0064	0.029	0.069
wt of Fe in slag, g.	0.04	0.06	0.28	0.43
wt of "FeS" in slag, g.	0.063	0.095	0.44	0.675
wt of Mn in slag, g.	0.351	0.490	0.671	0.684
wt of MnS in slag, g.	0.55	0.775	1.06	1.085
wt of Na_2S, g.	2.4	2.17	1.55	1.30
$X_{"FeS"}$	0.019	0.0285	0.135	0.21
$Y_{"FeS"}$	0.205	0.225	0.215	0.33

Substituting the calculated values of a_{Fe}, $a_{"FeS"}$ and $h_{\underline{Mn}}$ in

$$a_{MnS} = 14.8 \frac{a_{"FeS"}\ h_{\underline{Mn}}}{a_{Fe}}$$

we obtain activity of MnS in the slag

Time, Hours	1/2	1	3	8
a_{MnS}	0.156	0.157	0.1225	0.194
X_{MnS}	0.167	0.235	0.33	0.34
γ_{MnS}	0.935	0.67	0.37	0.57

Time, Hours	1/2	1	3	8
wt of Mn in slag	0.351	0.490	0.671	0.684
wt of MnS in slag	0.55	0.775	1.06	1.085
(%Mn)slag	11.62	16.1	22.0	22.35
[%Mn]metal	1.82	1.12	0.193	0.128
Distribution ratio $\eta = \frac{(\%Mn)\ \text{slag}}{[\%Mn]\ \text{metal}}$	6.4	14.4	114	175

APPENDIX VI

Rosenbrock's Optimization Search Technique

The optimization method used is based on the "hill climbing search" technique of Rosenbrock. Figure 51 illustrates the contours of constant value of $f(x_1,x_2)$. It is desired to locate the minimum (or max) point A. The starting point b_1 is chosen arbitrarily. Trial steps of size ϵ are taken in the direction parallel to the x_1 axis on both sides of b_1. It is found c_1 is better than b_1. The criterion used is that the summation of the squares of the differences between the calculated and observed values is better at point c_1 than at b_1. Next, starting from c_1 trial steps are taken along the x_2 direction and it is found that b_2 is again a better point than c_1 using the same criterion mentioned above. From b_2 exploratory steps are again taken but this time with step size $\alpha\epsilon$, where α is greater than 1. A better point b_3 is found. Now, the step size is again increased by a factor of α to $\alpha^2\epsilon$. At b_3 when a step to F_1 is tried, it indicates a failure. That means an increase in the summation of the squares of the differences between the calculated and observed values. The search is then returned to b_3 and proceeds to b_4 which is a success. Since F_1 was a failure, a step in the opposite direction with the step size reduced by a factor of β to $\beta\alpha^2\epsilon$ was taken at b_4 which is again proved to be a failure. The search returns to b_4 and proceeds to F_3 which is also a failure.

Now at least one success followed by a failure is encountered in all directions. A so-called stage ends at b_4. The exploratory axes

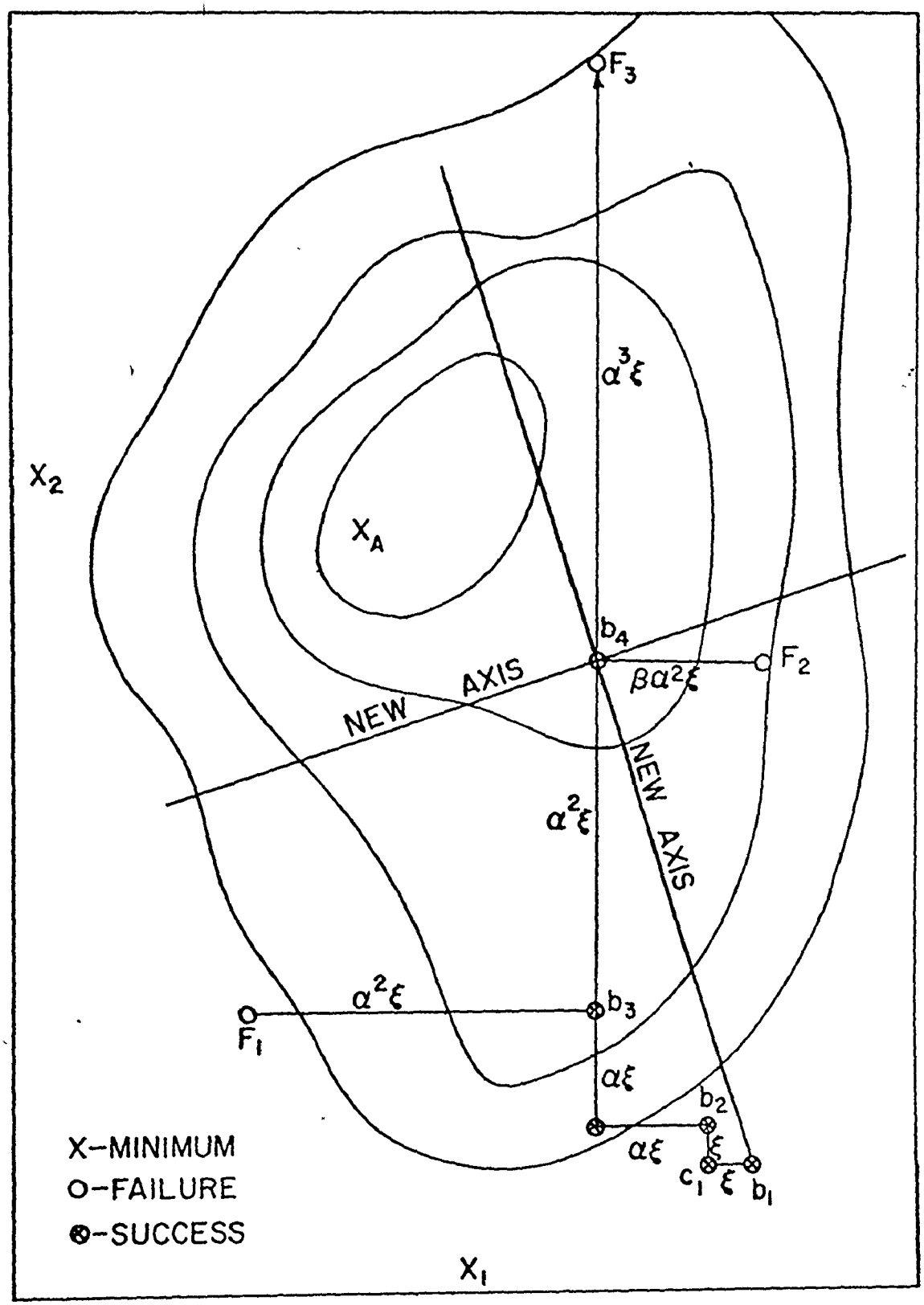

Fig. 51: Rosenbrock's search pattern

are then rotated according to the following rules. The first new axis is established by joining the first and last points of the stage. The other axes are derived from the first by the Gram-Schmidt orthogonalization process. The search pattern can now be repeated along the new axes. The local optimum point may be found, hopefully, after some stages.

The values obtained by this optimization technique depend on the complexity of the surface, i.e., the shape and slopes near the minimum point. The starting point b_1 is also important particularly in the presence of more than one minimum.

The Notations used in the Program

AKE(I):		Initial guessed values for variables
EPS(I):		Initial step sizes of variable perturbation
NV	:	Number of variables
K(I)	:	Rate constants
AR1	:	Gas/slag interfacial area
AR2	:	Slag/metal interfacial area
VMS	:	Volume of metal sulphide (FeS or Cu_2S)
VNAS	:	Volume of sodium sulphide
SODZ	:	Initial concentration of sodium in the slag
P	:	Concentrations in the metal phase
M,N	:	Number of experimental points
C1(I)	:	Concentration of sodium in the slag
C2(I)	:	Concentration of iron or copper in the slag

C1CAL(I): Calculated concentration of sodium in the slag

C2CAL(I): Calculated concentration of iron in the slag

TOL : Tolerance required

DIFF2 : Summation of squares of differences between experimental and calculated values

T(I) : Time of reaction

XM : Maximum time of reaction, seconds

The Input Values Used

ε = EPS(I) = AKE(I)/10.0

TOL = $1.0*10^{-5}$

XM = 28800

M,N = 8

NV = 2,4 or 6

α = 1.5

β = 0.5

```
ROSENBROCK  OPTIMIZATION  SEARCH  PROGRAM  FOR          ION
    OF FOUR  UNKNOWN  RATE  CONSTANTS.
HWLT,T100.                                                    TOPKAYA
FTN.
LGO.
1         6400 END OF RECORD
      PROGRAM TST (INPUT,OUTPUT,TAPE5=INPUT,TAPE6=OUTPUT)
      COMMON/B/X(500),Y1(500),Y2(500)
      COMMON/BLK1/C1(10),T(10),C1CAL(10),N,XM,C2(10),C2CAL(10),NXM
      COMMON/BLK3/AR1,AR2,VMS,VNAS,SODZ,P
      REAL K(4)
      DIMENSION AKE(4),EPS(4)
C *** READ  EXPERIMENTAL  CONDITIONS
      READ(5,400)AR1,AR2,VMS,VNAS,SODZ,P
      READ(5,500) M, N
C *** READ  IN  OBSERVED  C1  AND  C2  VS  TIME  RELATION
      READ(5,510)(T(I),C1(I),C2(I), I=1,M)
      WRITE(6,400)AR1,AR2,VMS,VNAS,SODZ,P
C *** CALCULATION  OF  CONSTANT  PARAMETERS
C *** PREPARE  FOR  CALLING  ROSENBROCK  SEARCH
      NV=4
      READ( 5,300) K(1),K(2),K(3),K(4)
      DO 20 I = 1,4
      AKE(I) = K(I)
      EPS(I)=AKE(I)/10.0
   20 CONTINUE
      TOL=1.0E-05
      CALL  ROSEN (AKE,EPS,NV,100,100,50,1.5,0.5,TOL)
      CALL OBJECT(AKE,DIFF2)
      WRITE(6,600) ( AKE(I) , I = 1,4) ,DIFF2
      WRITE(6,610)
      WRITE(6,620) (T(I),C1(I),C1CAL(I),C2(I),C2CAL(I), I = 1,N)
  300 FORMAT(4F10.0)
  400 FORMAT(6F10.6)
  500 FORMAT(2I10)
  510 FORMAT( 3F10.0)
  600 FORMAT(//10X,*BEST SET OF K1 AND K2*/15X,*K1F= *,E12.5,
     115X,*K1B= *,E12.5/15X,*K2F= *,E12.5,15X,*K2B= * , E12.5
     2/15X,*DIFF2= *,E12.5/)
  610 FORMAT(20X,*T*,10X,*C1*,5X,*C1CAL*,10X,*C2*,5X,*C2CAL*/)
  620 FORMAT(10X,F10.0, 4F17.6 )
      WRITE(6,601)(X(I),Y1(I),Y2(I),I=1,289)
  601 FORMAT(3E15.6)
      STOP
      END
      SUBROUTINE OBJECT (AKE,DIFF2)
      COMMON/B/X(500),Y1(500),Y2(500)
      COMMON/BLK1/C1(10),T(10),C1CAL(10),N,XM,C2(10),C2CAL(10),NXM
      COMMON/BLK2/ARK1,ARK2,ARK3,ARK4,ALPHA,BETA,GAMA,ZETA
      COMMON/BLK3/AR1,AR2,VMS,VNAS,SODZ,P
      REAL K1,K2,K3,K4
      DIMENSION AKE(4)
C *** DEFINE  CONSTANTS   USED
      K1=AKE(1)
      K2=AKE(2)
      K3=AKE(3)
      K4=AKE(4)
      ARK1=K1*AR1
      ARK2=K2*AR1
```

```
      ARK3=K3*AR2*P
      ARK4=K4*AR2
C *** SOLVE THE DIFFERENTIAL EQUATION WITH ASSUMED K1 AND K2
      X0=0.0
      Y01=SODZ
      Y02=0.0
      XM=28800.0
      NXM=XM
      CALL RK4 (X0,Y01,Y02,XM,X,Y1,Y2,100.0)
C *** FIND C1 AND C2 AT EXPERIMENTAL T
      DO 100 J=1,N
      DO 105 I=1,NXM
      IF( ABS( X(I) - T(J) ) .LT. 1.0E-10 )  GO TO 106
  105 CONTINUE
  106 C1CAL(J)=Y1(I)
      C2CAL(J)=Y2(I)
C *** WRITE(6,900) X(I),C1(J),C1CAL(J)  ,C2(J),C2CAL(J)
  100 CONTINUE
C *** CALCULATE  DIFFERENCE
      DIFF2=0.0
      DO 110 I=1,N
  110 DIFF2=DIFF2+(C1(I)-C1CAL(I))**2 +(C2(I) - C2CAL(I) )**2
  898 FORMAT(//,15X,*K1*,10X *K2*, 5X, *SUM OF SQUARE*, 20X,
     1*A1 AND A2*, 3(1PE14.5)//30X,*TIME , X(I)*,5X,*CU EXPT*,
     25X,*C1 CALCD*,5X,*C2 EXP*,5X,*C2 CALCD*)
  900 FORMAT(30X, 5( 1PE14.5)/)
      RETURN
      END
     ( SUBROUTINE RK4(XC,Y01,Y02,XM,X,Y1,Y2, H )
      DIMENSION X(500),Y1(500),Y2(500)
      COMMON/BLK2/ARK1,ARK2,ARK3,ARK4,ALPHA,BETA,GAMA,ZETA
      COMMON/BLK3/AR1,AR2,VMS,VNAS,SODZ,P
C
C *** THIS PROGRAM SOLVE SETS OF SIMULTANEOUS ORDINARY FIRST
C *** ORDER DIFFERENTIAL EQUATIONS  DY1/DX=F1(X,Y1,Y2) AND
C *** DY2/DX=F2(X,Y1,Y2) BY 4-TH ORDER RUNGE-KUTTA METHOD
C *** WITH  GIVEN INITIAL VALUE Y1=Y01,Y2=Y02 AT X=X0
C
C     X         INDEPENDENT VARIABLE, OUT PUT VALUE, X(1)=X0
C     Y1        DEPENDENT VARIABLE, OUT PUT VALUE, Y1(1) = Y01
C     Y2        DEPENDENT VARIABLE, OUT PUT VALUE, Y2(1) = Y02
C     H         STEP SIZE, INPUT VALUE, MODIFIED WITHIN THE PROGRAM
C     STEP SIZE IS INTERNALLY CONTROLLED WHEN EE.GT.100.0
C
C *** DEFINE DERIVATIVE EQUATIONS DY1/DX=F1(X,Y1,Y2) AND
C *** DY2/DX=F2(X,Y1,Y2)
C *** X=TIME , Y1=NO OF MOLES OF NA , Y2= NO OF MOLES OF EE
      F1(X,Y1,Y2)=-((ARK1*Y1)/(0.5*Y1*VNAS+Y2*VMS))+(ARK2)
      F2(X,Y1,Y2)=(ARK3)-((ARK4*Y2)/(0.5*Y1*VNAS+Y2*VMS))
C
C *** START WITH GIVEN H AND CHECK ITS PROPERNESS IN EVERY 10 STEP
      NHALF=0
      I=1
      X(1)=X0
      Y1(1) = Y01
      Y2(1) = Y02
      HH = 0.5 * H
      HHH = 0.166666667 * H
```

```
  100 I=I+1
      IF(I.GT.500) GO TO 160
      X(I)=X(I-1)+H
      IF(X(I).GT.XM) RETURN
  101 CONTINUE
      AK11 = F1(X(I-1),Y1(I-1),Y2(I-1))
      AK21 = F2(X(I-1),Y1(I-1),Y2(I-1))
      AK12 = F1(X(I-1)+HH,Y1(I-1)+AK11*HH,Y2(I-1)+AK21*HH)
      AK22 = F2(X(I-1)+HH,Y1(I-1)+AK11*HH,Y2(I-1)+AK21*HH)
      AK13 = F1(X(I-1)+HH,Y1(I-1)+AK12*HH,Y2(I-1)+AK22*HH)
      AK23 = F2(X(I-1)+HH,Y1(I-1)+AK12*HH,Y2(I-1)+AK22*HH)
      AK14 = F1(X(I-1)+H ,Y1(I-1)+AK13*H ,Y2(I-1)+AK23*H )
      AK24 = F2(X(I-1)+H ,Y1(I-1)+AK13*H ,Y2(I-1)+AK23*H )
      Y1(I)=Y1(I-1)+HHH*(AK11+2.0*AK12+2.0*AK13+AK14)
      Y2(I)=Y2(I-1)+HHH*(AK21+2.0*AK22+2.0*AK23+AK24)
      IF(Y1(I).LT.1.0E-10) GO TO 201
      IF(Y2(I).LT.1.0E-10) GO TO 201
      GO TO 100
  201 WRITE(6,202)(X(I),Y1(I),Y2(I))
  202 FORMAT(3E15.5)
      RETURN
C *** H WAS FOUND TOO LARGE, NOW REDUCE INTO HALF
  150 HF=H/2.0
      H=HF
      X(I)=X(I-1)+H
      NHALF=NHALF+1
      WRITE(6,605) NHALF,H
      IF(NHALF.GT.10) GO TO 200
      GO TO 101
  160 WRITE(6,620) X(500)
  620 FORMAT(10X,*X(500) = *,1PE10.3, * .LT. XM*/)
      STOP
  200 WRITE(6,600)
  600 FORMAT(10X,*H REDUCED TO HALF 10 TIMES*)
  605 FORMAT(20X,I2,*   H REDUCED TO *,1PE10.3)
      STOP
      END
      SUBROUTINE ROSEN(AKE,EPS,KM,MAXK,MKAT,MCYC,ALPHA,BETA,EPSY)
      DIMENSION AKE(20),D(20),V(20,20),BL(20,20),BLEN(20,20),
     1EPS(20),AJ(20),E(20),AL(20,20),AFK(20)
      NSTEP=2
      NSTEP=1
      DO 100 I=1,KM
      DO 100 J=1,KM
      V(I,J)=0.0
      IF(I.EQ.J) V(I,J)=1.0
  100 CONTINUE
      KAT=1
      CALL OBJECT(AKE,SUMN)
      WRITE(6,481) KAT,(AKE(IJJ),IJJ=1,KM),SUMN
      SUMO=SUMN
      DO 812 K=1,KM
      AFK(K)=AKE(K)
  812 CONTINUE
      KK1=1
      IF(NSTEP.EQ.1) GO TO 1000
      DO 350 I=1,KM
      E(I)=EPS(I)
```

```
  350 CONTINUE

 1000 DO 250 I=1,KM
      AJ(I)=2.0
      IF(NSTEP.NE.1) GO TO 250
      E(I)=EPS(I)
  250 D(I)=0.0
      III=0
  397 III=III+1
  258 I=1
  259 DO 252 J=1,KM
  251 AKE(J)=AKE(J)+E(I)*V(I,J)
      IF (AKE(J).GE.1.0E-10) GO TO 252
      AKE(J)=AKE(J)-E(I)*V(I,J)
      E(I)=0.5*E(I)
      GO TO 251
  252 CONTINUE
      CALL OBJECT(AKE,SUMN)
      WRITE(6,481) KAT,(AKE(JJ),JJ=1,KM),SUMN
C     PRINT HERE IF DESIRED NO OF TIMES OBJECTIVE FUNCTION
C *** BEING CALLED
  481 FORMAT(1X,I5,8E13.5/)
      KAT=KAT+1
      IF(SUMN.LE.EPSY) GO TO 1001
      IF(KAT.GE.MAXK) GO TO 1001
      IF(SUMN.LT.SUM0) GO TO 253
      DO 254 J=1,KM
  254 AKE(J)=AKE(J)-E(I)*V(I,J)
      E(I)=-BETA*E(I)
      IF(AJ(I).LT.1.5) AJ(I)=0.0
      GO TO 255
  253 D(I)=D(I)+E(I)
      E(I)=ALPHA*E(I)
      SUM0=SUMN
      DO 813 K=1,KM
  813 AEK(K)=AKE(K)
      IF(AJ(I).GT.1.5) AJ(I)=1.0
  255 DO 256 J=1,KM
      IF(AJ(J).GT.0.5) GO TO 299
  256 CONTINUE
      GO TO 257
  299 IF(I.EQ.KM) GO TO 399
      I=I+1
      GO TO 259
  399 DO 398 J=1,KM
      IF(AJ(J).LT.2.0) GO TO 258
  398 CONTINUE
      IF(III.LT.MCYC) GO TO 397
      GO TO 1001
  257 CONTINUE
      DO 290 I=1,KM
      DO 290 J=1,KM
  290 AL(I,J)=0.0
C
C     ORTHOGONALIZATION
C
      WRITE(6,280) KK1
      WRITE(6,294)
```

```
      WRITE(6,815) ((V(I,J),J=1,KM),I=1,KM)
      WRITE(6,281) SUMO,(AKF(I),I=1,KM)
      DO 260 I=1,KM
      KL=I
      DO 260 J=1,KM
      DO 261 K=KL,KM
  261 AL(I,J)=D(K)*V(K,J)+AL(I,J)
  260 BL(I,J)=AL(I,J)
      BLEN(1)=0.0
      DO 351 K=1,KM
      BLEN(1)=BLEN(1)+BL(1,K)*BL(1,K)
  351 CONTINUE
      BLEN(1)=SQRT(BLEN(1))
      DO 352 J=1,KM
      V(1,J)=BL(1,J)/BLEN(1)
  352 CONTINUE
      DO 263 I=2,KM
      II=I-1
      DO 263 J=1,KM
      SUMAVV=0.0
      DO 264 KK=1,II
      SUMAV=0.0
      DO 262 K=1,KM
  262 SUMAV=SUMAV+AL(I,K)*V(KK,K)
  264 SUMAVV=SUMAV*V(KK,J)+SUMAVV
  263 BL(I,J)=AL(I,J)-SUMAVV
      DO 266 I=2,KM
      BLEN(I)=0.0
      DO 267 K=1,KM
  267 BLEN(I)=BLEN(I)+BL(I,K)*BL(I,K)
      BLEN(I)=SQRT(BLEN(I))
      DO 266 J=1,KM
  266 V(I,J)=BL(I,J)/BLEN(I)
      KK1=KK1+1
      IF(KK1.EQ.MKAT) GO TO 1001
      GO TO 1000
 1001 CONTINUE
      IF(SUMN.GT.EPSY) GO TO 1002
      DO 1008 I=1,KM
 1008 AFK(I)=AKF(I)
      SUMO=SUMN
 1002 CONTINUE
      WRITE(6,1003) KK1,KAT,III
      WRITE(6,1004) SUMO
      WRITE(6,1006) (AFK(I),I=1,KM)
      DO 1009 I=1,KM
      AKF(I)=AFK(I)
 1009 CONTINUE
      WRITE(6,294)
      WRITE(6,815) ((V(I,J),J=1,KM),I=1,KM)
      WRITE(6,1501) (E(I),I=1,KM)
 1501 FORMAT(/10X,*THE FINAL STEP SIZES ARE*,5X,5E12.3/)
  280 FORMAT(//3X,*NO OF STAGE= *,3X,I5/)
  281 FORMAT(10X,*SUMO AND VARIABLES*,3X,6E12.4/)
  294 FORMAT(/3X,*ORTHOGONAL UNIT VECTORS*/)
  815 FORMAT(3X,9E12.4/)
 1003 FORMAT(/3X,*NO OF STAGE = *,I5,3X,*AND OBJECT BEING
     1CALLED*,I5,3X,*TIMES*,3X,*NO OF SUCCESSIVE FAILURES =
```

```
     2*,[5/)
 1004 FORMAT(/3X,*OBJECT = *, F15.5/)
 1006 FORMAT(/3X,*THE VARIABLES ARE*, 6E12.5/)
      RETURN
      END
$          6400 END OF RECORD
1.77        2.55        18.565      42.026      0.0769      0.1091
           R           R
3600.0      0.0639      0.0068
7200.0      0.0574      0.0100
10800.0     0.0517      0.0123
14400.0     0.0474      0.0141
18000.0     0.0452      0.0155
21600.0     0.0422      0.0166
25200.0     0.0396      0.0175
28800.0     0.0387      0.0182
0.000116    0.000004170.000005240.0000429
$            END OF FILE
```

APPENDIX VII

1. Sensitivity of Calculated Rate Constants

An effective way to illustrate the sensitivity of k* with respect to $k^{**}p^B$ and k_2 with respect to k_2' is given below for the case of carbon-saturated iron - Na_2S system.

With the electroneutrality assumption, the values of k*, $k^{**}p^B$ and k_2, k_2' which gave the closest agreement between the experimental data and the calculated results were already given (refer to page 153).

As defined in Eq. (6.42),

$$k^* = 0.14 * 10^{-3} \text{ cm/sec}$$
$$k^{**}p^B = 0.47 * 10^{-5} \text{ moles/cm}^2\text{. sec}$$

As defined in Eq. (6.43),

$$k_2 = 0.62 * 10^{-5} \text{ cm/sec}$$
$$k_2' = 0.44 * 10^{-4} \text{ cm/sec}$$

First, holding k* constant at the best value as listed above, $k^{**}p^B$ was perturbed and the calculated results were compared with the experimental data by a least squares criterion. The process was then repeated for other chosen values of k*, in the range of 0.5 k* and 2k* about its optimum value, see Fig. 52. The calculated results are very sensitive to the variation of the value of $k^{**}p^B$ and to a lesser extent to that of k*. However, perturbations of k* within ±25% of the best value does not cause substantial shifts

in the closeness of the fit. In fact, variations are comparable to the reproducibility of experimental results obtained from duplicate runs.

Similar calculations were done for the case of k_2 and k_2'. Sum of squares of differences between experimental and calculated concentration values against k_2' is plotted in Fig. 53 for different k_2 values. As before, perturbations of k_2 by a factor of 0.5 and 2 cause significant shifts in the closeness of the fit between the calculated values and the experimental data. However, in the case of k_2 and k_2' the curves do not have as sharp minima as in Fig. 52. This means that the calculated results are not as much sensitive to changes in k_2' as in the case of $k^{**}p^B$.

It was concluded from the computer outputs that the changes of k's by a factor of 0.5 and 2 would give calculated values within the limits of ±20% of the observed concentrations. However, when the perturbations of the rate constants were within ±25% of the optimum values, the calculated and experimental concentrations were within ±5% of each other. Therefore, it may be suggested that the uncertainty in the numerical values of rate constants is about ±25% of the above listed values.

The uniqueness of the set of values of rate constants cannot be verified rigorously. However, there is some further evidence about the accuracy of rate constants. The data for Fe-C and Cu-C systems were analysed separately, but similar values for k^* and $k^{**}p^B$ were obtained, i.e., within the uncertainty limits given above. The rate constants evaluated based on the experimental data from the binary alloys were also in good agreement with the rate constants evaluated for the ternary Fe-Cu-C system. Furthermore, the same set of rate constants fitted the data obtained from different size crucibles.

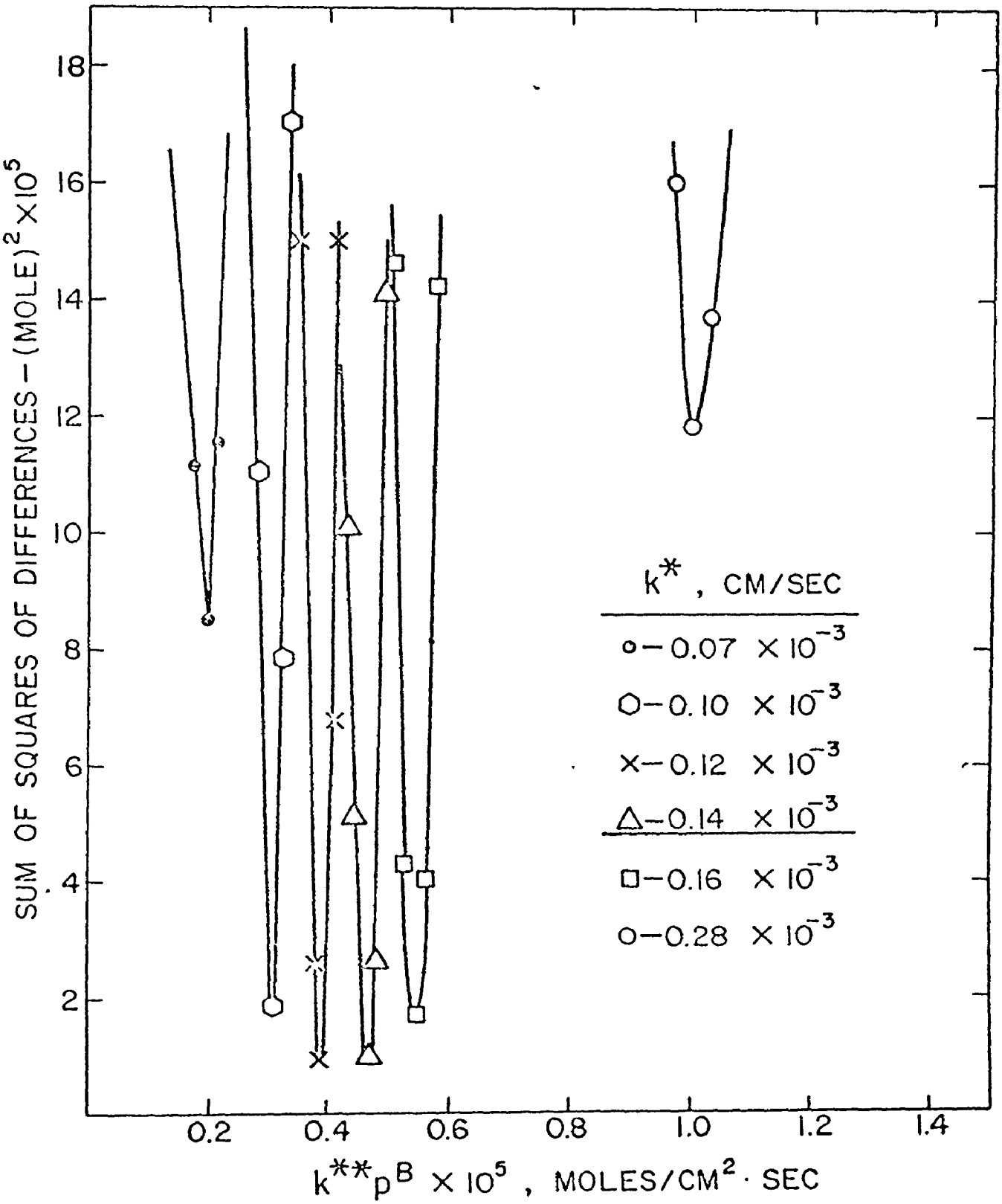

Fig. 52: Values of k* and k**p^B were perturbed and the resulting solutions compared with the experimental points by a least squares criterion

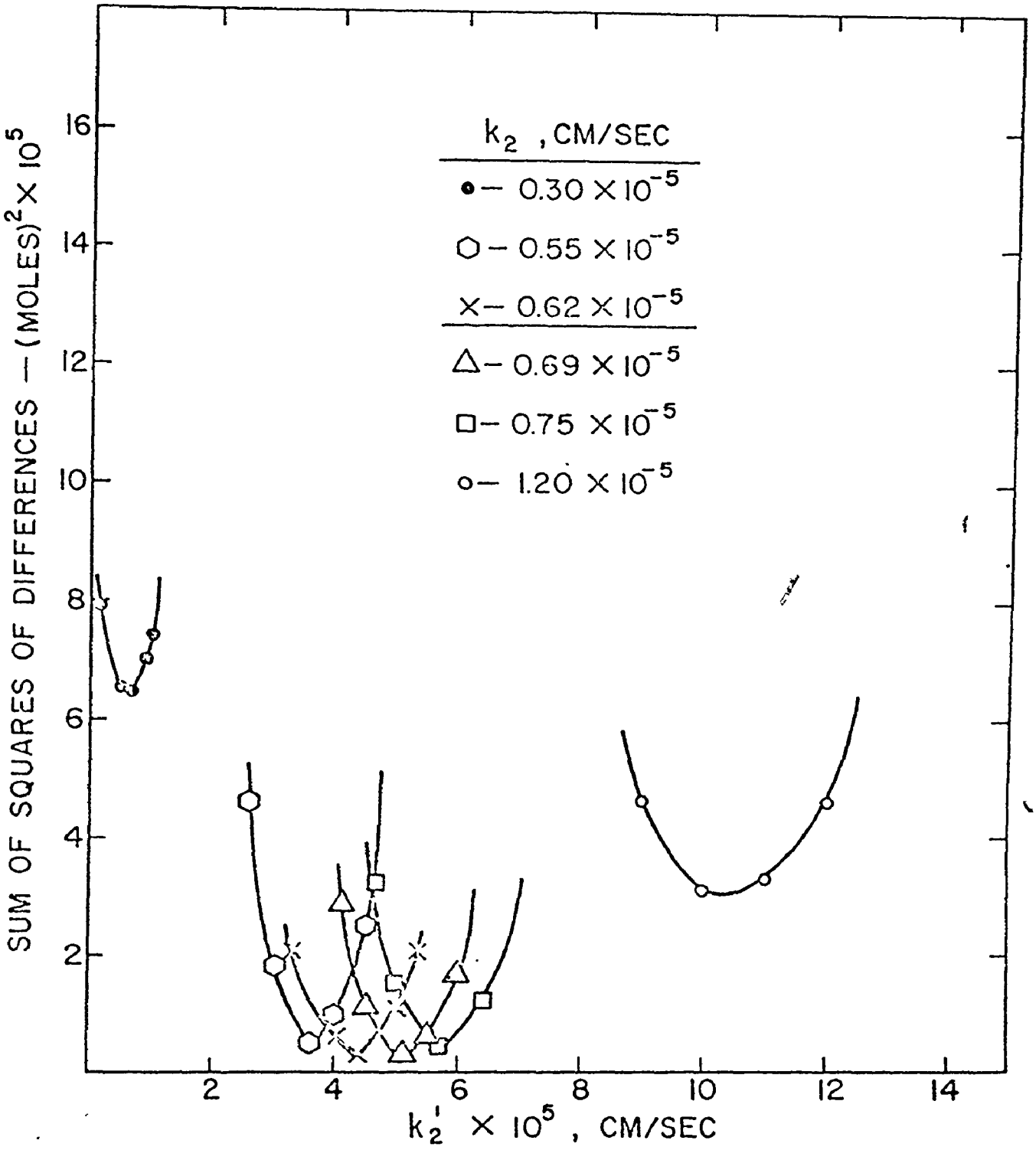

Fig. 53: Values of k_2 and k_2' were perturbed and the resulting solutions compared with the experimental points by a least squares criterion

2. Sources of Experimental Error

In the present system, the errors arise in chemical analysis, sampling, weighing of slag and metal and the measurement of temperature.

The chemical analysis errors are usually within ±1% of the reported analysis. However, accuracy of the analysis of the various elements in slag and metal phases varies from element to element and also varies with concentration. In the present system, carbon, copper, silicon, manganese and sulphur in the metal phase were determined within the following accuracies: ±0.05 wt%C (for C ≥ 4.0%), ±0.02 wt%Cu, ±0.01 wt%Si, ±0.03 wt%Mn (for Mn ≥ 3.0%) and ±0.003 wt%S (for S ≤ 0.03%), ±0.01 wt%S for higher sulphur contents. The copper content of the slag was also determined within an accuracy of ±0.02 wt%, the sulphur was determined to ±0.25 wt%, the sodium to ±0.5 wt% and the iron to ±1% of its content. However, the relative importance of the errors in analysis of each of the constituents is different, as may be seen from the stoichiometry of the reactions. This error is not appreciable when alloy contents are low, which was generally the case in the present system (i.e., 0.7 wt%S, 0.9%Cu, 1%Si, etc.).

The sampling errors are difficult to estimate. However, to minimize the errors from this source, whenever possible, all of the slag was taken for chemical analysis, so that average values for the components of the slag could be obtained. In the sampling of metal specimens, first the surface of the metal was machined with a lathe to remove any sulphide layer that might have been present. Only after this step could a longitudinal machining of the surface be done to collect sufficient sample for chemical analysis.

The other errors that should be considered are in determination of the weights of metal and slag and temperature measurement. The temperature of the crucible was determined with a Pt/Pt-13%Rh thermocouple and is expected to be within ±5°C. The error in weighing of slag was difficult to estimate due to the hygroscopic nature of the slag. However, it was noticed that during the duration of weighing, the change in recorded weight was not significant.

The reproducibility of results obtained from duplicate runs under identical conditions was good. The variations of the values reported were within ±5%.

APPENDIX VIII

Alternate Mechanisms of Reaction

Two alternate mechanisms to the one given in Chapter 6 were proposed in the oral defense of this thesis. The first alternate model involves double displacement reactions with ionic diffusion steps in the present multi-component system. Sodium sulphide which is most probably a p-type semi-conductor will have S^- (electron holes) and $S^=$ ions present in the liquid slag. So the reactions at the gas/slag and slag/metal boundaries can be written as follows:

At the gas/slag interface $\quad Na^+ + S^= \longrightarrow S^- + \{Na\}_{gas}$

At the slag/metal interface $\quad Fe + 2S^- \longrightarrow Fe^{++} + 2S^=$

This means that under the condition of electroneutrality there will be diffusion and possibly convection of S^- ions from gas/slag interface to the slag/metal interface. At the same time Fe^{++} and $S^=$ ions will move from the slag/metal boundary to the gas/slag boundary.

Another mechanism could be based on local anodic and cathodic reactions at the slag/metal boundary. This mechanism is very likely if the Debye-Hückel screening distance requirements has to be satisfied, i.e , the separation of charge should be within a few angstroms. Under these circumstances, the slag phase will not be required to support a large potential difference. The local anodic and cathodic reactions at the slag/metal boundary can be represented as follows:

At the slag/metal boundary $Fe \longrightarrow Fe^{++} + 2e^-$

$Na^+ + e^- \longrightarrow Na^*$ (Dissolved atomic sodium in slag phase)

At the gas/slag boundary $Na^* \longrightarrow \{Na\}_{gas}$

The atomic sodium which forms at the slag/metal interface may be transported to the gas/slag interface by diffusion and convection that is present in the system.

In conclusion, it can be said that additional investigations are needed in order to differentiate between some of the possible mechanisms.

REFERENCES

1. K.M. Goldman, G. Derge, and W.O. Philbrook. Trans. AIME, 200, 534, 1954
2. S. Ramachandran, T.B. King, and N.J. Grant, Trans. AIME, 206, 1549, 1956
3. C. Wagner, "The Physical Chemistry of Steelmaking", M.I.T. Symposium, p.237, John Wiley, N.Y., 1958
4. C. Wagner and W. Traud, Z. Electrochem., 44, 391, 1938
5. T.B. King and S. Ramachandran, "The Physical Chemistry of Steelmaking", M.I.T. Symposium, p.125, John Wiley, N.Y., 1958
6. X. de Hemptinne, H. Eyring, and T. Ree, "Physical Chemistry of Process Metallurgy", Part I, p.65, Interscience, N.Y., 1961
7. W.O. Philbrook, 1971 AIME Annual Meeting, Howe Memorial Lecture, March 1971
8. W-K.Lu, Trans. ISIJ, 11, 32, 1971
9. W-K. Lu, Trans. ISIJ, 10, 473, 1970
10. I. Prigogine, "Introduction to Thermodynamics of Irreversible Processes", p.57, Interscience, N.Y., 1967
11. J.F. Jordan, "Process for the removal of sulphur from ferrous metal", U.S. Patent No. 2,509,189 May 23, 1950
12. J.F. Jordon, "Method of desulphurizing and decopperizing ferrous metal", U.S. Patent No. 2,512, 578 June 20, 1950
13. F.C. Langenberg and R.W. Lindsay, Trans. AIME, 200, 967, 1954

14. F.C. Langenberg and R.W. Lindsay, "The removal of the copper from iron-carbon-copper melts", Contributions to the Metallurgy of Steel, No.51, American Iron and Steel Institute, New York, March 1957.

15. F.C. Langenberg, R. Lindsay, and D.P. Robertson, Blast Furnace and Steel Plant, 1142, Oct. 1955

16. A. Simkovich and R.W. Lindsay, Trans. AIME, 218, 569, 1960

17. H. Schenck and G. Perbix, Archiv. für das Eisenhüttenwesen, Heft7, 417, 1962

18. F.A. Settino and E.J. Stofka, "Treatment of molten automotive scrap to reduce copper content", Prepared for U.S. Bureau of Mines, Contract No. 14-09-0070-363, PPG Industries, 1967

19. H.V. Makar, B.W. Dunning, and H.S. Caldwell, U.S. Bureau of Mines Investigation Report 7199, Nov. 1968

20. H.V. Makar and B.W. Dunning, J. of Metals, 21, 19, 1969

21. H.V. Makar and R.E. Brown, U.S. Bureau of Mines Investigation Report 7914, 1974

22. H. Schenck, H. Roth, and E. Steinmetz, Archiv. für das Eisenhüttenwesen, heft7, 595, July 1970

23. A. Safiah and F.R. Sale, J. Iron and Steel Inst., 210, 52, 1972

24. F.D. Richardson and J.E. Antill, Trans. Faraday Soc., 50, 22, 1954

25. W. Olsen, Stahl und Eisen, Heft11/12, 175, May 1948

26. E.G. Bunzel and E.J. Kohlmeyer, Z. Anorg. Allgem. Chem., 254, 1, Sept. 1947

27. Chemical Abstracts, 45:4621h, Ball. Sci. Facolto Chim. Ind., Bologna 8, No.3, 1950

28. F. Uhlig, "General Motors' efforts in junk car processing", Proceedings of 52nd National Open Hearth and Basic Oxygen Steel Conference, TMS-AIME, 52, 83, 1970

29. R.R. Brown and F.E. Black, U.S. Bureau of Mines Investigation Report 7218, Dec. 1968

30. J.S. Poliskin, Electric Furnace Conference Proceedings, TMS-AIME, Vol.27, p.141, 1969

31. C.M. Hsido and A.W. Schlechten,J. of Metals, Trans. AIME, 194, 65, 1952

32. O.C. Roberts, D.G.C. Robertson and A.E. Jenkins, Trans. AIME, 245, 2413, 1969

33. F.D. Richardson and J.H.E. Jeffes, JISI, 171, 165, 1952

34. J.F. Elliott and M. Gleiser, "Thermochemistry for Steelmaking", Addison-Wesley Publishing Co. Inc., Reading, Mass., 1960

35. "Handbook of Physics and Chemistry", 53rd Edition, The Chemical Rubber Company, 1972-1973

36. E. Zintl, A.Dauth, Z. Elektrochem., 40, 588, 1934

37. G. Courtois, Compt. Rend., 207, 1220, 1938

38. P. Ley, Chem. Ztg., 58, 859, 1934

39. T.G. Pearson and P.L. Robinson, J. Chem. Soc., London, 137, 1473, 1930

40. Von E.J. Kohlmeyer and H. Brinkmann, Z. Anorg. Allgem. Chem., 299, 182, 1959

41. T.W. Bauer and R.M. Dorland, Canad. J. Tech., 32, 91, 1954

42. O. Kubaschewski, E. Evans, C.B. Alcock, "Metallurgical Thermochemistry", Pergamon Press, N.Y. 1967

43. D.R. Stull and H. Prophet, "Janaf thermochemical tables", U.S. Government Printing Office, Washington, D.C. 1971

44. "Mellor's Comprehensive Treatise on Inorganic and Theoretical Chemistry", The alkali metals, Part 1, p.980, Longmans, 1960

45. "Gmelins Handbuch der Anorganischen Chemie", Natrium, system nummer 21, p.466, 1969

46. Metals Handbook, Vol.8, "Metallography, structures and phase diagrams", ASM, Metals Park, Ohio, 1973

47. M. Hansen, "Constitution of Binary Alloys", McGraw Hill Book Company, Inc., New York, 1958

48. E.T. Turkdogan and R.A. Hancock, JISI, 179, 155, 1955

49. C.S. Smith and E.W. Palmer, Trans. AIME, 188, 1486, 1950

50. W.R. Maddocks and G.E. Claussen, ISI Alloy Steels Research Committee, Special Rep. 14, 97, 1936

51. K. Iwase, Sci. Rep. Tôhoku Univ., 26, 618, 1937

52. N.I. Kopylov, Russian Journal of Inorganic Chemistry, 13(2),276 1968

53. "ASTM Methods for Chemical Analysis of Metals", p.22, 184, ASTM, Philadelphia, 1960

54. W. Westwood and A. Mayer, "Chemical analysis of cast iron and foundry materials", Ruskin House, 1960

55. S.Z. Lewin, J. of Chemical Education, 43, 1, 1966

56. Kirk-Othmer, "Encyclophedia of Chemical Technology", Vol.18, p.510, Interscience Publishers, N.Y., 1969

57. Arthur I. Vogel, "A Textbook of Quantitative Inorganic Analysis", Longmans, London, 1961

58. "A.S.T.M. Methods Chemical Analysis of Metals", American Society for Testing Materials, Philadelphia, Pa., 1960

59. "Techniques of Metals Research", Vol.IV, Part 1 and 2, Edited by Robert Rapp, Interscience Publishers, N.Y., 1970

60. K.L. Fetters and J. Chipman, Trans. AIME, 145, 95, 1941

61. C.R. Taylor and J. Chipman, Trans. AIME, 154, 228, 1943

62. "Basic Open Hearth Steelmaking", Physical Chemistry of Steelmaking Committee, AIME, p.752, 1964

63. N.I. Kopylov, Russian Journal of Inorganic Chemistry, 12, 1494, 1967

64. "Electric Furnace Steelmaking", Vol.II, Iron and Steel Division AIME, P.136, 1967

65. N.I. Kopylov and S.S. Novoselov, Russian Journal of Inorganic Chemistry, 9, No.8, 1964

66. R.G. Ward, "Physical Chemistry of Iron and Steelmaking", Arnold, 1962

67. F.D. Richardson and B. Fincham, JISI, 178, 4, 1954

68. "Progress in semi-conductors", Editor Gibson, Vol.4, John Wiley and Sons, Inc., 1960

69. D. Argyriades, G. Derge, and G.M. Pound, Trans. AIME, 215, 909, 1959

70. G.M. Pound, G. Derge, and G. Osuch, Trans. AIME, 203, 481, 1955

71. M. Bourgon, G. Derge, and G.M. Pound, Trans. AIME, 212, 338, 1958

72. F.C. Langenberg, Trans. AIME, 206, 1024, 1956

73. P.J. Koros and J. Chipman, Trans. AIME, 206, 1102, 1956

74. H.H. Rosenbrock and C. Storey, "Computational Techniques for Chemical Engineers", Pergamon Press, Oxford, 1966

75. L.S. Darken and R.W. Gurry, "Physical Chemistry of Metals", McGraw Hill Book Co., N.Y., 1953

76. W. Jost, "Diffusion in Solids, Liquids and Gases", Academic Press N.Y., 1960

77. J. Crank, "The Mathematics of Diffusion", Clarendon, Oxford, 1964

78. R.E. Grace and G. Derge, Trans. AIME, 203, 839, 1955

79. L. Yang, M.T. Simnad, and G. Derge, Trans. AIME, 206, 1577, 1956

80. J.D. Verhoeven, Trans. AIME, 242, 1937, 1968

81. R.E. Grace and G. Derge, Trans. AIME, 221, 331, 1958

82. T. Saito, Y. Kawai, K. Maruya, and M. Maki, "Physical Chemistry of Process Metallurgy", p.1. International Symposium, Pittsburgh, 1959 (Interscience Publishers, N.Y., 1961)

83. von A. Majdic, D. Graf, and H. Schenck, Archiv. für das Eisenhüttenwesen, Heft8, 627, 1969

84. Shiro Banya and J. Chipman, Trans. AIME, 242, 940, 1968

85. J.P. Morris and R.C. Buehl, Trans. AIME, 188, 317, 1950

86. Shiro Banya and J. Chipman, Trans. AIME, 245, 133, 1969